

**Fate of biodegradable disposables in high-solids anaerobic
digestion followed by hydrothermal liquefaction**

by

Parisa Niknejad

A thesis submitted in partial fulfilment of the requirements for the degree of

Master of Science

in

Environmental Engineering

Department of Civil and Environmental Engineering

University of Alberta

© Parisa Niknejad, 2023

Abstract

To address the growing concern of environmental sustainability and waste management, recent research efforts have been dedicated to investigating innovative methods for the treatment and conversion of biodegradable disposables and bioplastics. These studies delve into the potential of high solid anaerobic digestion (HSAD) followed by hydrothermal liquefaction (HTL) as integrated processes to facilitate the transformation of these materials. However, several fundamental and engineering bottlenecks are associated with their practical application. To date, limited information is available on the fate of bioplastics during HSAD and HTL process. Thus, this thesis aims to address these research gaps by investigating the degradability of bioplastics during HSAD and their subsequent degradation during HTL under various operating conditions.

First, the biodegradability and transformation of biodegradable disposables through an integrated process of HSAD followed by HTL was investigated. During the HSAD phase, the paper-based disposables demonstrated efficient degradation. Conversely, compostable plastic bags and utensils showed resistance to degradation, leading to a reduction of 29.5% and 8.99%, respectively, in methane yield compared to the control group. However, the HTL process exhibited promising results, as it was able to completely convert the undegraded plastic bags and utensils present in the HSAD digestate into biocrude. This transformation significantly lowered the potential environmental risks associated with bioplastic pollution from digestate application on land. Furthermore, by increasing the HTL temperature from 280 to 350 °C, the yield and quality of biocrude, particularly in terms of heavy oil content, were improved.

Second, the co-digestion of bioplastics and source-separated organic waste (SSO) using an integrated approach involving HSAD and followed by HTL under various operating conditions at 280 °C, 330 °C, and 370 °C was explored. During the HSAD process, bioplastics underwent fragmentation, resulting in a notable reduction in methane recovery. Nonetheless, the HTL process proved to be highly effective in completely converting bioplastics, thereby mitigating the potential environmental risks associated with bioplastic pollution. Experimental observations indicated that an increase in temperature from 280 to 330 °C led to a higher weight percentage of biocrude. However, when the temperature was further increased from 330 to 370 °C, both the weight percentage of biocrude and hydrochar decreased, while the weight

percentage of total gas showed a peak rise. At a temperature of 330 °C, the maximum higher heating value for bioplastics was achieved, surpassing that of the control group.

Preface

Chapter 1 and 2 of this thesis encompass a thorough examination of the research background and a comprehensive literature review in which fundamental concepts, technical terminology, different technology and operational concepts. We present a review that meticulously summarizes and discusses the most recent observations and results concerning the biodegradability and transformation of bioplastics in high solid anaerobic digestion followed by hydrothermal liquefaction.

Chapter 3 of this thesis has been published as Niknejad, P., Azizi, S.M.M., Hillier, K., Gupta, R., Dhar, B.R., 2023. *“Biodegradability and transformation of biodegradable disposables in high-solids anaerobic digestion followed by hydrothermal liquefaction”* in Resources, Conservation & Recycling, vol 193, 106979. Niknejad, P was responsible for experimental design, experiment and data collection, writing original draft, review, and editing. Azizi, S.M.M and Hillier, K assisted with conducting the experiments. Gupta, R and Dhar, B.R were responsible for the review, editing, and supervising this work.

Chapter 4 of this thesis has been submitted as Niknejad, P., Azizi, S.M.M., Gupta, R., Dhar, B.R.,2023. *“Unveiling the Impact of Bioplastic Bags on High-Solids Anaerobic Digestion and Subsequent Hydrothermal Liquefaction of Source Separated Organics”* in Environmental Research Journal. Niknejad, P was responsible for conceptualization and experiment design, experiment and data collection, writing original draft, review, and editing. Azizi, S.M.M assisted with conducting the experiments. Gupta, R and B.R. Dhar were responsible for the review, editing, and supervising this work.

Dedication

To my dear family, you have been the pillars of strength and the guiding lights in my life. Your constant belief in my abilities, your patience during moments of struggle, and your profound understanding have been the bedrock of my achievements. From the earliest days of my education, you nurtured my curiosity, cultivated my passions, and instilled in me an unyielding determination to pursue knowledge. Your sacrifices and selflessness have paved the way for me to stand here today. This work is a tribute to your love, and it reflects the values and wisdom you have instilled in me.

To my loving husband, you are my rock, my confidant, and my most fervent cheerleader. Your unwavering belief in my dreams and your unwavering support through every triumph and setback have been the wind beneath my wings. Your love has been a source of inspiration and motivation, and it has given me the courage to conquer challenges and reach new heights. This thesis is a dedication to the profound impact you have had on my life and the boundless joy you bring to each moment we share together.

Acknowledgments

I am profoundly grateful to my esteemed supervisors, Dr. Bipro Ranjan Dhar and Dr. Rajender Gupta. Your guidance, expertise, and mentorship have been instrumental in shaping this thesis and my academic growth. Your constructive feedback, dedication to fostering critical thinking, and support during challenging times have made an indelible impact on my research journey. I have been fortunate to have you both as my supervisor, and I am grateful for the wisdom and knowledge you have imparted.

My sincere thanks also go to my MSc defense committee for their generous time and invaluable constructive input on my thesis. Their valuable feedback has been instrumental in refining and enhancing the quality of my research work. Their expertise and keen observations have offered fresh perspectives that have contributed significantly to the overall academic rigor of this study.

I extend my heartfelt gratitude to both my past and present colleagues for their invaluable support throughout my academic journey. I would like to specially thank Seyed Mohammad Mirsoleimani Azizi and Basem Zakaria for generously sharing their expertise and providing me with essential training in the equipment and laboratory techniques. Their guidance has been instrumental in honing my skills and navigating the intricacies of research work.

I am grateful as well for the support provided by the Discovery Grant from the Natural Sciences and Engineering Research Council of Canada (NSERC).

Table of contents

Abstract	ii
Preface	iv
Dedication	v
Acknowledgments	vi
List of Tables	x
List of Figures.....	xi
Abbreviations and Units	xii
Chapter 1	1
Introduction	1
1.1. Background	1
1.2. Scope and Objective.....	3
1.3. Thesis Outline	3
Chapter 2	4
Literature Review.....	4
2.1. Bioplastics	4
2.2. Anaerobic digestion processes	6
2.2.1. Co-digestion.....	9
2.3. Thermochemical processes	11
2.3.1. Combustion.....	12
2.3.2. Pyrolysis.....	12
2.3.3. Gasification	13
2.3.4. Hydrothermal process	13
2.3.4.1. Hydrothermal Carbonization.....	14
2.3.4.2. Hydrothermal Gasification.....	14
2.3.4.3. Hydrothermal Liquefaction	15
2.4. HTL Reaction's mechanism.....	17
2.5. HTL's products	19

2.5.1. Bio-crude.....	19
2.5.2. Hydrochar	21
2.5.3. Water soluble substance.....	21
2.5.4. Gases	22
2.6. Operating parameters affecting HTL	23
2.6.1. Reaction temperature	23
2.6.2. Pressure	24
2.6.3. Retention time	25
2.6.4. Type of solvent	27
2.6.5. HTL’s catalyst.....	27
Chapter 3	29
Biodegradability and transformation of biodegradable disposables in high-solids anaerobic digestion followed by hydrothermal liquefaction	29
3.1. Introduction	29
3.2. Material and Methods.....	31
3.2.1. High-solids anaerobic digestion experiments	31
3.2.2. Hydrothermal liquefaction experiments	32
3.2.3. Analytical methods	33
3.3. Results and Discussion.....	34
3.3.1. Anaerobic biodegradability of biodegradable disposables	34
3.3.2. FTIR analysis of digestate	36
3.3.3. Hydrothermal liquefaction of digestate	38
3.3.3.1. Product distribution	38
3.3.3.2. Biocrude composition	39
3.3.3.3. Gaseous products.....	41
3.3.3.4. FTIR spectra	42
3.4. Conclusions	44
Chapter 4	46
Unveiling the Impact of Bioplastic Bags on High-Solids Anaerobic Digestion and Subsequent Hydrothermal Liquefaction of Source Separated Organics	46
4.1. Introduction	46
4.2. Material and Methods.....	48

4.2.1. High-solid anaerobic digestion experiments.....	48
4.2.2. Hydrothermal liquefaction experiments	50
4.2.3. Analytical Methods.....	50
4.2.3. Data analysis	51
4.3. Results and Discussion.....	51
4.3.1. High-solids anaerobic digestion.....	51
4.3.1.1. Impact of bioplastic bags on methane potential and kinetics.....	51
4.3.1.2. Fourier transform infrared spectroscopy of digestate	54
4.3.2. Hydrothermal liquefaction of digestate	56
4.3.2.1. Product distribution	56
4.3.2.2. Biocrude composition	57
4.3.2.3. Gaseous products.....	60
4.3.2.4. Elemental analysis, atomic ratio, and higher heating value	61
4.3.2.4.1. Hydrochar	61
4.3.2.4.2. Biocrude.....	63
4.3.2.5. FTIR spectra.....	65
4.3.3 Principal component analysis	67
4.4. Conclusions	69
Chapter 5	71
Conclusions and Recommendations.....	71
5.1. Conclusion.....	71
5.2. Recommendations	72
References	74
Appendix A	95
<i>Supplementary Information for Chapter 3</i>	<i>95</i>
Appendix B.....	105
<i>Supplementary Information for Chapter 4</i>	<i>105</i>

List of Tables

Table 2.1. Assessing the differences between LSAD and HSAD processes (Fagbohunbe et al., 2015)	7
Table 2.2. Investigation of HTL studies: effects of biomass types, temperatures, and retention times on process outcomes.....	26
Table 3.1. Characteristics of inoculum and feedstocks.	32
Table 4.1. Characteristics of inoculum and feedstocks.	49
Table 4.2. Initial elemental analysis of source-separated organics, inoculum, and initial bioplastic bag; CHNO (wt.%), and their molecular formula.	49
Table 4.3. The molecular formula of source-separated organics and biomethane recovery efficiencies obtained based on elemental analysis results.	53
Table 4.4. Kinetic parameters estimated with the first-order and modified Gompertz model.	54
Table 4.5. Elemental analysis and higher heating value for hydrochar at different conditions.	62
Table 4.6. Elemental analysis and higher heating value for biocrude at different conditions.	63
Table A-1. Summary of literature used for identifying different functional groups present in samples based on their wavenumber.....	95
Table A-2. GC-MS results for heavy oil (HO) from different digestate samples under different HTL experimental condition: (a) Control (280 °C) (b) Control (350 °C) (c) Paper-based disposables (280 °C) (d) Paper-based disposables (350 °C) (e) Compostable plastic bag (280 °C) (f) Compostable plastic bag (350 °C) (g) Plant-based utensils (280 °C) (h) Plant-based utensils (350 °C)	96
Table B-1. GC-MS results for heavy oil (HO) from different digestate samples under different HTL experimental condition: (a) Control (280 °C) (b) Control (330 °C) (c) Control (370 °C) (d) Bioplastic (280 °C) (e) Bioplastic (330 °C) (f) Bioplastic (370 °C)	105

List of Figures

Figure 2.1. The gaseous phase composition during HTL at 350 °C (Basar et al., 2021b; Brown et al., 2010; Cherad et al., 2016; Jena et al., 2012).....	23
Figure 3.1. Cumulative methane yield for different feedstocks.....	35
Figure 3.2. FTIR spectra of initial feedstocks and digestate from HSAD: (a) control, (b) paper-based disposables, (c) compostable plastic bags, and (d) plant-based utensils.	37
Figure 3.3. Product yields from different digestate samples in HTL at 280 and 350°C.	39
Figure 3.4. GC–MS analysis results for biocrude from different HTL test conditions.....	40
Figure 3.5. GC–TCD analysis results for gaseous products from different HTL tests.	42
Figure 3.6. FTIR spectroscopy of biocrude and hydrochar (HC) samples after HTL of digestate samples: (a) control, (b) paper-based disposables, (c) compostable plastic bags, and (d) plant-based utensils.....	43
Figure 4.1. Cumulative methane yields for control and bioplastics-loaded reactors.	52
Figure 4.2. Fourier transform infrared spectroscopy of initial feedstocks and digestate from high-solid anaerobic digestion under different test conditions.	55
Figure 4.3. Product yields from hydrothermal liquefaction of digestate under different conditions.....	57
Figure 4.4. Heatmap showing gas chromatography–mass spectrometry analysis results for biocrude under different hydrothermal liquefaction conditions	59
Figure 4.5. Gas chromatography-thermal conductivity detector analysis results for gaseous products from different hydrothermal liquefaction tests.	61
Figure 4.6. Fourier transform infrared spectroscopy of biocrude and hydrochar samples after hydrothermal liquefaction of digestate samples: (a) control, (b) bioplastic	66
Figure 4.7. Principal component analysis of different functional groups in biocrude with products distribution.	69

Abbreviations and Units

AD	Anarobic digestion
LSAD	Low-solid anaerobic digestion; so-called wet-type AD
HSAD	High-solids anaerobic digestion
HTL	Hydrothermal liquefaction
SSO	Source-separated organics
OFMSW	Organic fraction of municipal solid wastes
TS	Total solids
HTC	Hydrothermqal carbonization
HTG	Hydrothermal gasification
MSW	Municipal solid wastes
OLR	Organic loading rate
VS	Valotile solids
d	Day
m ³	Cubic meters
°C	Celsius
CH ₄	Methane
CO ₂	Carbon dioxide
H ₂	Hydrogen
CO	Carbon monoxide
H ₂ O	Water
C ₂ H ₄	Ethylene
C ₂ H ₆	Ethane
wt. %	Weight percentage
N	Nitrogen

O	Oxygen
HHV	Higher heating value
PA	Polyamides
PTT	Polytrimethylene terephthalate
TPS	Thermoplastic starch
PHA	Polyhydroxyalkanoate
PCL	Polycaprolactone
PVA	Polyvinyl alcohol
PVOH	Polyvinyl alcohol
PBAT	Poly butylene adipate-co-terephthalate
PGA	Polyglycolide
PBS	Polybutylene succinate
HRT	Hydraulic Retention Time
PLLA	Poly-L-lactic acid
O/C	Oxygen per carbon
C/N	Carbon per nitrogen
Psi	Pounds per square inch (pressure's unit)
bar	Baros (pressure's unit)
DSS	Domestic sewage sludge
Bio-PE	Bio-Polyethylene
Bio-PP	BioPolypropylene
S	Sulfur
DCM	Dichloromethane
HO	Heavy oil
AO	Aqueous oil

MJ/kg	Megajoules per kilogram
WSS	Water soluble substance
HC	Hydrochar
COD	Chemical oxygen demand
L	Liter
g	Gram
g/L	Gram per liter
N ₂	Nitrogen
OH ⁻	Hydroxide ion
H ⁺	Hydrogen ion
Kg	Kilogram
MPa	Mega pascal
min	Minute
Na ₂ CO ₃	Sodium carbonate
MC	Moisture content
EWMc	Edmonton waste management centre
mL	Milliliter
mL/g	Milliliter per gram
F/M	Feedstock to microorganism
cm	Centimeter
rpm	Revolutions per minute
pH	Potential of hydrogen
NaOH	Sodium hydroxide
BMP	Biochemical Methane Potential
TCD	Thermal conductivity detection

ATR-FTIR	Attenuated Total Reflectance Fourier Transform Infrared Spectroscopy
FTIR	Fourier Transform Infrared Spectroscopy
m	Meter
mm	Milimeter
μm	Micrometer
μL	Microleter
GC-MS	Gas Chromatography-Mass Spectrometry
H	Hydrogen
C	Carbon
ARGs	Antimicrobial resistance genes
PCA	PNPrincipal component analysis
MPs	Microplastics
NPs	Nanoplastics
HDPE	High-density polyethylene
L/d	Liter per day
R	Maximum rate
λ	Lag phase
PLA	Polylactic Acid

Chapter 1

Introduction

1.1. Background

Plastic pollution has become a global environmental concern due to the extensive use of plastic products and improper waste management practices (Abraham et al., 2021; Na et al., 2021). The global production of plastics exceeds 300 million tons, and a significant portion, approximately 13 million tons, finds its way into the environment (Enfrin et al., 2019a). Mostly derived from fossil fuels, these plastics constitute approximately 6% of global oil consumption and possess chemical stability, making them persistent and non-biodegradable. Consequently, the accumulation of such plastics in ecosystems poses a serious threat (Cucina et al., 2022a; Enfrin et al., 2019a; Matthews et al., 2021; Unmar and Mohee, 2008). In response to these concerns, bioplastics have emerged as an eco-friendly substitute for conventional plastics derived from fossil fuels (Cucina et al., 2021a). Bioplastics, which are either biodegradable or derived from renewable sources, are designed to naturally degrade in the environment within a shorter period than traditional plastics (Cucina et al., 2022a). In response to the growing awareness of plastic pollution, many countries have implemented directives to ban single-use plastics, leading to an increased usage of biodegradable disposables, including bioplastics and paper-based materials (Cucina et al., 2021a).

Nonetheless, the presence of disposable bioplastics in waste streams presents challenges, particularly in municipalities lacking residential source separation programs (Cucina et al., 2021a; Pereira de Albuquerque et al., 2021). Commingling these bioplastics with the organic fraction of municipal solid waste (OFMSW) can lead to complications in waste management procedures, such as composting and anaerobic digestion (AD) (Cucina et al., 2021a). Studies have shown that bioplastics may not fully degrade within typical composting time frames, requiring a longer duration for complete degradation (Ruggero et al., 2020). Additionally, the degradability of bioplastics in AD varies depending on their composition (Cucina et al., 2022a).

In addition to the challenges posed by plastic pollution, the growing global population and rapid urbanization have led to a significant rise in the production of source-separated organics (SSO) (Dastyar et al., 2021c). By 2050, SSO generation is projected to reach a critical level of

approximately 3.4 billion tonnes (Kaza et al., 2018). In certain municipalities, bioplastic bags have been utilized as liners for green bins used for SSO storage and collection, simplifying the waste management process and enhancing convenience for both municipalities and residents (Peng et al., 2022).

The utilization of high-solid anaerobic digestion (HSAD) has gained significant attention as it offers the notable benefit of diverting OFMSW and SSO from landfills (Dastyar et al., 2021b, 2021a). HSAD, with a total solids (TS) content exceeding 15%, presents numerous advantages, including decreased water usage, reduced heating expenses, the capability to manage heterogeneous feedstocks, higher organic loading rates, and eliminates the necessity for sophisticated dewatering techniques for digestate prior to agricultural utilization (Dastyar et al., 2021a, 2021c). Nevertheless, a comprehensive understanding of the destiny of biodegradable disposables and their decomposition in the context of the HSAD process remains limited. During HSAD, biodegradable disposables experience incomplete decomposition, as they could persist in significant amounts within the digestate, posing potential environmental risks when the digestate is utilized for land application (Karamanlioglu et al., 2017).

Consequently, additional treatment may be necessary for HSAD residuals before final disposal. Moreover, because of the existence of solubilized organic materials and high carbon content, digestate holds significant energy value that can be harnessed through thermochemical biomass processing techniques such as hydrothermal processes (Sharma et al., 2022). Hydrothermal processes involve various thermochemical techniques conducted at high temperatures and elevated pressures. Notably, hydrothermal carbonization (HTC), hydrothermal liquefaction (HTL), and hydrothermal gasification (HTG) are the main categories of hydrothermal processes (Ruiz et al., 2013). HTL, in particular, holds significant potential for the valorization of water-containing organic wastes, as it enables the conversion of complex molecules into biocrude oil without the need for energy-consuming drying processes (Ruiz et al., 2013).

In the last few years, there have been several inquiries focusing on exploring the application of HTL for the valorization of AD digestate. These studies have highlighted the crucial influence of digestate properties regarding the productivity and chemical characteristics of the resultant biocrude (Posmanik et al., 2018; Sudibyo et al., 2022). Nevertheless, through an in-depth review

of the literature, a significant research gap exists concerning the HTL of HSAD digestate, particularly with regard to undegraded biodegradable disposables.

1.2. Scope and Objective

This study aims to investigate the degradability and transformation of common bioplastics in during high-solid anaerobic digestion (HSAD) followed by hydrothermal liquefaction (HTL) processes. Furthermore, this study sheds light on the impact of co-digestion of bioplastics and source separated organics (SSO) in the HSAD process, as well as the effects of different temperatures in the HTL process on the quality of the final product and the degradation of bioplastics. Two specific objectives of this thesis were:

- a) To investigate the biodegradability and transformation of biodegradable disposables in HSAD followed by HTL.
- b) To assess the impact of bioplastic bags on HSAD and subsequent HTL of SSO.

1.3. Thesis Outline

This thesis consists of five chapters. Chapter 1 focuses on the background of the topic under investigation and provides a concise overview of the research objectives. Chapter 2 conducts a comprehensive literature review relevant to the proposed research. The experimental findings of this thesis are then presented in Chapter 3 and Chapter 4 in the format of research articles. Lastly, Chapter 5 summarizes the key results, discusses their scientific and engineering implications, and offers recommendations for future research.

Chapter 2

Literature Review

2.1. Bioplastics

Bioplastics encompass a range of polymers with biodegradable, biobased, or combined properties. Biobased plastics are manufactured using materials derived from biomass. However, it should be emphasized that while some biobased plastics are biodegradable, not all of them possess this characteristic. On the other hand, bioplastics derived from petroleum or other sources may still demonstrate degradable properties (Abraham et al., 2021). Biodegradable bioplastics are typically engineered to break down naturally through biological processes, including landfill decomposition, composting, or degradation in natural settings like water ecosystems and soils (Folino et al., 2020; Siegenthaler et al., 2012). Biodegradable plastics are a type of plastic that microorganisms can break down into H₂O and CO₂ in aerobic conditions, or into CH₄ and CO₂ (biogas) in anaerobic conditions (Abraham et al., 2021; Dilkes-Hoffman et al., 2019). Within the biobased polymers that are not degradable, we can find bioPET, bio-PE (bio-Polyethylene), bio-PP (bioPolypropylene), PA (Polyamides), and PTT (Polytrimethylene terephthalate). On the other hand, there are biobased and decomposable polymers, such as PLA, PHA (Polyhydroxyalkanoates), starch blends, and TPS (thermoplastic starch). In addition to these, there are biodegradable polymers of petrochemical origins that exhibit a certain degree of degradability. Notable examples of biobased polymers that lack biodegradability include PCL (Polycaprolactone), PVA/PVOH (Polyvinyl alcohol), PBAT (Polybutylene adipate terephthalate), PGA (Polyglycolide), PBS (Polybutylene succinate) (Vardar et al., 2022).

The biopolymers that have been extensively researched in the scientific literature include PLA, PHA, and their combinations (Choe et al., 2021). PLA blends are widely employed in various industries and are viewed as a promising substitute for fossil fuel-derived polymers (Ahmed et al., 2018). The mechanical features of these blends are impacted by their crystallinity, with amorphous PLA being more flexible and crystalline PLA being more rigid (Folino et al., 2020). In addition to PLA, PHA, and cellulose, starch-based polymers have also gained extensive usage and hold the distinction of being the earliest widely adopted bioplastics. Even in 2020, they retained a

considerable share (20%) within the bioplastics market (Cucina et al., 2021b; Folino et al., 2020). In 2020, combined production and utilization of PLA, PHA, and starch blends accounted for 70% of all bioplastics (Cucina et al., 2021a). The materials are employed to create eco-friendly alternatives, contributing to sustainability efforts. Numerous products including biodegradable bags, eco-conscious mulching films, compostable stirrers for coffee, disposable dishes and glasses, plant-based pots, recyclable bottles, environmentally friendly packaging materials, and even biocompatible medical appliances, are produced (Folino et al., 2020; Narancic et al., 2020; Zhao et al., 2020).

The OFMSW is a complex waste type that may contain intentional polymers used in waste collection, as well as impurities originating from improperly discarded food packaging or household activities. Nevertheless, OFMSW represents a valuable biomass resource for composting and AD facilities, where it can be utilized to produce biogas. Globally, the OFMSW consists of approximately 46% food waste, which contains substantial moisture levels, varying from 80% to as high as 85-90% in certain waste streams (Bátori et al., 2018). The collection process for this fraction can present challenges since plastic bags commonly used for waste collection can contaminate the feedstock delivered to composting and biogas plants (Bátori et al., 2018). The primary contaminants found in OFMSW are plastics, bioplastics, and cellulosic materials, primarily originating from collection bags and accidental leakages (Bátori et al., 2018; Cucina et al., 2021b).

Bioplastics and cellulosic materials are suggested as environmentally friendly substitutes for conventional plastics, offering biodegradability and compatibility with biological processes. Their use could potentially eliminate the necessity to separate bags from collected waste streams, especially considering the increasing adoption of bioplastic bags in waste collection systems. For instance, in 2019, bioplastic bags constituted approximately 3-4% of Italy's OFMSW, with expectations of further growth (Cucina et al., 2021b). The program is specifically designed to exclusively utilize bioplastic bags for waste collection. Mixing plastics and bioplastics makes it challenging to separate them from each other, so using only bioplastic bags is crucial to avoid any potential plastic contamination. Co-digestion of bioplastics and the residual organic matter present in the plastic bags can contribute to elevated biogas generation and enhanced mass mineralization. By embracing this co-digestion approach, sustainability objectives are effectively supported,

promoting improved resource utilization and adopting a comprehensive ecosystem management strategy (Dolci et al., 2021; Hobbs et al., 2021; Patrício Silva, 2021). The majority of biogas plants function at mesophilic conditions due to their advantages, such as reduced investment requirements, lower energy consumption, and process stability. These plants typically maintain a hydraulic retention time (HRT) of 20–40 days (Cucina et al., 2021b; Nsair et al., 2020). Hence, the decomposition of polymers should align with the time frame and operating temperatures of AD plants. It is crucial to note that not all bioplastics are biodegradable, and some specific commercial bioplastics could potentially hinder biogas production in the AD process, as stated in the literature (Niknejad et al., 2023; Peng et al., 2022). Therefore, implementing co-digestion strategies should involve a comprehensive assessment of biodegradability and compatibility to ensure optimal biogas generation and efficient waste management.

2.2. Anaerobic digestion processes

In order to decrease the quantity of MSW sent to landfills and address the mentioned problems, there has been an increasing focus on converting non-recyclable materials and the OFMSW into valuable products. This involves utilizing various thermochemical and biochemical activities such as composting, incineration, landfilling, and anaerobic digestion to produce biofuels, bio-fertilizers, and other valuable bioproducts (Kumar and Samadder, 2020; Lim et al., 2016; Zhang et al., 2019). Among these available technologies, AD has emerged as a reliable, environmentally sustainable, and appealing method for converting the OFMSW into renewable biomethane (Chowdhury et al., 2020; Guilford, 2009; Panigrahi and Dubey, 2019). The AD process mainly encompasses a bunches of interconnected biochemical stages, such as hydrolysis, fermentation, and methanogenesis (Rocamora et al., 2020). AD processes can be divided into two categories : (I) low solid anaerobic digestion (LSAD) and (II) high solids anaerobic digestion (HSAD) (Fagbohunge et al., 2015; Pennington, 2018; Shahriari et al., 2012). Each approach has its own specific operational requirements, advantages, and disadvantages, specifically identified in Table 1 (Fagbohunge et al., 2015; Pennington, 2018; Shahriari et al., 2012).

Table 2.1. Assessing the differences between LSAD and HSAD processes (Fagbohunge et al., 2015)

Factor	LSAD	HSAD
Total solid content	<15%	15% - 40%
Operational state	Single and multi-stage AD	Single and multi-stage AD
Feeding method	Semi and continuous	Batch, sequential batch, semi and continuous
Biogas feature	High biogas production with high moisture content	Low biogas production, but low moisture
Volatile solid removal	50% - 70%	< 40%
Feedstock loading rate	<7 kg VS/m ³ .d	7-15 kg VS/m ³ .d
Inhibitory factors	More dispersion and diffusion	Less dispersion and high adsorption into substrate
Mixing regime	Internal mixing device, or liquor and biogas recirculation	Mixing by recirculating percolate and biogas, or by partial mixing
Heating condition	Requiring high heating due to large digester volume	Requiring low heating due to smaller digester volume
Operational issues	Requiring less sophisticated pumping device, due to higher water or moisture	Requiring complex pumping equipment due to dry nature of operation
Feedstock requirement	Not appropriate for hydrophobic feedstock like lignocellulosic biomasses	Most proper for hydrophobic organic biomasses
Digestate management	Requiring considerable dewatering of digestate	Minimal dewatering is needed
Digestate characteristic	Less stable but with higher nutrient content	More stable but with lower nutrient content

In recent times, there has been notable interest in HSAD, also referred to as dry-type AD. This method has garnered significant attention for its unique benefits in handling the OFMSW

(Guilford et al., 2019; Pereira de Albuquerque et al., 2021; Ting et al., 2020). HSAD systems are specially engineered to handle organic solid wastes containing higher total solids (TS) content, typically ranging from 15% to 40% TS (Fagbohunge et al., 2015). Unlike conventional wet-type anaerobic digesters, which are designed for liquid slurry feedstock with generally less than 10% TS content, HSAD can efficiently treat organic solid waste due to its ability to handle higher TS content. HSAD systems offer several notable advantages, including: (i) reduced water consumption, (ii) decreased heating costs, (iii) capability to handle higher organic loading rates (OLRs), and (iv) production of high-quality digestate without the need for complex dewatering technologies (Fagbohunge et al., 2015). However, despite the positive aspects of HSAD, it should be emphasized that the underlying biochemical processes in both HSAD and wet-type AD systems remain unchanged. In both cases, the AD procedure decomposes organic matter without oxygen, generating biogas and digestate.

Recently, AD has received considerable attention for handling bioplastics and biodegradable disposables in waste streams. For instance, Cucina et al. researched the degradation of different types of commercial bioplastics, including starch-based shopping bags and polylactic acid (PLA) tableware (Cucina et al., 2021a). They found that bioplastics degraded up to 27% during AD, with the remaining portion persisting in the digestate. Also, Yagi et al. explored the biodegradation of PCL powder (125-250 μm) using mesophilic AD over a prolonged duration of 277 days. The study observed a notably slow rate of biodegradation, with just 3 to 22% of the PCL being transformed into methane. The microorganisms were found to solely break down lower molecular weight PCL as a consequence of the ester bonds' random hydrolytic chain breaking (Yagi et al., 2014). Likewise, other plastics like Poly(butylene succinate) (PBS) and poly(butylene adipate-co-terephthalate) (PBAT), which are among the plastics discovered to be capable of breaking down naturally in industrial composting environments, did not experience substantial biodegradation when subjected to mesophilic anaerobic digesters (Cho et al., 2011; Massardier-Nageotte et al., 2006; Narancic et al., 2018; Shin et al., 1997; Svoboda et al., 2019). For instance, in an extensive investigation by Svoboda et al. the biodegradation behavior of the aromatic-aliphatic biodegradable polyester PBAT was investigated under both mesophilic and thermophilic anaerobic conditions. Under mesophilic conditions, the biodegradation after 126 days was relatively limited, yielding a degradation rate of only 2.2%. In contrast, thermophilic anaerobic conditions (55°C) led to more substantial changes, with a biodegradation rate of 8.3% after 126

days (Svoboda et al., 2019). These findings emphasize the significance of considering the specific properties of the materials and waste streams when investigating their biodegradability and suitability for AD processes. In summary, while HSAD holds promise for effectively handling organic solid waste with higher TS content, understanding biodegradation mechanisms and the influence of waste composition remains crucial for optimizing AD process and ensuring sustainable waste management practices.

2.2.1. Co-digestion

Traditionally, anaerobic digesters have been used to process a single type of organic material. However, co-digestion involves the concurrent treatment of two or more biodegradable materials to produce biogas. This approach enables the appropriate management of organic waste from several origins and improves the stability of the digester. The key advantage is that existing anaerobic digesters can be utilized with minor modifications and additional steps (Esposito et al., 2012; Karki et al., 2021). By adding a complementary feedstock with a primary feedstock in anaerobic co-digestion, the system's efficiency can be enhanced. The additional substrates during the digestion procedure can lead to either a beneficial synergy, providing vital nutrients that may be lacking for the microorganism growth in the digestion medium, or potentially hinder the AD process (Abraham et al., 2021; Hoelzle et al., 2014). Subsequently, the biogas production in the co-digester can either increase as a result of the improved nutritional balance within the system, or decrease the release of inhibitory compounds to the digesters (Alvarez and Lidén, 2008). The main co-substrates available for utilization include agricultural residues, municipal biowaste, and household-generated food waste (Ye et al., 2013).

Anaerobic co-digestion can be utilized in order to manage biodegradable plastics and generate renewable energy by making slight adjustments to the existing anaerobic digesters (Abraham et al., 2021). In the co-digestion process, anaerobic digesters receive biodegradable plastics and additional supplementary materials, like municipal sludge, through separate channels. Bioplastics can be employed in different types of anaerobic digesters, and the characteristics of the bioplastics and other process factors influence the degradation rate in these digesters. Microbes found in various environments possess varying abilities to break down bioplastics, and it is important to note that not every kind of bioplastics is appropriate for AD (Abraham et al., 2021; Endres and Siebert-Raths, 2011).

Bioplastics offer a valuable solution for co-digestion with substrates having lower C/N ratio values. Since bioplastics contain only carbon, their inclusion in the feedstock mix during AD can raise the overall C:N ratio. This increased C:N ratio creates a more favorable environment for anaerobic microorganisms, enhancing their ability to break down organic matter and produce biomethane (Abraham et al., 2021). In AD systems, an optimal C:N ratio typically ranges from 20:1 to 30:1 (Stroot et al., 2001). Throughout the AD of bioplastics, a combination of oxidation, hydrolysis, and depolymerization reactions works together to break down bioplastic polymers into smaller monomeric units (Chua et al., 2013). Afterwards, water-soluble monomers are released from the bioplastics, becoming easily accessible for microbial metabolism (Yoshie et al., 2002). These monomers serve as a carbon-rich substrate for the microorganisms, complementing the carbon-deficient substrates found in waste streams with lower C/N ratios. As a result, the digestion process becomes more efficient, resulting in increased production of biomethane. The study conducted by Vasmara et al. assessed the biodegradability of maize starch-based film and PLA bioplastics under different anaerobic digestion conditions (Vasmara and Marchetti, 2016). Specifically, the biodegradation of PLA bioplastics was evaluated alone in a batch reactor, as well as in co-digestion with pig slurry or partially deproteinized cheese whey. The investigation's findings demonstrated that the co-digestion of PLA bioplastics with pig slurry resulted in an increase of 12% in methane production compared to the mono-digestion of PLA (Vasmara and Marchetti, 2016). Maragkaki et al. conducted a pilot-scale study to investigate the co-digestion of OFMSW with poly-L-lactic acid (PLLA) (Maragkaki et al., 2023). Their findings revealed that the co-digestion of PLLA and OFMSW caused an 8% rise in biomethane production. Additionally, the co-digestion process showed that the overall operation of the AD process showed no apparent adverse effects (Maragkaki et al., 2023). Additionally, the study carried out by Kang et al. demonstrated that co-digestion of food waste with PLA and polyhydroxyalkanoate (PHA) led to a notable growth in methane production (Kang et al., 2022). The PLA-fed tests showed an 8.5–26.6% rise in methane production, while the PHA-fed tests showed a 12.7–25.5% increase compared to their respective mono-digestion reactors (Kang et al., 2022).

Nevertheless, Peng et al. performed a study exploring the degradation of poly (butylene adipate-co-terephthalate) (PBAT) and PLA-based biopolymer bags co-digested with food waste (Peng et al., 2022). Surprisingly, no significant biological degradation was observed after the AD process for any of the PBAT/PLA polymers, and they did not convert into biogas. Co-digestion of

PBAT/PLA with food waste at mesophilic conditions did not improve their biodegradability either. The addition of food waste created a weak acidic environment during the hydrolysis phase, which was expected to act as an acid pretreatment to aid PBAT/PLA degradation (Battista et al., 2021). However, the acidic pretreatment did not lead to higher methane production from PLA. Furthermore, the researchers noticed that under thermophilic conditions, the co-digestion of food waste with PBAT/PLA resulted in lower methane generation compared to food waste mono-digestion, indicating inhibition of methane production (Peng et al., 2022). Although the authors did not reveal the underlying mechanism behind the inhibition of the AD process, another study suggested that the incomplete breakdown and release of harmful additives from the bioplastic could interfere with the activity of key enzymes of anaerobic microorganisms (Niknejad et al., 2023). Additionally, the existence of bioplastic bags might restrict mass transfer within the digester, leading to a reduction in methane generation (Niknejad et al., 2023). Lastly, the physical presence of bioplastic bags could act as a barrier, limiting microorganisms' access to and degradation of organic matter (Abraham et al., 2021; Lallement et al., 2021; Mu et al., 2018). These factors collectively could contribute to the observed inhibition of the AD process in the presence of bioplastic bags. These observations suggest that the co-digestion of PBAT/PLA with food waste may not be an effective approach to enhance biodegradability or biogas production in AD processes.

Overall, it is important to note that not every kind of bioplastics is suitable for degradation in AD, and some may inhibit methane production. Despite the potential challenges, the co-digestion of bioplastics with compatible substrates, especially those with lower C:N ratio values, holds great promise in improving the overall sustainability of waste treatment processes and resource recovery. Further research and optimization efforts are needed to fully harness the potential benefits of anaerobic co-digestion with bioplastics and other organic materials.

2.3. Thermochemical processes

Thermochemical processes are a set of techniques that involve various chemical and physical transformations of waste at high temperatures. These processes are fundamental in converting biomass, waste, and other feedstocks into valuable products, such as biofuels, syngas, and biochar. The four main thermochemical processes commonly used are combustion, pyrolysis, gasification, and hydrothermal processes which are discussed below.

2.3.1. Combustion

Combustion is a process where fuel, including biomass, undergoes a chemical reaction with oxygen, generating a substantial quantity of heat energy. Waste biomass can be used as a fuel for combustion, providing energy for various applications, such as thermal power plants, factories, and boilers. Biomass combustion involves a series of complex heterogeneous and homogeneous reactions, including drying, devolatilization, gasification, char combustion, and gas phase oxidation (Nussbaumer, 2003). To ensure cost-effective operation, biomass combustion is typically suitable for feedstocks with a moisture content below 50%. During the combustion process of biomass, high-temperature hot gases are generated, typically ranging from 800 to 1000 °C (McKendry, 2002). This elevated temperature facilitates efficient energy production and is utilized in a variety of industrial and energy conversion processes.

2.3.2. Pyrolysis

Pyrolysis of waste biomass is a crucial thermochemical conversion process that takes place in the absence of oxygen. It holds great potential for producing a variety of valuable products, including solid char, liquid tar, and gaseous substances (Balat et al., 2009). Pyrolysis can be approached in two main ways: slow pyrolysis and fast pyrolysis. Slow pyrolysis involves lower temperatures (around 350-550 °C), slower heating rates, and longer residence times. This method predominantly yields solid char as the major product (Greenhalf, 2014). On the other hand, fast pyrolysis (around 450-600 °C), which is considered more favorable in modern applications, employs rapid heating of the biomass to intermediate and/or high temperatures without oxygen. It utilizes higher heating rates and primarily produces liquid tar and gaseous fuels as the main products (Balat et al., 2009). The advancement of fast pyrolysis holds significant promise for various applications, including bio-oil production for renewable energy, chemicals, and bio-based products. Both slow and fast pyrolysis processes offer unique advantages and can be tailored to meet specific needs, making pyrolysis a versatile and sustainable technology for converting biomass into valuable materials and contributing to the transition to a greener and more sustainable energy future.

2.3.3. Gasification

Gasification is a two-stage thermochemical process that transforms biomass into syngas and char. In the initial stage, biomass is partially combusted to produce gas and char. The resulting gases mainly consist of carbon dioxide and water vapor. In the second stage, these gases are reduced by the charcoal (char) produced in the first stage, leading to the formation of CO and H₂ (Singh and Gu, 2010). Additionally, the gasification process can yield methane and other higher hydrocarbons, which may vary differ based on the specific design and operational parameters of the gasification reactor (Singh and Gu, 2010). Syngas produced through gasification can be applied in diverse ways, including power generation, heat production, and the synthesis of valuable chemicals and fuels (Singh and Gu, 2010).

2.3.4. Hydrothermal process

Thermochemical processes, such as hydrothermal technology, have been garnering significant research interest as a promising environmentally friendly approach to convert biomass into different chemicals or energy carriers (Ruiz et al., 2021). Hydrothermal processing is a thermochemical method conducted at high temperatures and pressures above saturation, creating a sequence of reactions that modify water's physical and chemical properties, including its density, dielectric constant, and ionic product (Ruiz et al., 2021). This unique process leads to the production of energy-rich fuels and valuable chemicals from biomass feedstocks (Ruiz et al., 2021).

When biomass is converted into sub- or supercritical water, a multitude of reactions can occur simultaneously. These reactions encompass hydrolysis, depolymerization/polymerization, isomerization, dehydration, decarboxylation, aromatization, condensation, methanation, hydrogenation/dehydrogenation, and various additional processes others (Lachos-Perez et al., 2022b; Ruiz et al., 2021). Hydrothermal processes can be categorized into three primary categories depending on the desired products and temperature range : Hydrothermal Carbonization (HTC), Hydrothermal Gasification (HTG), and Hydrothermal Liquefaction (HTL) (Lachos-Perez et al., 2022a; Ruiz et al., 2021).

2.3.4.1. Hydrothermal Carbonization

Recently, hydrothermal carbonization (HTC,) also known as wet torrefaction, has attracted increased attention as an environmentally-friendly approach for producing a solid product called hydrochar, with a mass yield ranging from approximately 35% to 80% (Heidari et al., 2019). Hydrochar has various applications in fields such as environmental solutions, energy generation, biosensing, supercapacitors, and catalysts (Kambo and Dutta, 2015; Sun et al., 2020). Biomass materials with high moisture content, usually ranging from 70% to 90%, are particularly suitable for HTC due to the process's reliance on the inherent presence of water. Unlike conventional thermal technologies such as pyrolysis and dry torrefaction, HTC eliminates the need for pre-drying, which is an energy-intensive phase. As a result, the energy-intensive drying process is completely bypassed in HTC, leading to significant energy savings. (Antero et al., 2020; Kambo and Dutta, 2015).

Additionally, the production of hydrochar in HTC requires relatively less energy compared to pyrolysis (Antero et al., 2020; Kumar et al., 2018). This is mainly due to two factors: Firstly, HTC eliminates the need for feedstock drying, which is a significant energy-intensive step in pyrolysis. Secondly, HTC operates at lower temperatures, commonly from 180 to 250°C, in contrast to the higher temperatures used in pyrolysis, which can be as high as 500°C (Antero et al., 2020; Kumar et al., 2018). These lower temperatures in HTC contribute to its energy efficiency and make it an attractive alternative for generating hydrochar from biomass with higher moisture content.

2.3.4.2. Hydrothermal Gasification

Hydrothermal gasification is a thermochemical process that occurs at temperatures exceeding 350 °C without oxidants. This process results in the production of a flue gas, which is primarily enriched in either H₂ or CH₄, depending on the specific reaction conditions (Cherad et al., 2016). HTG can be performed in either batch or continuous mode. The batch process allows for experiments to be conducted using different concentrations and catalysts, while the continuous system enables the study of reaction kinetics and facilitates the study of the process under continuous flow conditions (de Vlieger et al., 2012; Kumar et al., 2018). HTG encompasses three main types: aqueous phase refining, catalytic gasification in a near-critical state, and supercritical

water gasification (de Vlieger et al., 2012; Kumar et al., 2018). During hydrothermal gasification, various products are produced, including CO₂, H₂, CO, CH₄, and minor amounts of C₂H₄ and C₂H₆ (Kumar et al., 2018). The specific type and quantity of products generated are influenced by the temperature and pressure conditions, which can significantly impact the efficiency and effectiveness of the process (Kumar et al., 2018). Hydrothermal gasification holds promise as a versatile and environmentally sustainable technology for converting biomass into valuable gases and products for renewable energy and resource recovery applications.

2.3.4.3. Hydrothermal Liquefaction

Hydrothermal liquefaction (HTL) is a method of converting biomass that takes place in a water-based environment, typically operating within a temperature range of 250-374 °C and a pressure range of 10-25 MP (Basar et al., 2021a; Lachos-Perez et al., 2022b). One of the primary benefits of the HTL process is its capability to handle biomass sources with elevated moisture content, without requiring a distinct drying phase (Basar et al., 2021a; Lachos-Perez et al., 2022b). This characteristic simplifies the process and reduces energy requirements compared to other methods.

HTL systems offer versatile capabilities for processing various substrates, making them suitable for direct fuel production and waste valorization (Basar et al., 2021a; Lachos-Perez et al., 2022b). The process's flexibility and efficiency make it particularly attractive for converting different types of biomass into valuable products, such as biofuels, bio-oils, and other high-value chemicals. Moreover, HTL operates at reduced reaction temperatures in contrast to alternative biomass conversion techniques, such as pyrolysis or gasification. This low temperature operation helps reduce the risk of corrosion in HTL reactors, improving the overall system durability (Basar et al., 2021a). Additionally, the compatibility of HTL with alkaline catalysts further enhances its applicability and opens opportunities for process optimization and product yield improvements. (Basar et al., 2021b; Lachos-Perez et al., 2022a). The synergy between HTL and alkaline catalysts promotes better reaction kinetics and allows to convert biomass into a wider array of valuable products.

The HTL process can convert biomass into a substance known as bio-crude within a time range of 1 to 60 minutes. Bio-crude is a liquid resembling petroleum and can be further refined

and utilized in petroleum refineries. This process takes advantage of water's unique properties as it stays in a liquid phase up to a temperature of 373.94 °C and a pressure of 220 bar (Yang, 2007). Additionally, at high temperatures, water exhibits a reduced dielectric constant, making it an effective solvent for various chemical reactions. The ability to adjust the process temperature allows for control over the dielectric constant of water, enabling precise manipulation of the hydrolysis process severity (Lachos-Perez et al., 2022a; Luong et al., 2015). During conditions of 20 °C, the dielectric constant of water is 80.1. However, as the temperature increases to 300 °C, the dielectric constant drops below 20 (Akerlof and Oshry, 1950; Basar et al., 2021a). This decrease in dielectric constant at high temperatures makes water a more effective solvent compared to widely employed solvents like ethanol, methanol, or acetone (Basar et al., 2021b).

The HTL process replicates the natural formation of fossil fuels from organic matter, a process that typically takes millions of years. While HTL offers the advantage of converting biomass into liquid bio-crude within a short timeframe, the resulting bio-crude is of lower quality compared to petroleum-derived crude oil, containing 8-20% oxygen (Basar et al., 2021b). To overcome this limitation, fuel upgrading techniques like hydrodeoxygenation can be employed to enhance the quality of bio-crude (Basar et al., 2021a). Moreover to bio-crude, the HTL process also generates hydrochar, HTL aqueous phase, and gas phase as co-products (Gollakota et al., 2018; Lachos-Perez et al., 2022b; Mathanker et al., 2020a).

The HTL process can be executed using either batch or continuous-flow systems, each having its own set of advantages and disadvantages (Gollakota et al., 2018). To understand the impact of the reactor type on bio-crude yield and quality, a study conducted by Biller et al. HTL experiments were compared under batch and continuous-flow configurations, operating at 350 °C (Biller et al., 2017). The results showed that the continuous-flow system produced a higher bio-crude yield of 44.3%, compared to the batch system's yield of 34.5%. The difference in yields was attributed to the reduced temperature achieved within the batch reactor, which reached only 340 °C, and the enhanced mixing achieved in the continuous-flow setup (Biller et al., 2017). Interestingly, the bio-crude generated in the continuous-flow system demonstrated higher energy recovery (Biller et al., 2016). This finding indicates that continuous-flow systems hold promise for maximizing the energy recovery potential of the HTL process, making them particularly appealing for large-scale applications where efficient bio-crude production and energy utilization are

essential. Overall, the choice of reactor type in the HTL process should be carefully considered, weighing factors such as yield, energy recovery, system complexity, and the scale of the application. As the technology continues to advance, a deeper understanding of the optimal reactor configuration for different biomass sources will further drive the commercial viability and widespread adoption of the HTL process as a sustainable and efficient biomass conversion technique.

Overall, the efficiency and adaptability of HTL demonstrate its potential as a promising biomass conversion technique. By effectively processing high-moisture biomass without pre-drying, HTL offers a simplified and energy-efficient solution for sustainable biomass utilization. As ongoing research and advancements continue, HTL is expected to play a crucial role in shaping a greener and more sustainable energy future.

2.4. HTL Reaction's mechanism

The HTL process encompasses three primary reaction pathways: depolymerization, decomposition, and repolymerization (Akhtar and Amin, 2011; Basar et al., 2021a; Lachos-Perez et al., 2022b; Mathanker et al., 2020a). Although the precise details of these reactions remain incompletely understood due to the complexity of organic compounds involved, research studies have shed light on some of the key pathways (Basar et al., 2021b). The selectivity of these reactions may differ based on factors such as pH, the intensity of the HTL process such as temperature, pressure, retention time, solvent type and concentration, as well as the catalyst used (Akhtar and Amin, 2011; Basar et al., 2021b; Lachos-Perez et al., 2022a).

The initial phase of the HTL process involves depolymerization (hydrolysis) reactions. In this step, lipids undergo a process that leads to the formation of fatty acids and glycerol, while proteins are broken down into amino acids, and carbohydrates are broken down into simple sugars, known as monosaccharides. At this stage, no substantial formation of bio-crude takes place. By controlling the operating conditions of the HTL process particularly during the depolymerization step, the resulting effluent becomes suitable for utilization in fermentation processes, leading to the production of various biofuels such as methane, hydrogen, and ethanol (Balat, 2008). The depolymerization reaction typically happen in the range of 150–250 °C (Basar et al., 2021b).

Upon hydrolysis, smaller molecules undergo a sequence of thermal transformations including dehydration, decarboxylation, decarbonylation, deamination, dehydrogenation, and various bond cleavages due to the elevated temperatures. Decomposition process for various types of compounds in HTL takes place within the temperature range of 180–340 °C (Basar et al., 2021a). During the HTL process, the initial decomposition initiates with carbohydrates at a temperature of 180 °C. As the temperature rises beyond 200 °C, proteins and lipids then commence their decomposition. To achieve the complete decomposition of proteins, a temperature of 300 °C is necessary, while lipids require a higher temperature of 640 °C for full decomposition (Chen et al., 2018). In the HTL process, achieving the maximum efficiency is contingent on striking the right balance in decomposition reactions since certain lipids, like long-chain fatty acids, are incorporated into bio-crude, obviating the need for their complete decomposition. It is crucial to maintain a level of HTL operating conditions that are sufficiently intense to facilitate the decomposition of organic compounds into bio-crude forming compounds, without being overly severe as to cause the breakdown of bio-crude into gases. This optimized balance ensures optimal results.

Bio-crude compounds are generated as a consequence of the recombination of diverse reactive fragments, which occurs at temperatures exceeding 300 °C (Déniel et al., 2016). The formation of bio-crude is facilitated by the generation of substantial large molecules in these reactions, while basic molecules remain in the liquid phase (Basar et al., 2021b; Déniel et al., 2016). The recombination reactions of long-chain fatty acids play a pivotal role in producing various organic molecule groups found in bio-crude, including aromatics, ketones, amides, amines, and esters. Additionally, the complex alcohol molecules present in bio-crude result from the hydration and cyclization reactions of alkenes (Basar et al., 2021a).

The Maillard reaction plays a crucial role in the HTL process, contributing significantly to the formation of biocrude (Peterson et al., 2010). This reaction involves the interaction between reducing sugars' carbonyl groups and amino groups present in amino acids, leading to the formation of nitrogenous polymers and melanoidins, key components influencing bio-crude production (Rebollo-Hernanz et al., 2019). Tang et al. observed that the optimal conditions for obtaining the highest bio-crude yield were at 280°C and a retention time of 60 minutes, using a protein to glucose mixture ratio of 3:1 (by weight). When carbohydrates or proteins were used

individually as substrates, the resulting bio-crude yield was below 10% and 20%, respectively, underscoring the importance of leveraging Maillard reactions to attain increased bio-crude production (Tang et al., 2019).

Lu et al. conducted a study to examine the impact of HTL on various model compounds, including soybean oil, soy protein, cellulose, xylose, and lignin (Lu et al., 2018). They investigated binary, ternary, quaternary, and quinary combinations of these compounds to indicate the effect of the substrate's composition on the HTL products (Lu et al., 2018). They found that the composition of the substrate significantly influenced the HTL products. The quinary mixture yielded the highest energy recovery, highlighting the significance of utilization of a well-balanced substrate in the HTL process to harness synergistic impact and optimize energy recovery (Lu et al., 2018). By leveraging such valuable insights and further exploring the interaction between different biomass components and formation pathways, researchers can advance the HTL technology.

2.5. HTL's products

2.5.1. Bio-crude

The primary fuel product derived from the hydrothermal liquefaction process is bio-crude, a liquid with a dark brown color. It is rich in hydrocarbons, making it a valuable source of energy (Lavanya et al., 2016; Sharma et al., 2019). Bio-crude is widely recognized as an appropriate and sustainable alternative to fossil fuels for energy generation (Lavanya et al., 2016). The composition of bio-crude consists of a variety of organic compounds including saturated fatty acids, hydrocarbons, heterocyclic compounds, oxygen containing compounds, and nitrogen containing compounds. The composition of these compound categories in bio-crude is greatly influenced by the proportion of carbohydrates, proteins, and lipids in the substrate, the HTL process parameters, and the technique used for bio-crude separation. (Basar et al., 2021b).

The bio-crude can be refined to produce various fuels such as gasoline, jet fuel, diesel, naphtha, fuel oil, and a heavier component suitable for engine lubricants (Badoga et al., 2020; Haider et al., 2018). Fuels derived from bio-crude can be considered eco-friendly. Furthermore, they possess a renewable and sustainable nature attributed to their biomass origin. (Badoga et al., 2020; Haider et al., 2018; Xu et al., 2018). Throughout the HTL process, the primary objective is to optimize the fuel quality, which involves maximizing carbon and hydrogen content while

minimizing the presence of oxygen and nitrogen. Bio-crude is expected to have a typical elemental composition consisting of approximately 60-78% carbon, 6-12% hydrogen, 2-6% nitrogen, 0-2% sulfur, and 8-20% oxygen (Basar et al., 2021b).

The higher heating value (HHV) is a crucial factor in assessing the quality of bio-crude. It can be determined through two methods: direct measurement using a bomb calorimeter or calculation using the Dulong equation (equation (1)). In this equation, the percentages of carbon (C), hydrogen (H), and oxygen (O) in the bio-crude are used to compute the HHV (Basar et al., 2021b; Mathanker et al., 2020a; Xu et al., 2018). At temperatures above 300 °C, bio-crude yield may decrease owing to recombination reactions. However, these reactions can simultaneously reduce the oxygen content of the bio-crude and enhance HHV (Basar et al., 2021b).

$$\text{HHV}(\text{MJ/Kg}) = 0.338\text{C} + 1.428(\text{H}-\text{O}/\text{C}) + 0.095\text{S} \quad (1)$$

Following the HTL process, the extraction of bio-crude can be accomplished using physical methods or solvents. The commonly employed approach, particularly in experiments using batch-fed HTL systems, includes dissolving the bio-crude in dichloromethane (DCM) and acetone, separating it via rotavap. The bio-crude, extracted from the liquid fraction, is commonly known as light oil or aqueous oil (AO). On the other hand, the viscous residue that adheres to the reactor's surface and is trapped within the biochar pores is referred to as heavy oil (HO). This heavy oil can be effectively extracted through the application of specific solvents. (Basar et al., 2021b; Mathanker et al., 2020a). However, according to the existing literature, HO typically exhibits a higher HHV than AO, and as a result, the majority of research studies have been centered around investigating heavy oil (Mathanker et al., 2020a; Niknejad et al., 2023). For instance, Ankit et al. conducted HTL experiments on corn stover using various temperature conditions (250, 300, 350, and 375 °C), initial pressures (300 and 600 psi), and retention times (0, 15, 30, and 60 minutes). The resulting HO derived from this process exhibited a considerably higher carbon concentration in comparison to the original feed material and AO. Among the experimental conditions tested, the one with parameters of 375 °C, 600 psi, and 15 minutes produced HO with the highest carbon weight percentage (76.32 wt%) and HHV of 35.13 MJ/kg (Mathanker et al., 2020a).

2.5.2. Hydrochar

As the HTL process takes place, it generates a solid residue called hydrochar, which results from recombination reactions involving compounds present in the aqueous phase and bio-crude. Hydrochar also contains insoluble inorganic substances. Similar to bio-crude, hydrochar possesses distinct properties that are affected by the feedstock used and the HTL process conditions (Chen et al., 2014; Lachos-Perez et al., 2022a). According to the literature, hydrochar has various potential applications. It can be directly used for energy generation through combustion, utilized as a soil amendment to improve soil quality and carbon sequestration, or activated for adsorption purposes. (Saqib et al., 2019). Hydrochar also possesses significant amounts of trace elements and phosphorus, that have the potential to be extracted and utilized for commercial applications (Papadokonstantakis et al., 2018). One of the requirements for promoting the sustainable advancement of HTL is the essential need to either find valuable uses for hydrochar or ensure its safe disposal (Basar et al., 2021b). As research in the field continues, exploring innovative and economically viable applications for hydrochar will be crucial to maximize its potential as a valuable byproduct of the HTL process.

2.5.3. Water soluble substance

Water soluble substance (WSS) or the aqueous stream of HTL contains a mixture of organic and inorganic residues. The primary types of organic compounds found in the WSS include carboxylic acids, alcohols, ketones, glycerol, aldehydes, phenolics, esters, ethers, amides, pyrazines, pyridines, and N&O-heterocyclic compounds (Biller et al., 2016; Leng et al., 2018; Yang et al., 2014). the aqueous phase of lignocellulosic biomass HTL was observed to possess a significant concentration of carboxylic acids, primarily attributed to the abundant presence of carbohydrates such as cellulose and hemicellulose in the biomass structure (Biller et al., 2017). The aqueous phase of HTL also exhibits elevated levels of ammonia concentration, primarily resulting from protein deamination reactions. Just like hydrochar, the aqueous phase of HTL can serve as a favorable medium for recovering nutrients (Basar et al., 2021b).

AD is an alternative approach for the utilization of the HTL aqueous stream. Nevertheless, as highlighted by Zhou et al., the HTL aqueous phase, with a COD of 104 g/L, can inhibit AD under mesophilic conditions (Zhou et al., 2015). In a study conducted by Chen et al., it was found that in upflow anaerobic sludge blanket systems receiving HTL aqueous feed at a rate of 2.5 g

COD/L/d, approximately 61.6% and 45% of the COD originating from HTL aqueous with a concentration of 10 gCOD/L were successfully digested under mesophilic and thermophilic conditions, respectively (Chen et al., 2020). They also highlighted that phenolic compounds, furans, and pyrazines cannot be effectively digested within an up-flow anaerobic sludge blanket system. However, it is worth noting that batch anaerobic reactors have demonstrated the capability to digest these compounds, at lower concentrations (Barakat et al., 2012; Monlau et al., 2014). Notably, the challenge of effectively utilizing WSS, particularly in AD processes, requires further investigation and optimization.

2.5.4. Gases

The gaseous components produced in HTL can arise from a multitude of intricate reactions, encompassing water-gas shifts, thermal cracking, denitrogenation, methanization, and deamination (Basar et al., 2021b; Lachos-Perez et al., 2022a). The predominant component of the gaseous phase is CO₂, which typically accounts for approximately 80-95% (Lachos-Perez et al., 2022a; Sánchez-Bayo et al., 2019). Figure 2.1 presents the typical composition of gases in HTL (Basar et al., 2021b). The gaseous phase of HTL can contain small amounts of light hydrocarbons, including ethane, ethylene, propene, isobutane, n-butane, 1-butane, isopentane, and 1-pentene (Marrone et al., 2018; Wagner et al., 2016). Although gas production during the HTL process has a lower HHV compared to bio-crude, at higher temperatures, a portion of bio-crude may be converted to gas due to cracking reactions (Niknejad et al., 2023; Xu et al., 2018; Yuan et al., 2009). Efforts to minimize gas formation and optimize bio-crude yield are crucial in advancing the effectiveness and economic viability of the HTL process.

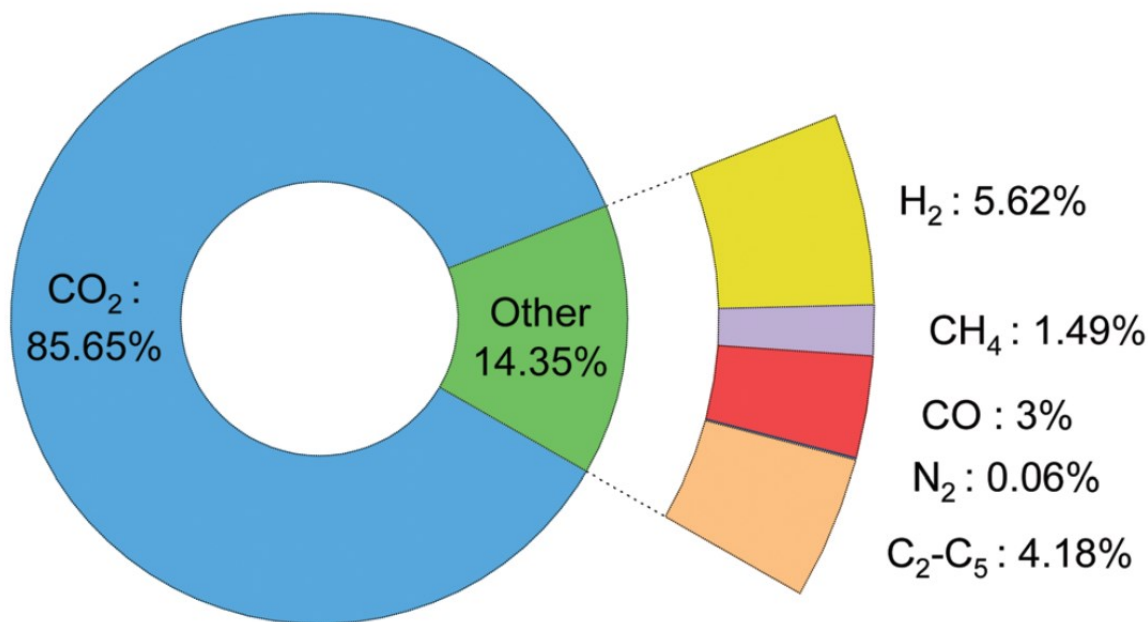


Figure 2.1. The gaseous phase composition during HTL at 350 °C (Basar et al., 2021b; Brown et al., 2010; Cherad et al., 2016; Jena et al., 2012)

2.6. Operating parameters affecting HTL

2.6.1. Reaction temperature

The temperature of the reaction is a critical parameter that significantly influences the HTL process. It plays a critical role in determining the reaction kinetics, product yields, and the composition of the resulting bio-crude, hydrochar, and gaseous products (Gollakota et al., 2018; Xu et al., 2018). In the HTL process, elevated temperatures enhance the solvency of water by reducing its dielectric constant, making it a highly effective solvent. This improved solvent capability enables water to hydrolyze organic substances and facilitate subsequent HTL reactions (Basar et al., 2021b; Mishra and Mohanty, 2020). During HTL, water functions as a catalyst because it undergoes dissociation into H⁺ and OH⁻ ions, which actively participate in the reaction (Lachos-Perez et al., 2022a; Mishra and Mohanty, 2020). After the hydrolysis process, higher temperatures induce decomposition and, under more extreme conditions, repolymerization reactions occur. To maximize the generation of bio-crude, it is essential to optimize the reaction

temperature for the purpose of reducing the occurrence of repolymerization reactions (Basar et al., 2021b).

The HTL process is commonly carried out within a temperature area of 250–374 °C (Basar et al., 2021a; Lachos-Perez et al., 2022a). The ideal temperature for HTL and the distribution of end products depend on the composition of the biomass being processed. By employing the appropriate catalyst type and quantity, it is possible to lower the temperature required for optimal bio-crude production (Basar et al., 2021b; Lachos-Perez et al., 2022a). The majority of research findings indicate that the optimal reaction temperature for HTL is below the critical point (≤ 374 °C) of water (Gollakota et al., 2018; Lachos-Perez et al., 2022a; Xu et al., 2018). When the temperature surpasses the critical point of water, the generation of bio-crude decreases as a result of syngas formation reactions and secondary cracking of the bio-crude (Mishra et al., 2018). Garcia Alba et al. conducted a study investigating the influence of HTL temperature on energy recovery from green algae (*Desmodesmus* sp.). The results showed that energy recovery of 60%, 67%, and 75% were achieved at temperatures of 325 °C, 350 °C, and 375 °C, respectively (Garcia Alba et al., 2012). Xu et al. explored the impact of HTL on the conversion of sewage sludge into biocrude and other products over a temperature range of 260-350°C. The findings revealed that higher temperatures led to an improvement in the quality of biocrude. Interestingly, as the temperature increased, both the biocrude production and the concentration of products in the liquid phase showed a rise, peaking at 340°C, and subsequently declined (Xu et al., 2018). This highlights the significance of temperature optimization in achieving optimal biocrude yield and product distribution during the HTL process.

2.6.2. Pressure

The HTL process operates within a pressure range of 10 to 25 MPa, allowing liquid water to remain in its liquid state until it reaches the critical point, thus minimizing energy losses associated with phase changes. While the combination of high temperatures and pressure already contributes to process efficiency, further increasing the pressure may not be cost-effective (Basar et al., 2021b; Lachos-Perez et al., 2022a; Peterson et al., 2008). Qian et al. found in their study that varying the pressure between 200 and 400 bar had no notable impact on bio-crude yield once the critical pressure of 221 bar was reached. This suggests that beyond the critical pressure, further adjustments to the pressure will not affect the production of bio-crude (Qian et al., 2017). On the

contrary, a study conducted by Sangon et al. focused on coal liquefaction employing a toluene-tetralin solvent and observed that elevating the pressure from 75 to 120 bar led to a 30% rise in the production of bio-crude (Sangon et al., 2006). To achieve optimal yields and process efficiency in HTL, careful consideration of pressure optimization is crucial, considering the specific feedstock and reaction conditions. Understanding the interplay between temperature, pressure, and other process parameters is essential for maximizing the production biocrude more cost-effectively.

2.6.3. Retention time

The retention time has an impact on various aspects of the hydrothermal process, including total conversion, biocrude yield, biochar, and gaseous products. Retention time refers to the duration the reactor is held at the final temperature once it has been reached, excluding the heating and cooling periods. The retention time in the HTL process is a crucial parameter that can significantly impact the outcomes, depending on the specific characteristics and composition of the feedstock (Mathanker et al., 2020a). While some studies suggest that longer retention times can potentially achieve effects similar to elevated temperatures, excessively extended retention times may lead to undesired outcomes, such as the conversion of bio-crude into hydrochar and coke. Therefore, while process severity is essential, it may not directly impact the quantity of biocrude produced (Basar et al., 2021b).

Mathanker et al. studied the effect of various retention times on product composition. They observed that with the increase in retention time from 0 to 15 minutes, the biocrude and gas fractions decreased, while the biochar content increased. However, beyond 15 minutes of retention time, both biochar and biocrude percentages started to decline, with a notable increase in the gaseous fraction. This indicates that longer retention times promoted oil decomposition and char formation. Table 2 presents a summary of HTL studies involving different biomass types, temperatures, and retention times, providing valuable insights into the impact of these parameters on the HTL process. Understanding these relationships will aid in optimizing HTL conditions to achieve desired product outcomes for various feedstocks.

Table 2.2. Investigation of HTL studies: effects of biomass types, temperatures, and retention times on process outcomes

Biomass type	Reaction temperature (°C)	Reaction time (min)	The highest bio-crude yield (wt%)	Ref.
Food waste	240-295	0-30	27.5% at 240 °C, 30 min	(Bayat et al., 2019)
Animal carcass	230 -350	10-80	55.6% at 320 °C, 60 min	(Yang et al., 2019)
Animal by-products	150-290	5-15	74% at 250 °C	(León et al., 2019)
Corn stover	250-375	0-60	42.61% at 300 °C, 0 min	(Mathanker et al., 2020b)
Secondary sewage sludge	260-350	10	22.9% at 340 °C	(Xu et al., 2018)
Mixed algae	260-340	30-90	8.4% at 300°C, 60 min	(Tian et al., 2015)
Domestic sewage sludge (DSS)	275-350	15-60	22% at 350°C, 30 min	(Mishra and Mohanty, 2020)
Microwave pretreated municipal sludge	340	30	35.4%	(Chen et al., 2019)
Dried sewage sludge	250-400	60	52% at 350 °C	(Badrolnizam et al., 2019)
Spend coffee grounds	200-300	5-30	35.29% at 275 °C, 10 min	(Yang et al., 2016)

2.6.4. Type of solvent

The HTL process facilitates the application of various solvents instead of water. Through the utilization of solvents like alcohol or acetone, it becomes feasible to attain supercritical conditions at reduced temperatures. Ethanol, methanol, isopropanol, and acetone are common solvents employed in the HTL process, each having critical points at 241 °C, 240 °C, 235.6 °C, and 235 °C, respectively (Basar et al., 2021b). While using different solvents may allow for improved hydrolysis conditions, it is not feasible to leverage the catalytic effects of water ions (H^+ and OH^-) at elevated temperatures (Basar et al., 2021b). Incorporating solvents in conjunction with water as co-solvents can be a beneficial approach to maximize the bio-crude production (Basar et al., 2021b; Zhang et al., 2020). Furthermore, the utilization of solvents prevents repolymerization reactions and enhances the stability of bio-crude throughout the process (Feng et al., 2018).

As the HTL conditions become more severe, the influence of solvents on HTL outcomes decreases. When considering bio-crude yield, solvents can be ranked from most to least effective as acetone, isopropanol, ethanol, and methanol. In general, organic solvents demonstrated greater effectiveness when used as co-solvents, while the using of pure solvents led to either a reduction in bio-crude yield or a negligible increase. Conversely, no significant alteration in the HHV of bio-crude was observed when different solvents were employed. It is important to note that the influence of solvents on HTL results varies depending on the composition of the substrate (Basar et al., 2021b). Nevertheless, it should be noted that using solvents instead of water may raise cost considerations in the HTL process.

2.6.5. HTL's catalyst

The HTL process is well-suited to the utilization of different types of catalysts. By utilizing the appropriate catalyst type and concentration, it is possible to decrease the necessary temperature and pressure for HTL while simultaneously increasing the production of bio-crude. (Dimitriadis and Bezergianni, 2017; Mishra et al., 2018). However it is important to acknowledge that the impacts of catalysts are specific to the type of substrate being used, as they work by modifying the reaction kinetics (Basar et al., 2021b). This effect is exemplified in the research conducted by Shakya et al., where they investigated the catalytic influence of Na_2CO_3 on three distinct microalgae species at a temperature of 350 °C. The research findings indicated that bio-crude production declined for *Nannochloropsis* sp., increased for *Pavlova* sp., and remained unaffected for *Isochrysis* sp. This demonstrates how the presence of Na_2CO_3 catalyst can have varying effects on different microalgae species in terms of bio-crude

production (Shakya et al., 2015). As researchers continue to explore and optimize the utilization of catalysts in the HTL process, a deeper understanding of their interactions with different feedstocks will contribute to the advancement of more efficient and tailored HTL systems for biomass conversion.

Chapter 3

Biodegradability and transformation of biodegradable disposables in high-solids anaerobic digestion followed by hydrothermal liquefaction

A version of this chapter was published in Resources, Conservation & Recycling; 193 (2023) 106979.

3.1. Introduction

The immense use of plastic products and their improper management has led to severe plastic pollution across the globe (Na et al., 2021). Reportedly, over 300 million tons of plastics are produced annually worldwide, and about 13 million tons are disposed of into the environment (Enfrin et al., 2019b). Almost 90% of plastics are derived from fossil fuels, accounting for 6% of worldwide oil consumption (Cucina et al., 2022b; Matthews et al., 2021). These fossil fuel-derived plastics are chemically stable and typically not biodegradable; therefore, they can accumulate and potentially persist in our ecosystem (Enfrin et al., 2019b). Thereby, bioplastics emerged as an environmentally friendly alternative to traditional fossil fuel-derived plastics (Cucina et al., 2021a).

Bioplastics are biodegradable or bio-based materials that are supposed to degrade naturally in the environment in a few years (Cucina et al., 2022b). The transition toward bioplastic and paper-based biodegradable disposables has emerged from recent directives banning single-use plastics in many countries worldwide (Cucina et al., 2021a). Nowadays, the fraction of biodegradable disposables in waste streams is increasing, especially in municipalities without residential source separated programs (Cucina et al., 2021a; Pereira de Albuquerque et al., 2021). Disposable bioplastics can be commingled with the organic fraction of municipal solid wastes (OFMSW) and pose substantial issues during waste management processes like biological processes (Cucina et al., 2021a). It should also be emphasized that the standards at which these bioplastics have been certified do not necessarily correlate with the conditions of biological processes (i.e., composting and anaerobic digestion (AD)) utilized to treat OFMSW (Cucina et al., 2021a). For instance, a recent study revealed that bioplastics might not be fully degraded during the typical operating time frame of the composting process, and a longer time is required (Ruggero et al., 2020). Another study suggested that bioplastics would degrade up to 27% (wet basis) in AD, but degradability would vary depending on their

composition (e.g., starch, polylactic acid, etc.) (Cucina et al., 2022b). Therefore, the vast presence of biodegradable disposables in the waste stream may become an increasing issue.

High-solid anaerobic digestion (HSAD) has attracted considerable attention due to its distinct advantage of diverting OFMSW from landfills (de Albuquerque et al., 2022). The key benefits of using HSAD (total solids (TS) greater than 15%) are less water consumption, less heating costs, the ability to handle heterogeneous feedstock and higher organic loading rates, and no requirement of advanced dewatering technologies for digestate before land application (Dastyar et al., 2021c, 2021b). However, limited information is available in the existing literature on the fate of biodegradable disposables and their degradation in HSAD. For instance, if biodegradable disposables only undergo partial degradation during HSAD, they may still be present in large amounts in the final digestate and can be released into the environment through the agricultural use of land application of digestate (Karamanlioglu et al., 2017). Thus, their post-processing may be required before the final disposal of HSAD residuals. However, due to the presence of dissolved organic matter and very high carbon content, digestate might have a very high energy value which needs to be valorized by thermochemical biomass processing methods like hydrothermal technologies (Sharma et al., 2022).

Hydrothermal Liquefaction (HTL) is as a promising process for valorizing wet organic wastes and converting macromolecules into biocrude oil by avoiding the energy-intensive drying process (Lachos-Perez et al., 2022b; Ni et al., 2022). The principal reaction agent in the HTL process is water, and the typical operating temperature range from 250 to 370 °C with a residence time of 10-60 mins (Lachos-Perez et al., 2022a; Posmanik et al., 2017). This operating condition enables water self-ionization of molecules, leading to the release of H^+ and OH^- (Lachos-Perez et al., 2022b). Consequently, due to the catalytic effect of these ions, self-ionization enhances feedstock decomposition and fractionation. In recent years, several studies investigated the valorization of digestate of AD with the HTL process, which suggested that digestate characteristics would significantly influence the yield and chemical characteristics of biocrude (Posmanik et al., 2018; Sudibyoy et al., 2022). However, an extensive literature review by the authors revealed that there had been no reports on the HTL of HSAD digestate that includes undegraded biodegradable disposables.

Considering these research gaps, this study systematically examined the biodegradability and transformation of biodegradable disposables in an integrated process of HSAD followed by HTL. First, the anaerobic biodegradability of three different biodegradable disposables, including compostable kitchen bags for food waste bin liners, plant-based compostable utensils, and a mixture of paper-based disposables (coffee cups, paper plates, and straws), was assessed

in mesophilic HSAD. Second, the residuals (digestate) from HSAD were utilized as a feedstock for HTL (280 and 350°C) process. HTL was selected over other thermochemical conversion processes, such as pyrolysis and gasification, due to the high moisture content of the digestate, as pre-drying feedstock (digestate) would be practically questionable due to high costs (Lachos-Perez et al., 2022b; Ni et al., 2022). A detailed characterization of the chemical properties of HTL products was conducted to understand the transformative potential of undegraded biodegradable disposables in HSAD residuals and the quality of the final products. Based on our knowledge, this study first reports the impact of various biodegradable disposables on the HSAD process and examines a process scheme combining HTL to manage and valorize digestate containing undegraded disposable items.

3.2. Material and Methods

3.2.1. High-solids anaerobic digestion experiments

Solid inoculum (dewatered anaerobic digester sludge or biosolids) was obtained from the Edmonton Waste Management Centre (EWMC) in Edmonton, Alberta, Canada. Liquid inoculum (mesophilic anaerobic digester sludge) was collected from the Gold Bar Wastewater Treatment Plant in Edmonton, Alberta, Canada. Three different biodegradable/compostable disposable items were used as feedstocks: compostable kitchen bags for food waste (source-separated organics) bin liners, plant-based compostable utensils, and disposable paper items with plastic linings (mixture of paper coffee cups, paper plates, and paper straws). Both solid and liquid inoculum were acclimated at 37°C for seven days before the experimental set-up for acclimation of microbial communities and residual organics degradation. The characteristics of solid inoculum, liquid inoculum, and feedstocks are summarized in Table 3.1. For assessing the anaerobic biodegradability of disposable items, 1 L lab-scale anaerobic bioreactors with a working volume of 750 mL and 250 mL headspace were used. Before the start-up, the acclimated solid inoculum (TS: $23.84 \pm 0.24\%$) was mixed with acclimated liquid inoculum (TS: $3.65 \pm 0.16\%$) to maintain a TS content $>15\%$, which is typical for HSAD. The experiments were conducted at the food-to-microorganism ratio (F/M) of 0.5 (g VS feedstock/g VS inoculum). Feedstocks were prepared by cutting materials into approximately 1 cm \times 1 cm squares and then added to the inoculum. After adding feedstocks and inoculum, N₂ gas was purged to create an anaerobic environment inside the reactors. Each reactor contained a mechanical mixer equipped with an electrical motor to mix continuously at 200 rpm during the experiment. The reactors were placed in a water bath (20 L General Purpose Water Bath, PolyScience, Illinois, USA) set at a mesophilic temperature (37 \pm 2 °C). The gas outlet of each

reactor was connected to an individual bottle containing an absorption solution (3 M NaOH solution + thymolphthalein pH indicator) to capture acidic gases such as carbon dioxide and hydrogen sulfide from the biogas (Mohammad Mirsoleimani Azizi et al., 2021a). Then, methane gas was collected in 1 L gas bags, and volume was measured daily using a glass syringe. Control digester bottles were loaded with only inoculum to determine the methane generation from the inoculum. The duration of the experiment was 45 days. All BMP tests were completed in triplicates to verify the results.

Table 3.1. Characteristics of inoculum and feedstocks.

Parameter	Solid Inoculum	Liquid Inoculum	Compostable Plastic Bags	Plant-based Utensils	Paper-based disposables
Moisture Content (MC)	76.16 ± 0.24%	96.35 ± 0.16%	0.33 ± 0.10%	0.74 ± 0.02%	4.61 ± 0.08%
Total Solids (TS)	23.84 ± 0.24%	3.65 ± 0.16%	99.67 ± 0.10%	99.26 ± 0.02%	95.39 ± 0.08%
Volatile Solid (VS)	12.31 ± 0.26%	2.23 ± 0.50%	81.39 ± 0.06%	70.55 ± 0.09%	89.67 ± 0.79%

3.2.2. Hydrothermal liquefaction experiments

After completing the HSAD tests, digestates were further used as feedstocks for the HTL experiments. The HTL tests were conducted with a 250 mL batch hydrothermal reactor (Parr 4843, T-316 SS, Max. pressure: 5000 psi, Max. temperature: 500°C, Parr Instruments Company, Moline, IL, USA). For each HTL experiment, about 150 mL of digestate was added. After sealing the reactor, N₂ gas was purged for a leak test. The digestate was stirred constantly throughout the process using a mechanical stirrer connected to the electric motor. Also, the reactor was equipped with a thermocouple connected to a control box to monitor the digestate temperature, a gas inlet line to purge nitrogen, a gas outline line to collect the generated gas produced during the HTL process, and a pressure gauge. A heating jacket covering the entire reactor was used to heat the reactor to the desired temperatures. The experiments were performed at two different temperatures of 280°C and 350°C at a retention time of 10 min. After this exposure period, chilled water was recirculated in the designated tubes to cool down the reactor temperature.

After completing each HTL test and cooling the reactor, gas samples were collected in gas bags for gas composition analysis. The reactor was then opened, and contents were

recovered and separated. The aqueous content was filtered on a Buchner funnel using Whatman filter paper using a vacuum pump. Also, the solids in the mixture tend to stick at the bottom of the reactor, which was recovered via washing with acetone (99.5% purity, Fisher Chemicals). Then, the mixture of acetone and sticky content was filtered. The solid residue from the acetone wash and the aqueous phase was washed once more to extract all trapped oils in the pores (Mathanker et al., 2020b). The remaining solids were dried at 70°C overnight; thus, the final residue or hydrochar (HC) was collected. Finally, the water from the aqueous phase and acetone from the acetone phase was removed using rotary evaporation under a vacuum to recover biocrude.

3.2.3. Analytical methods

The TS, volatile solids (VS), and moisture content (MC) were measured using standard methods [24]. All analyses were conducted in triplicates, and average values were reported here. Multiple gas samples were taken throughout the experiment and injected into gas chromatography (7890B, Agilent Technologies, Santa Clara, USA) equipped with thermal conductivity detection (TCD) to determine the gas composition and to verify that pure methane was collected in gas bags. ATR-FTIR (which uses germanium-tipped ATR) spectroscopy was utilized to analyze chemical groups found on the surface of the feedstocks before and after the 45-days of the mesophilic HSAD experiment. In addition, FTIR spectroscopy (FTIR Perkin-Elmer 2,000 spectrophotometer) was performed for the initial inoculum and final digestate in the control sample. Based on the wavenumber, different function group associated with each sample was identified based on the literature (see Table A-1).

The composition of heavy oil from HTL was analyzed using gas chromatography (Agilent GCD G1800A). The column used for the analysis was a DB-5MS 25m x 0.25mm, DF 0.25um. For the sample preparation, dichloromethane was used as a solvent to dissolve a small amount of the sample. Afterward, the mixture was micro-centrifuged, and the supernatant was filtered using a 0.2 µm PTFE filter. 1 µL of the sample for GC analysis was used and injected in split mode (50:1) with a carrier gas (Helium). The column heating in GC started at 40°C for 5 min and then at a heating ramp of 5°C /min reached 170°C for 5 min and eventually at the same ramp heated up to 280°C for 5 min. The NIST library for mass spectra was utilized to identify probable compounds in each sample. The composition of the gas (CH₄, H₂, and CO₂ content) collected from the HTL tests was analyzed using gas chromatography (7890B, Agilent Technologies, Santa Clara, USA) equipped with a thermal conductivity detector (TCD) and two

columns (Molsieve 5A 60/80 mesh and Hayesep N 80-100 mesh). FTIR (Perkin-Elmer 2,000 spectrophotometer) analysis was performed to determine the functional groups of HC and biocrude.

3.3. Results and Discussion

3.3.1. Anaerobic biodegradability of biodegradable disposables

Figure 3.1 shows the cumulative methane production profile for the different experimental conditions. The cumulative methane yield from the control after 45 days of batch incubation was 58.1 ± 2.94 mL/g VS. Interestingly, methane generation in control started on the first day without any noticeable lag phase. However, paper-based disposables showed 2.63 times higher methane production than the control, indicating that these items can be anaerobically degraded in HSAD. However, until the first 15 days of digestion, methane production from paper-based feedstocks was slightly lower than the control. In addition to slow hydrolysis, paper-based products might introduce mass transfer limitations during the initial phase. Moreover, the digester fed with paper-based disposables showed three distinct methane production profiles between days 0-15, 16-24, and 30-36. This might be attributed to the differences in hydrolysis or degradation kinetics of different macromolecules associated with the three specific paper-based disposables, i.e., coffee cups, paper plates, and paper straws. For instance, the degradability of paper wastes can be influenced by cellulose, hemicellulose, and lignin contents (Li et al., 2020). Nonetheless, the paper-based disposables were ultimately degraded in HSAD and led to higher methane production than the control.

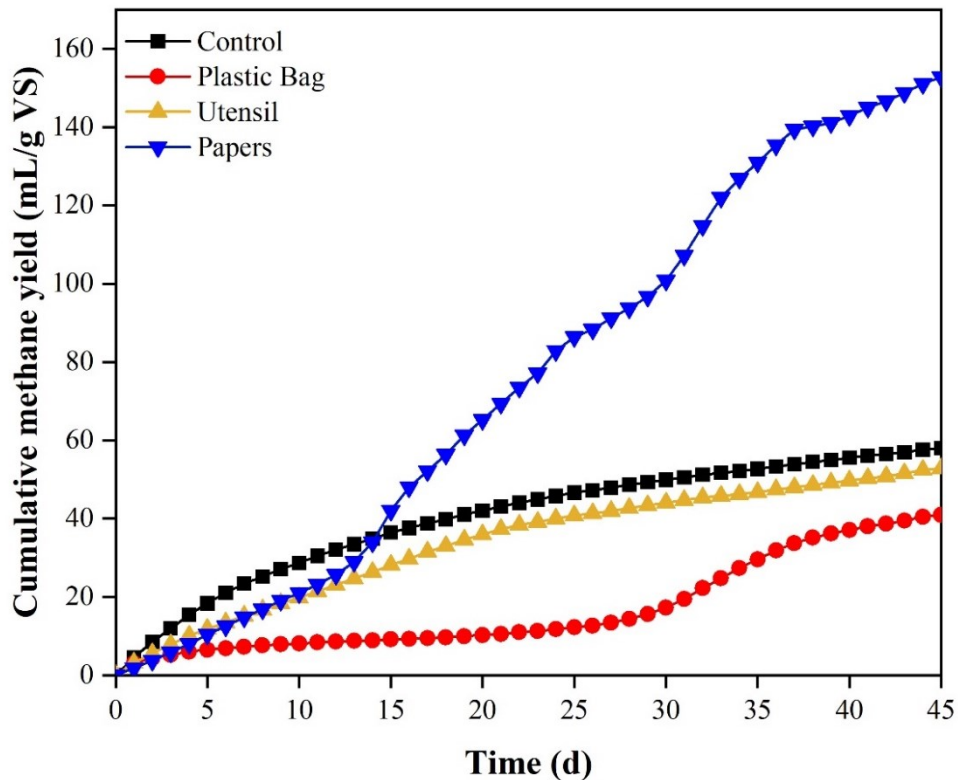


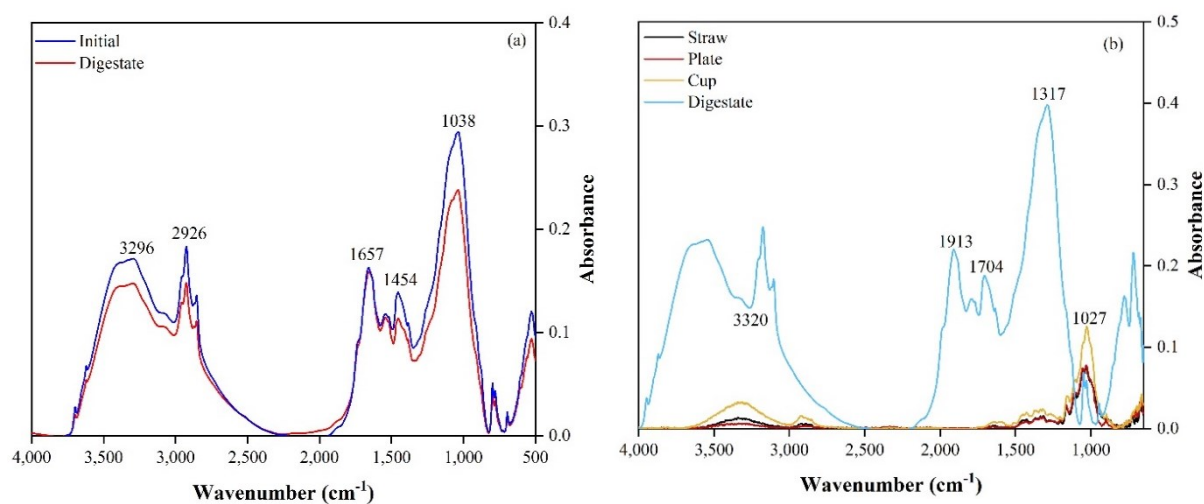
Figure 3.1. Cumulative methane yield for different feedstocks.

In contrast, compostable plastic bags as feedstock reduced the cumulative methane yield by 29.5% compared to the control with an extended lag phase of 26 days (Figure 3.1). This inhibition in methane generation and extended lag phase could be attributed to the partial degradation (discussed later) and leaching of toxic additives from plastic bags leading to restraining the activities of key enzymes of anaerobic microbes in AD (Mohammad Mirsoleimani Azizi et al., 2021b; Mohammad et al., 2022). Also, the presence of plastic bags may also cause mass transfer limitations in the digester and decrease methane production (Ahn and Chang, 2021). Their presence can create a physical barrier for the microorganism to access the organic matter for degradation (Abraham et al., 2021; Lallement et al., 2021; Mu et al., 2018). Such limited substrate availability can reduce the overall biodegradation rates. Furthermore, the compostable utensils produced 8.99% (52.85 mL/g VS) lower methane than the control. However, it can be noted that methane production followed a similar trend to that of the control, and no extended lag phase was observed. Analogous to plastic bags, the utensils also suppressed methane production. However, less inhibition than plastic bags might be related to the less mass transfer limitations and minor release of toxic additives from utensils. Our findings align with Cazaudehore et al., who reported that bioplastics have low biomethane

potentials when undergoing mesophilic anaerobic digestion (Cazaudehore et al., 2021). Battista et al. also found that starch-based bioplastics and polylactic acid (PLA)-based materials did not degrade significantly even after 250 days of anaerobic digestion (Battista et al., 2021). Overall, our results showed that not all biodegradable disposables available in the market could be efficiently degradable in AD. Paper-based disposables can be degraded and contribute to methane generation, whereas compostable plastic bags and utensils can suppress methane generation.

3.3.2. FTIR analysis of digestate

Figure 3.2 illustrates the FTIR spectrum of initial and final samples under different experimental conditions. The difference in the intensities indicates changes in functional groups and the solubilization of particulate macromolecules. Notably, each peak at a different wavenumber could be associated with a distinct functional group (Mohammad et al., 2022). Table A-1 listed the wavenumber and the associated functional group for each sample. For the control, peaks occur at the same wavelengths when comparing initial and final control samples (Figure 3.2a). However, a significant reduction in the intensity in the final sample was observed indicating the conversion of organic compounds (protein, carbohydrates, and lipids) to biomethane.



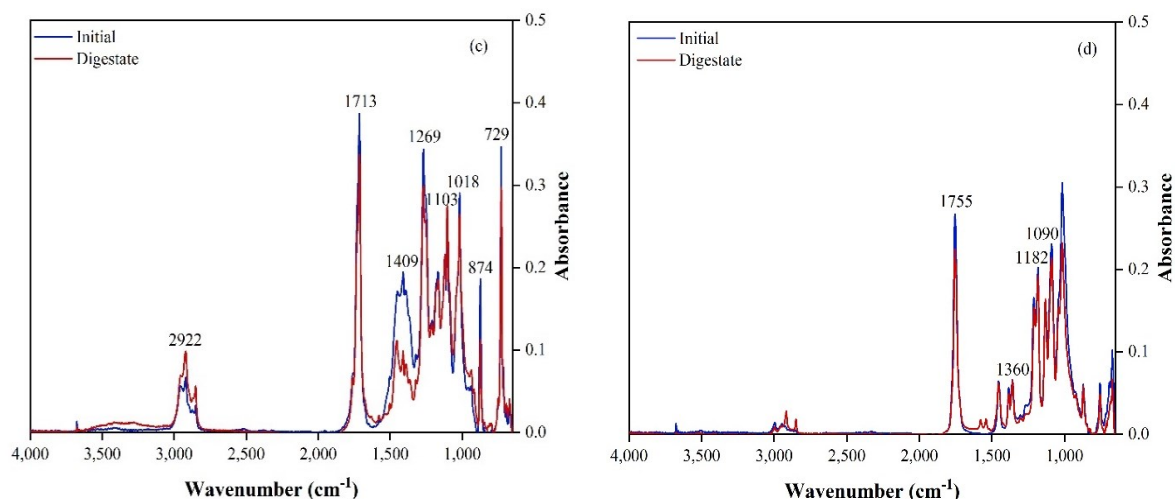


Figure 3.2. FTIR spectra of initial feedstocks and digestate from HSAD: (a) control, (b) paper-based disposables, (c) compostable plastic bags, and (d) plant-based utensils.

Moreover, Figure 3.2b shows the comparison between the FTIR spectrum of the raw paper-based products and digestate from the corresponding reactors. As demonstrated in Figure 3.2b, paper straws, plates, and cups, all displayed quite a similar spectrum with different intensities. The results indicated some shifts in the position and intensity of each peak after digestion. Although no paper-based feedstock was physically evident in the digestate after day 45, FTIR spectra showed that undegraded feedstock remained in the final digestate, which increased the intensity of the peaks of the FTIR.

Figure 3.2c represented ATR-FTIR spectra of initial plastic bags and the plastic bags collected from the digestate. Notably, comparing the initial and final spectrum, it can be inferred that most of the peaks occurred at the same wavenumber and minimal change in intensity occurred. However, a significant reduction in the absorbance and shifts in the peaks were observed in $1,400\text{-}1,500\text{ cm}^{-1}$ for the plastic bag sample after anaerobic digestion, which could be associated with the calcite form of calcium carbonate in biodegradable plastics (Patnaik et al., 2020b, 2020a). A previous study also suggested that calcite would be biodegradable (Kumar et al., 2010). Nonetheless, overall, minimal degradation of the plastic bags occurred during the 45 days of anaerobic digestion.

As shown in Figure 3.2d, most of the FTIR peaks for utensils and plastic bags were quite comparable, with some shifts in the position and intensity of the peaks. Analogous to plastic bags, spectrum of utensils exhibited a slight variation in the intensity of absorbance for initial

feedstock and utensil after anaerobic digestion, indicating that utensil feedstocks might have been minimally degraded.

3.3.3. Hydrothermal liquefaction of digestate

3.3.3.1. Product distribution

Figure 3.3 shows product yields from different digestate samples. The feedstocks were converted to HC, gases, biocrude, and water-soluble substances (WSS). With the increase in the temperature from 280 to 350°C, biocrude and gas yields increased, whereas HC and WSS percentages decreased which is consistent with previous studies (Xu et al., 2018). Thus, it can be inferred that temperature improved the conversion rate of feedstocks. Higher gas production at a higher temperature could be related to the reduction in the water dielectric constant, which can improve the solubility of organic compounds in the aqueous phase and promote gas production (Balagurumurthy et al., 2015; Lachos-Perez et al., 2022a). However, in most cases, the total gas yield was less than biocrude (8.4%-14.3%), which is desirable since biocrude has higher energy content (Xu et al., 2018). The highest biocrude yield at 280 °C (22.3%) was achieved for plastic bags. However, by further increasing HTL temperature to 350 °C, up to 32.86% of biocrude was attained in the utensil sample, which was almost 11% higher than that achieved at 280 °C. Also, high WSS contents in samples (22-33%) indicate the presence of a large amount of inorganic salts in the aqueous phase and the transfer of a considerable amount of organic matter into the water-soluble phase.

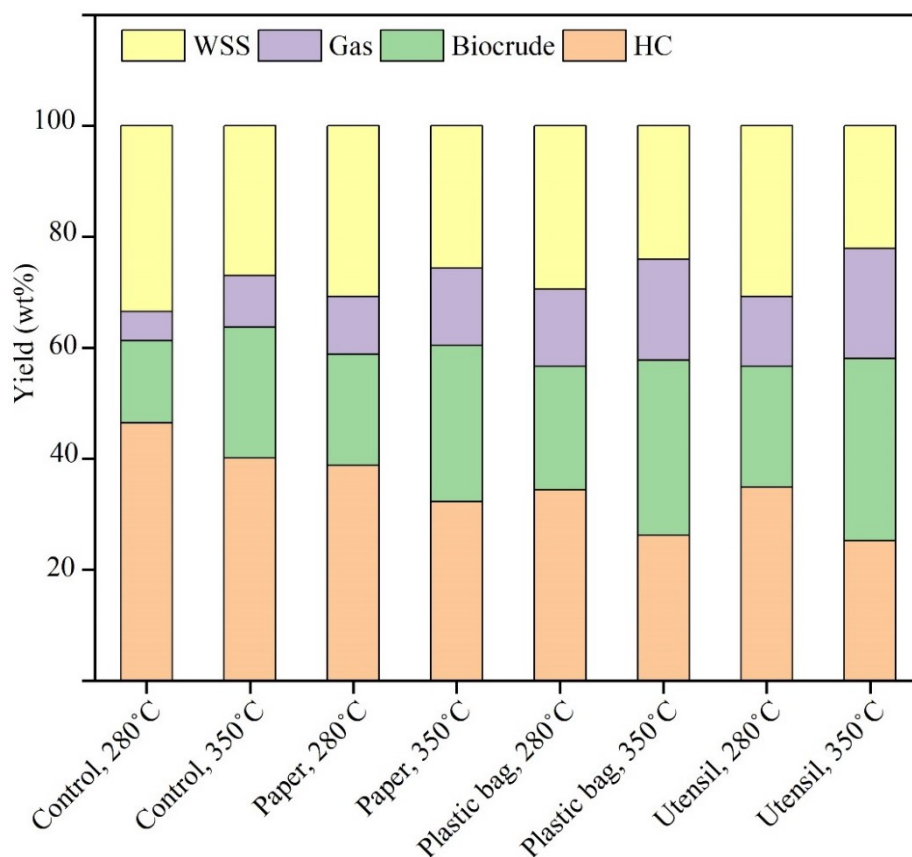


Figure 3.3. Product yields from different digestate samples in HTL at 280 and 350°C.

3.3.3.2. Biocrude composition

To grasp a better understanding of the molecular composition of biocrude, GC-MS analysis was performed. The detailed results, including retention time, compounds name, and peak area percent, are provided in Table A-2. GC-MS results indicated several compounds for each condition, and those compounds with an area of less than 0.75% were not considered here. Afterward, compounds were categorized based on the functional groups and presented in Figure 3.4. Based on GC-MS results, biocrude is classified into N-containing compounds (nitrogen and oxygen-heterocyclic compounds, amides), hydrocarbons (alkane and alkene), and oxygenated compounds like ketones, alcohols, acids, esters, carboxylic acid, and ethers. Due to the complex nature of the digestate (i.e., sludge + undegraded biodegradable disposables) used in this study, it is hard to specify the precise pathways of the formation of these compounds. Nonetheless, for each compound, different pathways can be involved. For instance, amides and N-containing compounds like dodecane amides or octadecane amides can be formed via decarboxylation, deamination, dehydration, and protein decomposition reactions (Ayaz A. Shah et al., 2020; Xu et al., 2018). Some heterocyclic compounds like pyrimidine, furan, pyrrole, and

indole can form via the Maillard reaction, which occurs when amino acids from the proteins chemically react with polysaccharides (Zhang et al., 2021). Moreover, phenolic compounds, such as epicholestanol, 3-pyridinol, and 2,4-di-tert-butylphenol, can be produced from cellulose by dehydration, hydrolysis, and ring closure reaction (Ayaz A. Shah et al., 2020; Xu et al., 2018). Similarly, the ketones like 2-hexadecanone, 8-pentadecanone, and 2-dodecanone can be produced from cellulose by cyclization and hydrolysis (Ayaz A. Shah et al., 2020). Fatty acids, including hexadecanoic acids, pentadecanoic acids, and tridecanoic acids, can be produced from lipid hydrolysis (Ayaz A. Shah et al., 2020). Hydrocarbons like tetradecane, 1-heptadecene, and hexadecane can form via the decarboxylation of fatty acids.

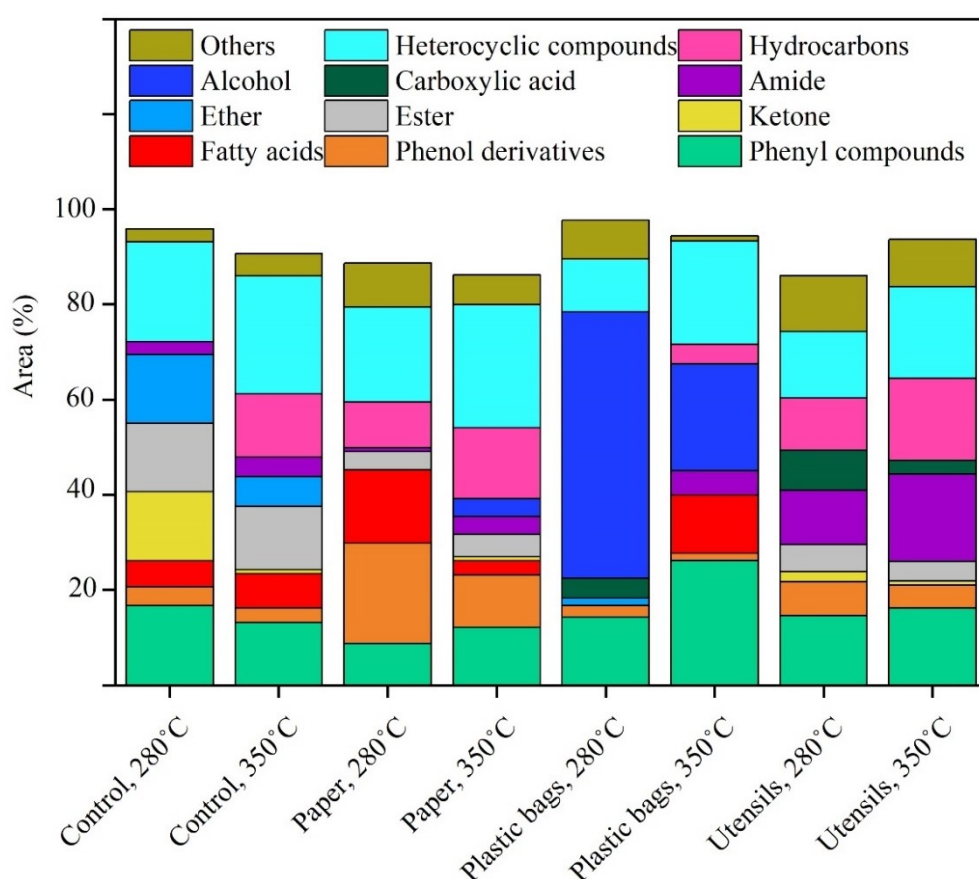


Figure 3.4. GC–MS analysis results for biocrude from different HTL test conditions.

As shown in Figure 3.4, with the increase in temperature, N-containing compounds (amide and heterocyclic compounds) increased. In contrast, oxygen-containing compounds like ketone, aldehydes, and alcohols decreased for most samples. For instance, 11.39% amide was detected in utensils containing digestate at 280 °C, which increased up to 18.25% at 350°C. This might be attributed to deoxygenation, decarboxylation, dehydration, and decarbonylation

reactions at higher temperatures (Wu et al., 2017). Also, hydrocarbon content in all samples increased with the increase in temperature. For instance, 10.9% of hydrocarbons was achieved in the HTL of utensils containing digestate at 280 °C, which increased to 17.23% at 350°C. Based on the literature, hydrocarbon compounds with higher C and H can have higher HHV (Xu et al., 2018). Thus, increasing the HTL temperature from 280 to 350°C could promote the biocrude quality with higher HHV. As shown in Figure 3.4, at both 280 and 350 °C, the hydrocarbon percent in utensils containing digestate is higher compared to other samples indicating that the quality of biocrude produced from this feedstock could be higher. On the other hand, plastic bags containing digestate demonstrated the lowest hydrocarbon percent compared to other samples. Overall, the GC-MS results demonstrated that biocrude had a significant amount of N and O-containing cyclic compounds, which would require further upgrading by deamination, decarboxylation, and dehydroxylation processes (Ayaz A. Shah et al., 2020; Xu et al., 2018).

3.3.3.3. Gaseous products

The gaseous products in HTL may originate from various complex reactions, including water-gas shifts, thermal cracking, denitrogenation, methanization, and deamination (Lachos-Perez et al., 2022b). Figure 3.5, shows the characteristics of gaseous products for different samples at 280°C and 350°C. The results indicated that CO₂ with 89-98% was the most dominant for all conditions, which could be attributed to the decarboxylation reaction under hydrothermal conditions (Xu et al., 2018). A high CO₂ content as a gaseous product from HTL is consistent with previous studies (Huang et al., 2013; Xu et al., 2018). Also, 1.6-5.9% of methane was detected in the gaseous analysis. H₂ (~5%) was only detected for the digestate from HSAD operated with paper-based disposables. Previous studies also reported low methane and hydrogen content in the gaseous product of HTL (Lachos-Perez et al., 2022b). However, with the increase in temperature from 280°C to 350°C, a slight increase in CH₄ was observed, which might be attributed to the cracking of high molecular hydrocarbons or decomposition reactions by free radicals, which happens close to the critical point temperature (340 and 350 °C) (Basar et al., 2021b; Xu et al., 2018). These results align with the findings from the research conducted by Xu et al., which showed that by increasing the HTL operating temperature from 260°C to 350°C, the CH₄ mol% can increase from 0.2 to 1.2 (Xu et al., 2018).

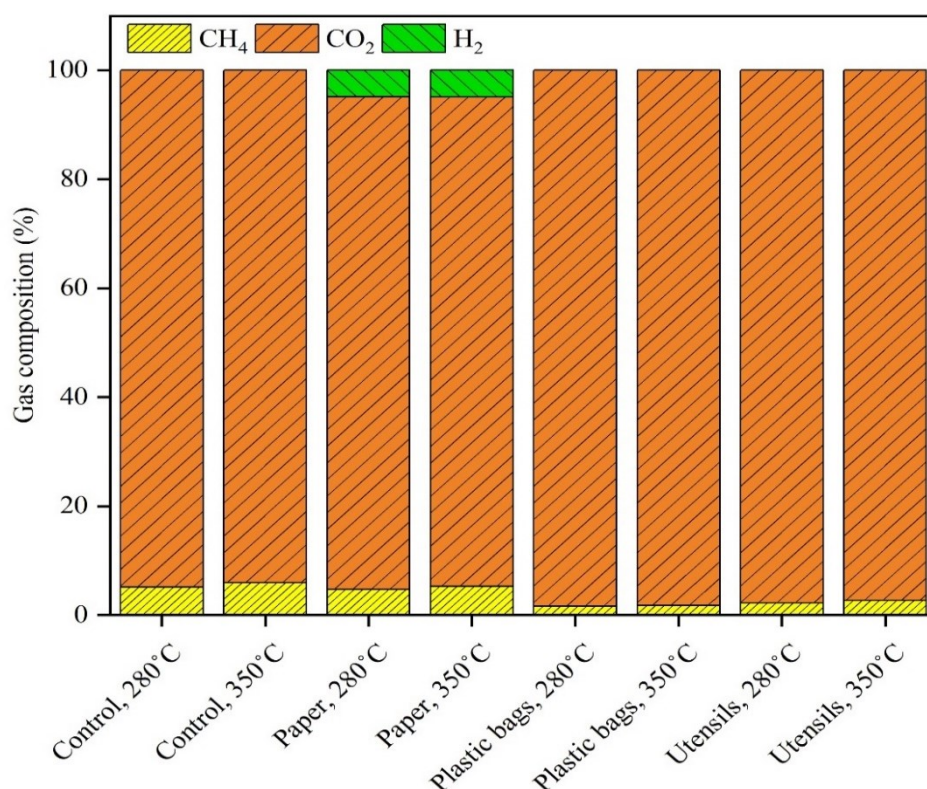


Figure 3.5. GC–TCD analysis results for gaseous products from different HTL tests.

3.3.3.4. FTIR spectra

Figure 3.6 shows the FTIR results for HC and biocrude from different conditions. The FTIR spectrum of control after HTL indicates that temperature significantly influenced the characteristics of HC and biocrude (Figure 3.6a). All of the peaks noticed in digestate (see Figure 3.2a) decreased in HC. Moreover, the intensity of different peaks in HC at 350°C was less than 280°C, indicating higher temperature led to a higher degradation of different functional groups in digestate samples. Also, the FTIR spectrum of biocrude showed two intense peaks at 1600-1700 cm^{-1} and 2,800-3,000 cm^{-1} . It can be inferred that biocrude contains a high amount of aliphatic methylene groups (with asymmetrical and symmetrical C-H stretching vibrations) and esters (Xu et al., 2018; Xu and Savage, 2014). Also, the sharp band in the range of 1400-1500 cm^{-1} could be due to the presence of some aromatic compounds in the biocrude (Xu et al., 2018).

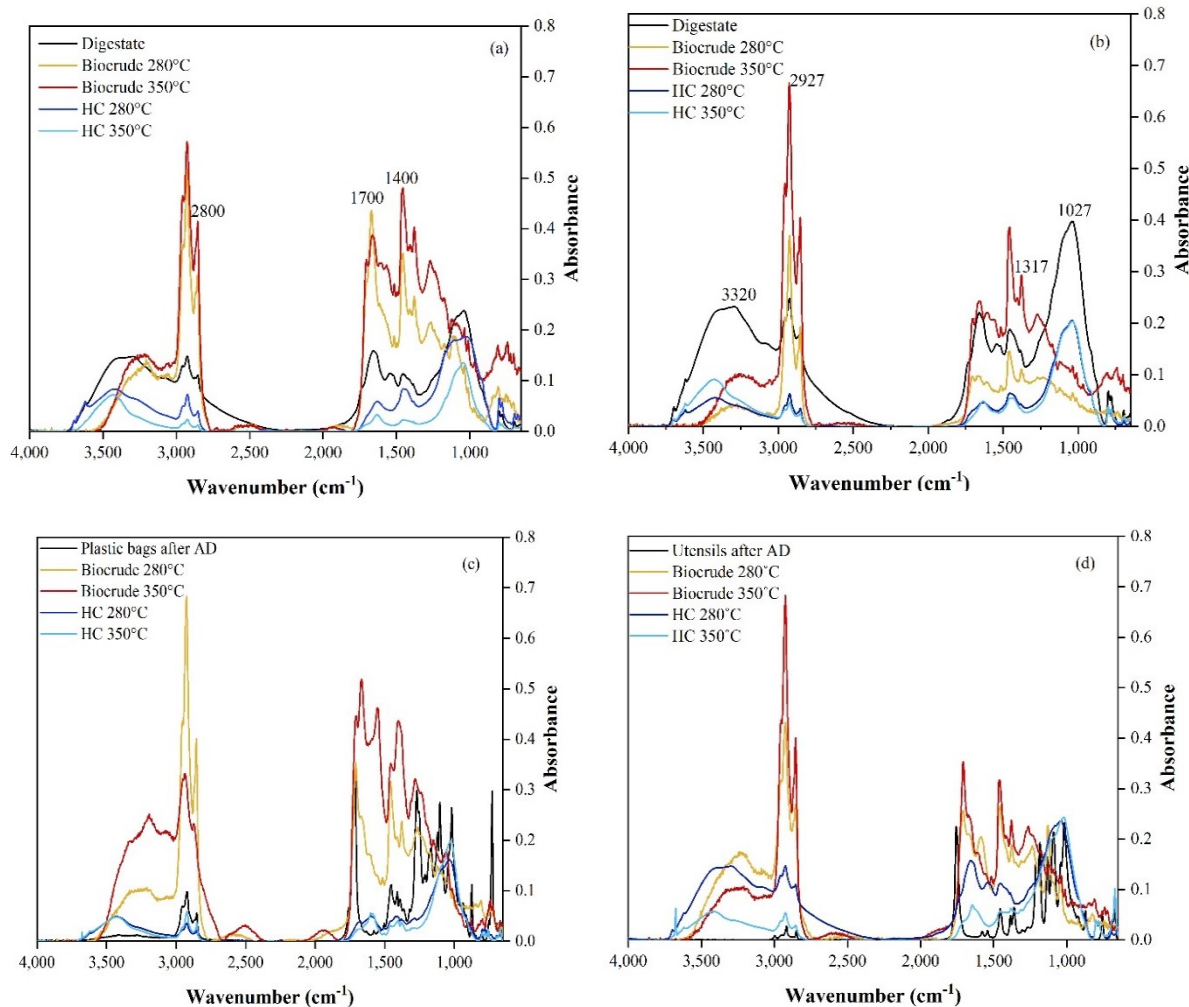


Figure 3.6. FTIR spectroscopy of biocrude and hydrochar (HC) samples after HTL of digestate samples: (a) control, (b) paper-based disposables, (c) compostable plastic bags, and (d) plant-based utensils.

As illustrated in Figure 3.6b, for digestate from HSAD of paper-based disposables, peaks at 663, 1,027, 1,317, 2,927, and 3,320 cm^{-1} decreased in HC. These peaks in HC after HTL demonstrate that there are still some unconverted organics like lignin in the solids, which might need more extreme operating conditions to be converted. Also, for biocrude at 350 °C, peaks were more intense than 280 °C since the temperature around the sub and near-critical region (critical point: 373.74 °C) can decrease the dielectric constant, density, and polarity of water, which accelerates hydrolysis reaction and improves the solubility of hydrophobic organic fractions (Seshasayee and Savage, 2020a). (Seshasayee and Savage, 2020a). Also, the difference in biocrude peaks implies that high operating temperatures in HTL enhance the

conversion of heteroatom compounds to biocrude (Xu et al., 2018). This is consistent with higher obtained biocrude at 350 °C.

Compared to the FTIR of digestate from HSAD of utensils and plastic bags (Figure 3. 2c and d), most functional groups from utensils and plastic bags disappeared in HC recovered from HTL (Figure 3. 6c and d). Thus, FTIR results implied that HTL efficiently removed plastic bags and utensils from digestate. However, for biocrude, FTIR peaks at 280 and 350°C demonstrated some sharp peaks like plastic bags and utensils. After opening the HTL reactor at the end of the experiment, no utensils and plastic bags were seen visually. Based on this, there is a high chance that some parts of plastic bags and utensils are degraded/melted, and some parts may be broken down into smaller parts of plastics (e.g., micro- and nanoplastics). Since the intensity of the FTIR peaks related to plastic bags and utensils are significantly higher in biocrude, it can be inferred that there is a high probability that utensils and plastic bags were transformed into biocrude. Previous studies indicated that by increasing the reactor temperature to 250°C, the plastics might pass through their glass transition temperature and further melt during the process (Seshasayee and Savage, 2020a). By increasing the temperature to 350°C and decreasing the dielectric constant of water, more plastics are more likely to dissolve or break down in the water (Seshasayee and Savage, 2020a). Overall, our results indicated that HTL could substantially remove plastic bags and utensils from digestate and decrease the potential environmental risk of plastic pollution when applying digestate as a biofertilizer in the fields (Chand et al., 2022).

3.4. Conclusions

The conversion of biodegradable disposables to biomethane and biocrude has been investigated in an integrated process of HSAD followed by HTL. The results evidently demonstrated that compostable plastic bags and plant-based utensils might not biodegrade in a conventional HSAD process. Moreover, their presence could reduce the cumulative methane yield by 29.5% and 8.99%, respectively. Despite minor lag phases, paper-based disposables could be degraded in the HSAD process, as indicated by 2.6 times higher methane production (compared to control). The post-processing of digestate using HTL could efficiently convert undegraded disposables to biocrude. Increasing HTL temperature from 280 to 350°C could lead to higher biocrude yields and superior biocrude quality in terms of biocrude content with higher HHV. FTIR results implied that no plastic bags and utensils remained in the biochar, indicating HTL could efficiently remove them from digestate and transform them into biocrude. Overall, it was evident that integrating HSAD with the HTL process would be needed for valorization and minimizing the potential environmental risk of biodegradable disposables made from

bioplastics. Although examining the synergistic effects between different types of disposable items was not part of the focus of this study, it is a valuable area for future research to consider, which could provide valuable insights and inform more effective strategies for managing and valorizing biodegradable disposables.

Chapter 4

Unveiling the Impact of Bioplastic Bags on High-Solids Anaerobic Digestion and Subsequent Hydrothermal Liquefaction of Source Separated Organics

A version of this chapter is submitted in a journal for peer-review and publication.

4.1. Introduction

Plastics have gained widespread popularity in modern society because of their versatility and wide range of applications (Abraham et al. 2021). They are used extensively in a wide range of products, including food packaging, household materials, construction supplies, textiles, farming equipment, electronics, and automotive components (Abraham et al. 2021). Annual plastic production has reached approximately 335 million tonnes, and almost 13 million tonnes of plastics end up as waste into the environment (Enfrin et al. 2019). At present, almost 90% of plastics are derived from fossil fuel substances and are not easily degradable, because their chemical structures are not vulnerable to the natural weathering processes, and they can persist in the environment for hundreds of years (Unmar and Mohee 2008). Their accumulation and persistence in the environment have detrimental effects on human life, wildlife, and ecosystems (Unmar and Mohee 2008). Fossil fuel-derived plastics have emerged as a major source of territorial and aquatic pollution (Enfrin et al. 2019). To tackle these issues, bioplastics have emerged as a promising environmentally friendly alternative to traditional fossil fuel-based plastics (Cucina et al. 2021a). Bioplastics are a category of materials that are either biodegradable or derived from renewable sources, and are intended to naturally degrade in the environment within a few years (Cucina et al. 2022). The feedstocks used for producing bioplastics include rice, corn, potatoes, soybeans, wood cellulose, and wheat fiber (Abraham et al. 2021). A wide range of bioplastics products are available in various forms, such as bottles, plates, cups, bags, furnishings, carpets, packaging materials, etc (Abraham et al. 2021). Currently, there is a growing presence of bioplastics in waste streams, particularly in municipalities that lack residential source separation programs (Pereira de Albuquerque et al. 2021; Cucina et al. 2021b).

Rapid urbanization and the increasing global population has resulted in a significant increase in the generation of source separated organics (SSO) worldwide (Dastyar et al. 2021b). It has been projected that by 2050, SSO generation will reach a critical level of approximately

3.4 billion tonnes (Dastyar et al. 2021b). In certain municipalities, bioplastic bags have been a favorable option as a liner for green bins used for SSO storage and collection because they eliminate the need to separate the plastic liner bags from the SSO (Peng et al. 2022) simplifying the waste storage and collection process and making it more convenient for both the municipality and the residents. These bioplastics are mixed with the SSO and undergo biological treatments such as high solid anaerobic digestion (HSAD), which is a common approach for diverting SSO from landfill (Dastyar et al. 2021a, b). These bioplastics are presumed to be degraded by microorganisms. However, Cucina et al. conducted a recent study revealing that different types of bioplastics, including starch-based and polylactic acid, are only degraded up to 27% during AD, with the remaining portion persisting in the digestate (Cucina et al. 2022). Similarly, Niknejad et al. examined the degradability of various biodegradable disposables, such as bioplastic food waste bin liners, plant-based compostable utensils, and a combination of paper-based disposables (coffee cups, paper plates, and straws) during HSAD (Niknejad et al. 2023). The findings indicated that only the paper-based disposables were degraded, while bioplastics-based bags and utensils remained intact after AD. Consequently, a substantial amount of bioplastics will likely persist in HSAD digestate, and will subsequently enter the environment through agricultural application of the digestate (Karamanlioglu et al. 2017). Therefore, additional post-processing procedures are recommended for the treatment of HSAD residuals before their final disposal. Notably, digestate contains a substantial amount of energy value because of its high carbon content and the presence of dissolved organic matter. To fully harness and use this energy potential, it is crucial to explore thermochemical biomass processing methods, such as hydrothermal technologies. These advanced techniques provide efficient means to valorize the digestate and extract its valuable energy content (Sharma et al. 2022).

Hydrothermal processes encompass a range of thermochemical methods conducted at elevated temperatures and above-saturated pressure. Among these approaches, hydrothermal carbonization (HTC), hydrothermal liquefaction (HTL), and hydrothermal gasification (HTG) are prominent (Ruiz et al. 2013). HTL, in particular, shows promise for the valorization of wet organic wastes, facilitating the conversion of complex molecules into biocrude oil while bypassing the energy-intensive drying process (Niknejad et al. 2023). The HTL process initiates a series of reactions that alter the physical and chemical properties of water, including density, dielectric constant, and ionic product (Lachos-Perez et al. 2022). The primary reaction agent in HTL is water, with operating temperatures typically ranging from 250 to 370 °C and residence

times between 10 and 60 min (Posmanik et al. 2017; Lachos-Perez et al. 2022). Under these conditions, water undergoes self-ionization, resulting in the release of H^+ and OH^- ions that act as catalysts, facilitating the decomposition and fractionation of feedstocks (Lachos-Perez et al. 2022). In recent years, there has been growing interest in the valorization of AD digestate using the HTL process. However, to the best of the authors' knowledge, there are no studies on HTL of HSAD digestate containing residual SSO and bioplastics.

Given this research gap, this study investigated the co-digestion of SSO and bioplastics during HSAD followed by HTL. First, the biodegradability of a mixture SSO and bioplastics under mesophilic HSAD conditions was evaluated. The digestate derived from HSAD was used as a feedstock for HTL at 280 °C, 330 °C, and 370 °C. To determine impact of HTL on bioplastics in HSAD digestate and the quality of the resulting products, a comprehensive analysis of the chemical properties of the HTL products was carried out.

4.2. Material and Methods

4.2.1. High-solid anaerobic digestion experiments

The solid inoculum (dewatered anaerobic digester sludge) and SSO were obtained from the Edmonton Waste Management Centre in Edmonton, Alberta, Canada, and preserved at 4 °C prior to the study. The liquid inoculum was mesophilic anaerobic digester sludge and was collected from the Gold Bar Wastewater Treatment Plant in Edmonton, Alberta, Canada. The compostable (bioplastics) kitchen bags used for food waste bin liners were purchased from a local store. The solid and liquid inoculum were acclimatized for 7 d at 37 °C before the experimental setup to facilitate the acclimation of microbial communities and degrade any remaining organic substances. The SSO consisted of food wastes, trimmed grass, residual fruit and vegetable matter, and lignocellulosic components, along with some fragments of paper, plastic, and small glass fragments. Prior to the experiment, the SSO sample underwent a manual inspection to eliminate any unwanted items, such as large particles of plastic, foam, and glass. Afterwards, the remaining material was thoroughly blended by hand to ensure a consistent sample for analysis and experimentation. Table 4.1 provides the characteristics of the solid inoculum, liquid inoculum, and feedstocks used in this study, and Table 4.2 shows the initial elemental analysis and the empirical molecular formula of SSO, inoculum, and bioplastic.

Table 4.1. Characteristics of inoculum and feedstocks.

Parameter	Solid Inoculum	Liquid Inoculum	Bioplastics	Source-separated organics (SSO)
Moisture Content (MC%)	75.8±0.06	97.71±0.01	0.33 ± 0.10%	56.24±13.94
Total Solids (TS%)	24.2±0.06	2.29±0.01	99.67 ± 0.10%	43.76±13.94
Volatile Solids (VS%)	9.97±0.01	0.71±0.03	81.39 ± 0.06%	8.24±0.96

Table 4.2. Initial elemental analysis of source-separated organics, inoculum, and initial bioplastic bag; CHNO (wt.%), and their molecular formula.

Item	Elemental composition (%)				C/N ratio	Empirical Molecular formula
Solid inoculum	31.43±0.34	4.31±0.04	4.23±0.08	45.19±0.96	7.43	C ₉ H ₁₄ O ₉ N
Liquid inoculum	35.16±0.57	5.14±0.06	5.77±0.01	52.88±0.04	6.09	C ₇ H ₁₃ O ₈ N
SSO	29.23±0.57	3.58±0.05	1.75±0.08	29.93±0.14	16.70	C ₁₉ H ₂₉ O ₁₅ N

Based on previous studies, SSO coming from municipalities will contain approximately 8%–10% (w/w) bioplastics (Cucina et al. 2021b). Consequently, a mixture of SSO and 10% (w/w) bioplastics was used to evaluate the biodegradability of bioplastics through HSAD. The bioplastics were first cut into small square pieces measuring roughly 1 cm × 1 cm. These squares were then introduced into the mixture containing the inoculum and SSO.

To evaluate the co-digestion of SSO and bioplastic under anaerobic conditions, small-scale anaerobic bioreactors were employed. These bioreactors had a working volume of 750 mL and a headspace of 250 mL. Before starting the experiment, a mixture of acclimated solid inoculum (Total solids [TS]: 24.2 ± 0.06%) and acclimated liquid inoculum (TS: 2.29 ± 0.01%) was created to maintain a TS content >15%, as commonly observed in HSAD. The biochemical methane potential (BMP) test using a food-to-microorganism ratio (F/M) of 2 (g volatile solids [VS] feedstock/g VS inoculum) was performed. A comprehensive description of the batch

reactors used for BMP tests can be found elsewhere (Niknejad et al. 2023). The BMP test condition included (I) the mixture of inoculum and SSO as the control, and (II) the mixture of inoculum, SSO, and bioplastics to determine the biodegradability of bioplastic during co-digestion and to compare the biomethane generation rates during the HSAD process. The BMP of the inoculum and deionized water was used as a blank to measure the methane production specifically derived from the inoculum. The experiment was conducted over a period of 45 d. All experiments were conducted in triplicate to ensure the accuracy and consistency of the results.

4.2.2. Hydrothermal liquefaction experiments

The digestate obtained from the HSAD tests was used as a feedstock for the subsequent HTL experiments. The comprehensive experimental protocol can be found elsewhere. (Niknejad et al. 2023) The experiments were conducted at three distinct temperatures of 280 °C, 330 °C, and 370 °C with a retention time of 10 min. Following the exposure period, designated tubes were used to recirculate chilled water to decrease the reactor temperature.

Following completion of the HTL tests, gas samples were collected and stored in gasbags for further analysis of their composition. Afterwards, the reactor was opened, and the contents were removed and separated. The aqueous phase was filtered through a Buchner funnel using Whatman filter paper and a vacuum pump. Any solids adhering in the reactor were retrieved by washing with pure acetone. The combination of acetone and adhesive substance was filtered, and the solid content obtained from the acetone wash, along with the aqueous phase, was subjected to another wash to extract any oils trapped in the pores (Niknejad et al. 2023). The solid residue remaining from the HTL test was dried overnight at 70 °C, resulting in the formation of the final residue known as hydrochar (HC). Rotary evaporation under vacuum was used to remove water from the aqueous phase and acetone from the acetone phase. This process allowed for the recovery of the desired end product of biocrude.

4.2.3. Analytical Methods

Detailed analytical methods for TS, VS, moisture content, gas composition, product distribution, and biocrude composition can be found elsewhere (Niknejad et al. 2023). The elemental composition of the initial inoculums, SSO, bioplastic, digestate, biocrude, and HC samples were measured using the Flash 2000 Organic Elemental Analyzer (Thermo Fisher, Cambridge, UK). The empirical molecular formula, and theoretical biomethane potential of the

feedstock were computed following the methodology described in the literature (Chae et al. 2008; Dastyar et al. 2021b). The higher heating value (HHV) of the samples was then calculated using the Dulong formula (Mathanker et al. 2020a).

4.2.3. Data analysis

Methanogenesis kinetics were evaluated using the first-order and modified Gompertz models based on the methane production data (Mohammad Mirsoleimani Azizi et al. 2021a). The first-order kinetic model was employed to determine the rate constant (k , d^{-1}), for methanogenesis, while the modified Gompertz model was used to determine the maximum rate of methane production (R , L/d) and the lag phase time (λ , d). The literature provides a detailed protocol for estimating the best-fit kinetic parameters (Meshref et al. 2021). Origin pro 2021 was used to conduct principal component analysis (PCA) to explore possible correlations and variances among various test conditions and the resulting products from the HTL process (Mirsoleimani Azizi et al. 2023).

4.3. Results and Discussion

4.3.1. High-solids anaerobic digestion

4.3.1.1. Impact of bioplastic bags on methane potential and kinetics

The cumulative methane production profile for the control and bioplastics-loaded reactor is presented in Fig.4.1. After initiating the experiment, both reactors quickly commenced methane production (Dastyar et al. 2021a). This rapid methane generation was a result of the decomposition of easily biodegradable organic matters present in the input materials. There was a brief delay in methane production following the initial surge, which aligns with findings from previous studies on HSAD (Dastyar et al. 2021b; de Albuquerque et al. 2022). After this short lag phase, methane production in both reactors exhibited an exponential increase, followed by a gradual decline accompanied by some fluctuations until the completion of the batch operation. The cumulative methane productions from the control and bioplastic-loaded reactors were 182.39 ± 2 and 95.91 ± 1.7 mL/g VS, respectively, after 45 d of batch operation. Although the bioplastics-loaded reactors demonstrated slightly higher methane production than the control during the initial 15 d of digestion, the methane production from the control ultimately

surpassed that of the bioplastics-loaded reactor (Fig. 1). The lower methane production in bioplastics-loaded reactor can be related to the incomplete breakdown and release of harmful additives from bioplastic bags (Niknejad et al. 2023) which may interfere with the activity of crucial enzymes of anaerobic microorganisms (Mohammad Mirsoleimani Azizi et al. 2021b; Mohammad et al. 2022). The presence of bioplastic bags could also impose constraints on mass transfer within the digester, leading to a decline in methane production (Niknejad et al. 2023). Lastly, the physical presence of bioplastic bags could act as a physical barrier and prevent microorganisms from accessing and degrading organic matter (Mu et al. 2018; Abraham et al. 2021; Lallement et al. 2021).

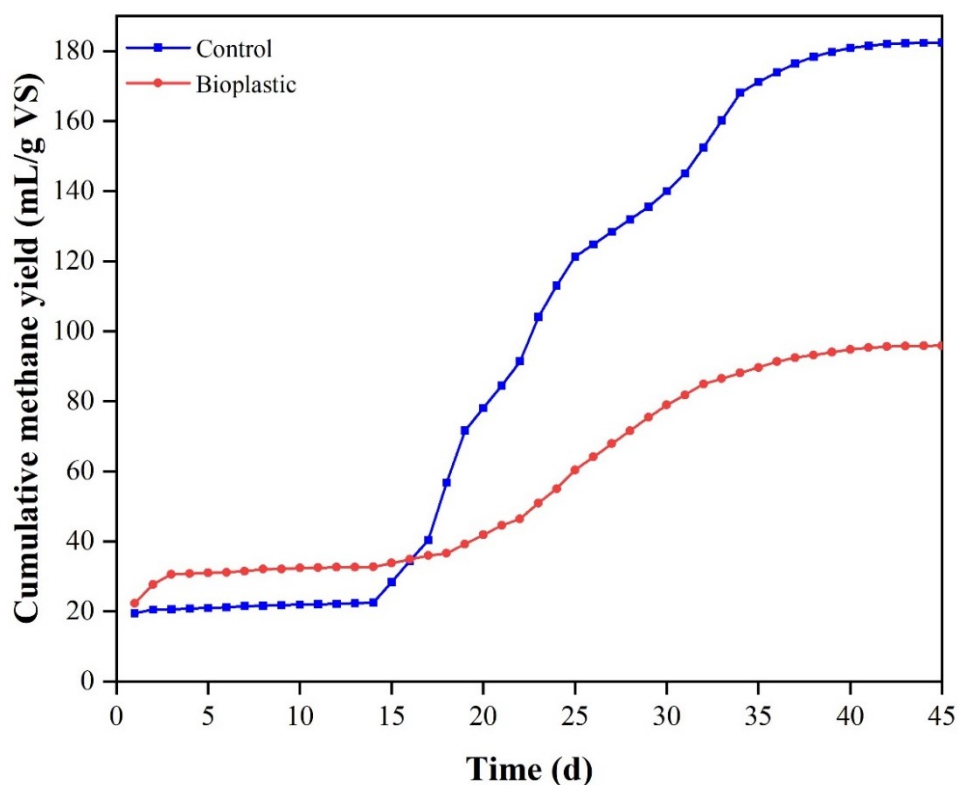


Figure 4.1. Cumulative methane yields for control and bioplastics-loaded reactors.

The experimental and theoretical extents of methane production were also examined for both conditions in Table 4.3. Using the elemental composition data, the empirical molecular formula of SSO + inoculum was $C_{13}H_{23}O_{14}N$. Hence, the theoretical methane potential of the initial SSO combined with the solid inoculum was calculated to be 9 L. Considering the actual cumulative methane production of 5.1 L and 2.68 L from the control and bioplastics-loaded reactors, respectively, the methane recovery efficiencies were calculated as 59.11% and 31.06%, respectively.

Table 4.3. The molecular formula of source-separated organics and biomethane recovery efficiencies obtained based on elemental analysis results.

Digester	The empirical molecular formula of initial SSO and inoculums	Methane potential (L) at 37°C		Methane recovery efficiency (%)
		Theoretical	Experimental	
Control	C ₁₃ H ₂₃ O ₁₄ N	9	5.1	59.11
Bioplastics			2.68	31.06

The methanogenesis kinetics was evaluated using the first-order and modified Gompertz models (see Table 4.4). The results from the first-order model showed that the addition of bioplastic bags increased the methanogenesis rate from 0.04 d⁻¹ to 0.05 d⁻¹. This observation is supported by the higher methane production in the bioplastic bags reactor than in the control reactor during the initial 15 d. Additionally, the modified Gompertz model indicated that the bioplastic bags reactor significantly reduced the lag phase for methane production when compared with the control (2.69 vs. 11.42 d). In general, the leaching of additives from most plastic materials can inhibit methane production in anaerobic digesters (Mohammad Mirsoleimani Azizi et al. 2021c); however, a few recent studies have demonstrated that the up to certain levels, the presence of certain plastic particles in anaerobic digesters can enhance the solubilization and activity of key enzymes because of leaching of additives that enhance the activity of key enzymes of methanogens (Chen et al. 2021; Mohammad et al. 2022). This could possibly explain the higher methanogenesis rate and shorter lag phase observed during the first 15 d of the experiment. Therefore, it is plausible that the leached additives were initially below the inhibitory thresholds, which could have enhanced the methanogenesis rate. By day 15, the concentration of leached additives could have escalated to inhibitory levels, which ultimately

arrested methanogenesis. The estimated R values from the modified Gompertz model for the control were 4.27 times higher than those for the bioplastic reactor, and this difference could be attributed to the breakdown of bioplastic bags into microplastics (MPs) and nanoplastics (NPs) (discussed later) in the digester (Niknejad et al. 2023). The increased concentration of MPs and NPs could suppress methane generation through various mechanisms, including the leaching of toxic additives, restraining the activity of key enzymes, and direct damage to cells through penetration (Mohammad Mirsoleimani Azizi et al. 2021b; Mohammad et al. 2022). In conclusion, the existence of bioplastics in the anaerobic digesters appeared to have both positive and negative effects on the methanogenesis process (Venkiteshwaran et al. 2019; Battista et al. 2021; Yu et al. 2023) increasing the initial rate of methane production but also potentially inhibiting it through the accumulation of MPs and NPs. Further research is needed to gain a comprehensive understanding of the complex interactions between bioplastics and the AD process and to develop strategies for optimizing methane production while mitigating any potential adverse impact caused by bioplastics.

Table 4.4. Kinetic parameters estimated with the first-order and modified Gompertz model.

Reactor	First-order model		Modified Gompertz model			
	Methanogenesis rate constant k (d ⁻¹)	Standard error of k	Maximum biomethane production rate, R (mL/g VS. d)	Standard error for R	Lag phase, λ (d)	Standard error for λ
Control	0.04	0.003	254.86	14.29	11.42	0.61
Bioplastics	0.05	0.002	69.96	5.94	2.69	1.78

4.3.1.2. Fourier transform infrared spectroscopy of digestate

Fig. 4.2 presents the Fourier transform infrared spectroscopy (FTIR) spectrum of the initial samples and digestate obtained from two reactors. The differences in the observed intensity reflect changes in the nature and distribution of functional groups, as well as the solubilization of particulate macromolecules (Mohammad et al. 2022). A detailed list of the

specific wavenumbers and their corresponding functional groups for each sample can be found in our previous publication (Niknejad et al. 2023). When comparing the initial SSO sample with the final sample from the control group, the peaks occurred at the same wavelengths. However, a remarkable decrease in intensity was noted in the digestate, indicating the successful conversion of organic compounds, such as proteins, carbohydrates, and lipids, into biomethane. Additionally, some peaks displayed changes in their positions.

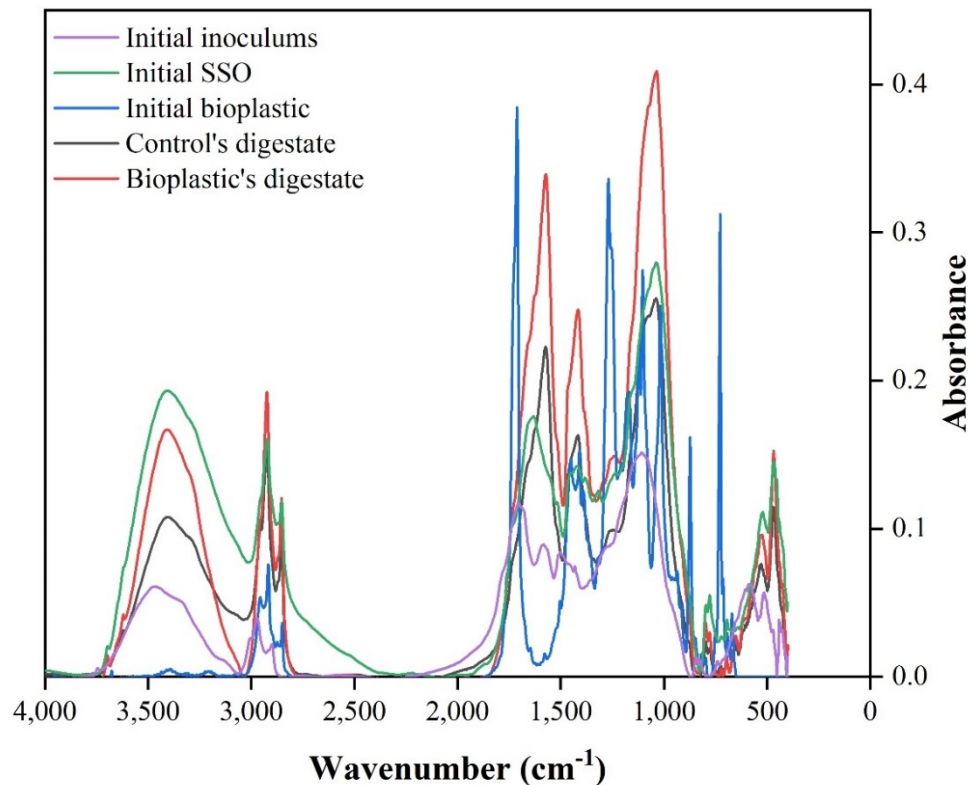


Figure 4.2. Fourier transform infrared spectroscopy of initial feedstocks and digestate from high-solid anaerobic digestion under different test conditions.

Comparing the attenuated total reflection-FTIR (ATR-FTIR) spectra of the initial bioplastic bags with the final digestate obtained from the bioplastics-loaded reactor, noticeable changes were observed in both the wavenumber and intensity of the peaks. Although there was no visual evidence, the FTIR analysis revealed the presence of bioplastic bags in the digestate, as evidenced by sharp peaks in the final spectrum, with some peaks having higher intensity than on the initial spectrum. Therefore, it can be inferred that co-digestion had a significant impact on the accelerated degradation of bioplastics, and some parts may have been fragmented into smaller plastic particles such as MPs and NPs (Niknejad et al. 2023). Previous studies also reported the degradation and breakdown of bioplastics during AD of bioplastics mixed with

organic wastes (Cucina et al. 2021a, 2022). These results highlight the need to address the environmental impact of digestate containing undegraded bioplastics and develop strategies to minimize potential adverse impacts on the environment. According to a few recent reports, bioplastics can serve as carriers for various secondary pollutants, such as antibiotics, antibiotic resistance genes, metals, and chlorinated phenols in the same manner as MPs and NPs from petro-plastics (Tubić et al. 2019; Di Cesare et al. 2021; Haffiez et al. 2023). Thus, thermochemical post-treatment of digestate might be an effective approach to mitigate these environmental risks.

4.3.2. Hydrothermal liquefaction of digestate

4.3.2.1. Product distribution

Fig.4.3 illustrates the yields of various products obtained during HTL of digestate samples. The digestates underwent conversion, resulting in the production of HC, gases, biocrude, and water-soluble substances (WSS). As the temperature increased from 280 to 330 °C, the weight percentage of biocrude increased. However, a further increase in temperature from 330 to 370 °C decreased the weight percentage of both biocrude and HC, while there was a peak rise in the weight percentage of total gas. This indicates that the higher temperatures led to a cracking process for biocrude and HC, resulting in the production of more gaseous compounds and WSS products (Xu et al. 2018; Niknejad et al. 2023). At lower temperatures, hydrolysis and dehydration can favor ionic reactions, leading to the formation of monomers in the polar medium through the initial ionization of biomass (Mathanker et al. 2020a). As the temperature increased, hemicellulose, cellulose, and lignin might decompose. Cellulose decomposes rapidly at approximately 250 °C, resulting in the generation of a significant amount of WSS products (Minowa et al. 1998; Akhtar and Amin 2011). The significant increase in the yield of WSS implies the presence of abundant quantities of soluble organic compounds and inorganic salts within the aqueous phase (Xu et al. 2018; Niknejad et al. 2023). Beyond 300 °C, two concurrent reactions might take place: the repolymerization of biocrude to form HC and the depolymerization of biocrude and HC to generate gaseous products (Akhtar and Amin 2011; Zhu et al. 2015). In this study, the depolymerization of biocrude and HC likely predominated, as evidenced by the increased production of gaseous products with rising temperature (see Fig. 3).

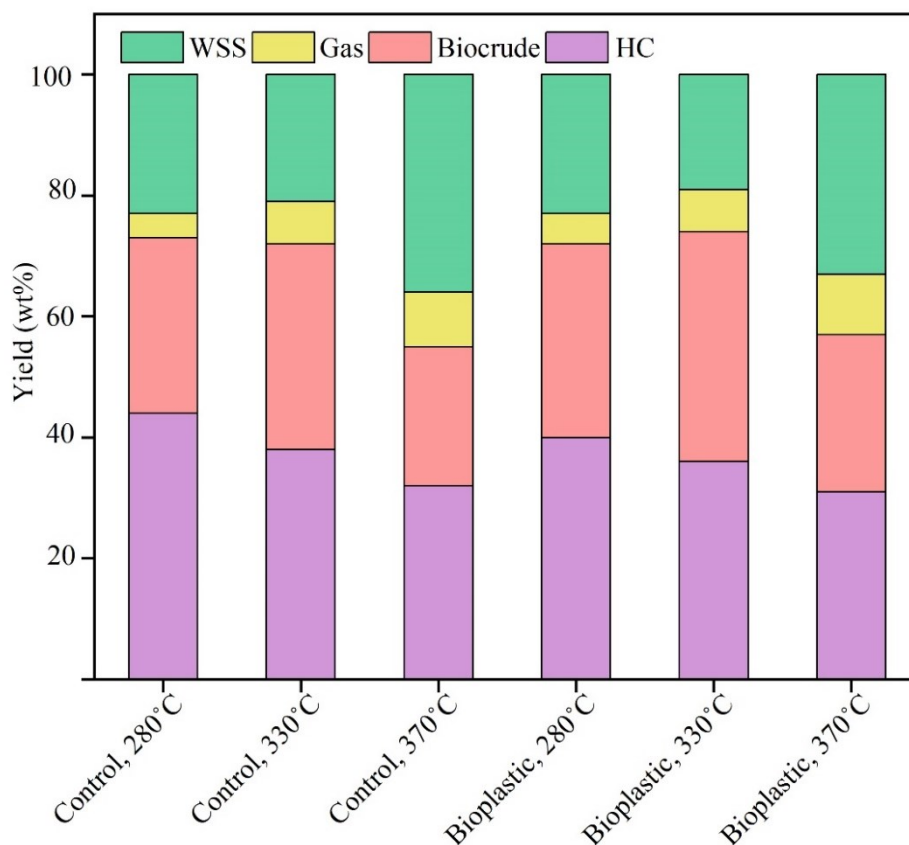


Figure 4.3. Product yields from hydrothermal liquefaction of digestate under different conditions.

Despite the increase in gaseous products with rising temperature, the overall yield of gas (4%–10%) remained lower than that of biocrude (23%–38%), which is desirable because of the higher energy content of biocrude (Xu et al. 2018). The maximum biocrude yield (38%) was achieved at 330 °C for the digestate from the bioplastics-loaded reactors. The production of biocrude involves a complex series of chemical reactions, including oligomerization, depolymerization, decomposition, and reformation (Toor et al. 2011; Vardon et al. 2012). The temperatures within the sub and near-critical range (373.74 °C) induce changes in water properties such as dielectric constant, density, and polarity (Seshasayee and Savage 2020a). These alterations expedite hydrolysis reactions and enhance the solubility of hydrophobic organic components (Seshasayee and Savage 2020a; Niknejad et al. 2023).

4.3.2.2. Biocrude composition

To gain a deeper understanding of the molecular composition of biocrude, gas chromatography–mass spectrometry (GC-MS) analysis was conducted. The comprehensive

results, including retention time, compound names, and percentage of peak area, can be found in Table B-1. The analysis revealed the presence of numerous compounds under various conditions. Compounds with a peak area below 0.75% were excluded from the analysis, and included compounds were classified according to their functional groups and illustrated in Fig.4.4. According to the findings from the GC-MS analysis, biocrude can be categorized into three main groups: (I) N-containing compounds (including nitrogen and oxygen-heterocyclic compounds, amides), (II) hydrocarbons (such as alkanes and alkenes), and (III) oxygenated compounds (ketones, alcohols, acids, esters, carboxylic acids, and ethers). Because of the complex nature of the digestate (i.e., inoculum + SSO + bioplastics), it is difficult to determine the specific pathways in which these compounds are formed, and the formation of each compound may involve multiple pathways, adding to the complexity of the process. Furthermore, the relative abundance of these compounds varied across different samples, highlighting the influence of specific conditions on their formation. For example, compounds such as amides and N-containing substances like nonanamides, octadecanamide, and benzamide can be generated through various processes, including decarboxylation, deamination, dehydration, and the decomposition of proteins, and incomplete hydrolysis reactions within a short residence time (10 min) (Xu et al. 2018; Shah et al. 2020a). The abundance of N-containing compounds increased with increasing temperature in both the control and bioplastic digestates. In the digestate from bioplastics-loaded reactor, the abundance of amides increased significantly from 7.97% to 24.15% as the temperature increased from 280 °C to 370 °C.

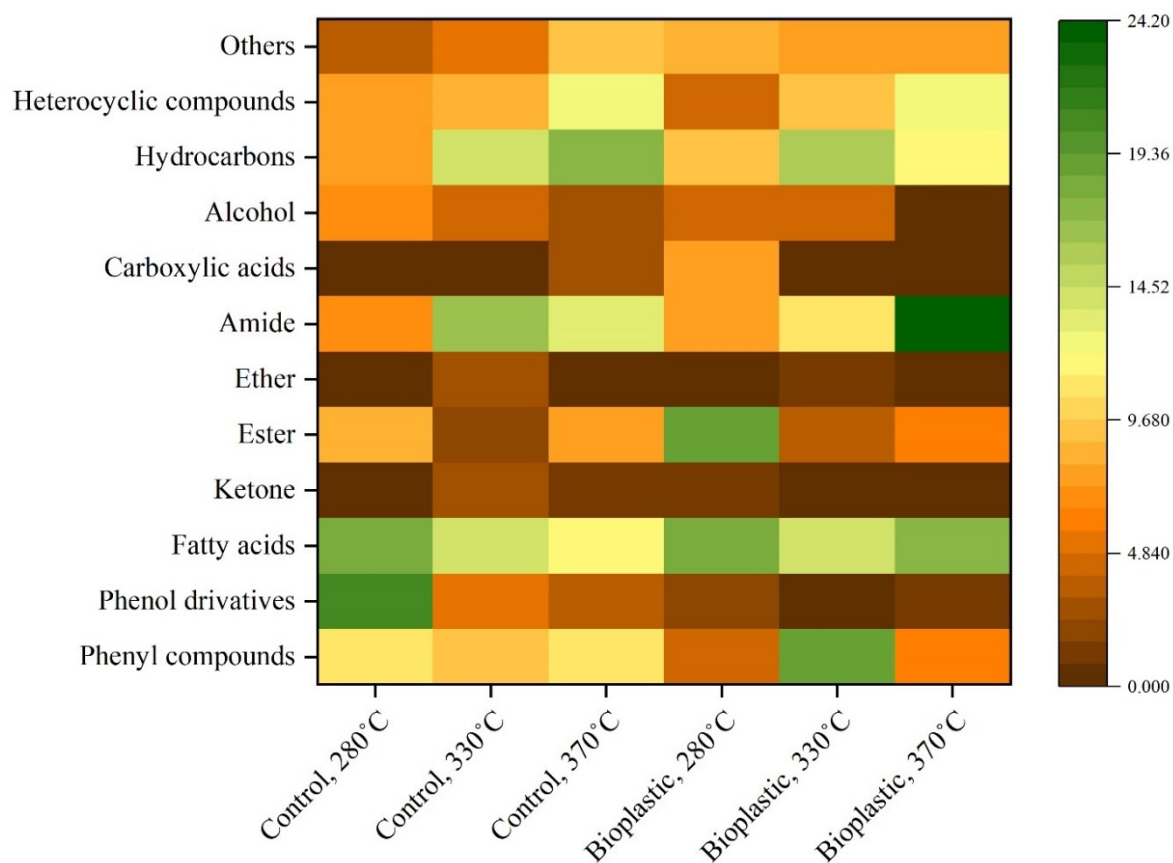


Figure 4.4. Heatmap showing gas chromatography–mass spectrometry analysis results for biocrude under different hydrothermal liquefaction conditions

Moreover, certain heterocyclic compounds like indolizine, quinoline, and pyridine can be formed through the Maillard reaction (Zhang et al. 2021). This reaction takes place when amino acids derived from proteins chemically interact with polysaccharides (Zhang et al. 2021). Phenolic compounds like 2-methoxy-5-methylphenol and 4-ethyl-2-methoxy-phenol can be generated from cellulose through dehydration, hydrolysis, and ring closure reactions (Xu et al. 2018; Shah et al. 2020a). Fatty acids such as octadecanoic acid, undecanoic acid, and *n*-hexadecanoic acid can be generated through lipid hydrolysis, which involves the breakdown of fats or lipids into their constituent fatty acids and other components (Shah et al. 2020a). The findings demonstrated a notable decrease in the abundance of oxygenated compounds as the temperature increased from 280 to 370 °C for both the control and bioplastics digestate. For instance, the percentage of alcohol detected in the control condition decreased from 7.09% at 280°C to 2.96% at 370°C. Overall, the reduction in N-containing and oxygenated compounds at higher temperatures can potentially lower the cost associated with further upgrading of

biocrude because it may require fewer deamination, decarboxylation, and dehydroxylation processes (Xu et al. 2018; Shah et al. 2020a).

Hydrocarbons such as nonadecane, 1-cetene, and heptadecane can be formed through the process of decarboxylation of fatty acids (Shah et al. 2020b). Ketones such as 2-hexadecanone, 8-pentadecanone, and 2-dodecanone can be formed from cellulose through processes involving cyclization and hydrolysis (Shah et al. 2020a). The hydrocarbon content in the biocrude obtained from the control digestate was enhanced from 7.41% at 280 °C to 17.73% at 370 °C, whereas the hydrocarbon content in the biocrude derived from the bioplastics-loaded HSAD digestate increased from 7.97% at 280 °C to 15.87% at 330 °C. However, at 370 °C, the hydrocarbon content in the bioplastics digestate decreased to 11.36%. This can be attributed to the cracking of long-chain aliphatic compounds into shorter chains and the formation of cyclic compounds, particularly near critical conditions (Zhu et al. 2014; Shah et al. 2020a). This is further reinforced by the higher presence of heterocyclic compounds in biocrude obtained from the digestate of the bioplastics-loaded reactor at 370 °C (12.87%) than at 330 °C (8.91%). Overall, these findings provide valuable insights into the composition and formation processes of biocrude, highlighting the complexity and influence of specific conditions on its composition.

4.3.2.3. Gaseous products

The gaseous products generated during HTL can result from a range of intricate reactions, such as water-gas shifts, thermal cracking, denitrogenation, methanization, and deamination (Xu et al. 2018). Fig.4.5 illustrates the gaseous products from the control and bioplastics bioreactors after HTL at 280–370 °C. The results indicated that CO₂ was the predominant gas component, accounting for 92.1%–95.8% of the gaseous products under all tested conditions. This could be ascribed to the occurrence of decarboxylation reactions under hydrothermal conditions (Xu et al. 2018). The high concentration of gaseous CO₂ observed during HTL aligns with previous research findings (Huang et al. 2013; Xu et al. 2018; Niknejad et al. 2023). Furthermore, the analysis of the gas composition indicated that methane constituted approximately 4.2%–7.9% of the total gas content. With the temperature increase from 280 to 370 °C, there was a progressive enhancement in the methane content. This can be explained by the breakdown of larger hydrocarbon molecules, the occurrence of methanation reactions, and decomposition reactions facilitated by free radicals (Xu et al. 2018; Basar et al. 2021). These reactions are known to be more prominent near the critical temperature of water (Basar et al. 2021). Therefore, elevated temperature plays a crucial role in facilitating gasification reactions,

leading to the preferential production of gases in the HTL process, as depicted in Fig.4.2. However, the overall gas yield remained relatively low, which is advantageous considering that gaseous products hold less value compared with biocrude. It is also essential to address the presence of flammable gases, and effective strategies for the collection, treatment, or reuse of these gases should be considered, particularly in large-scale HTL applications in the future.

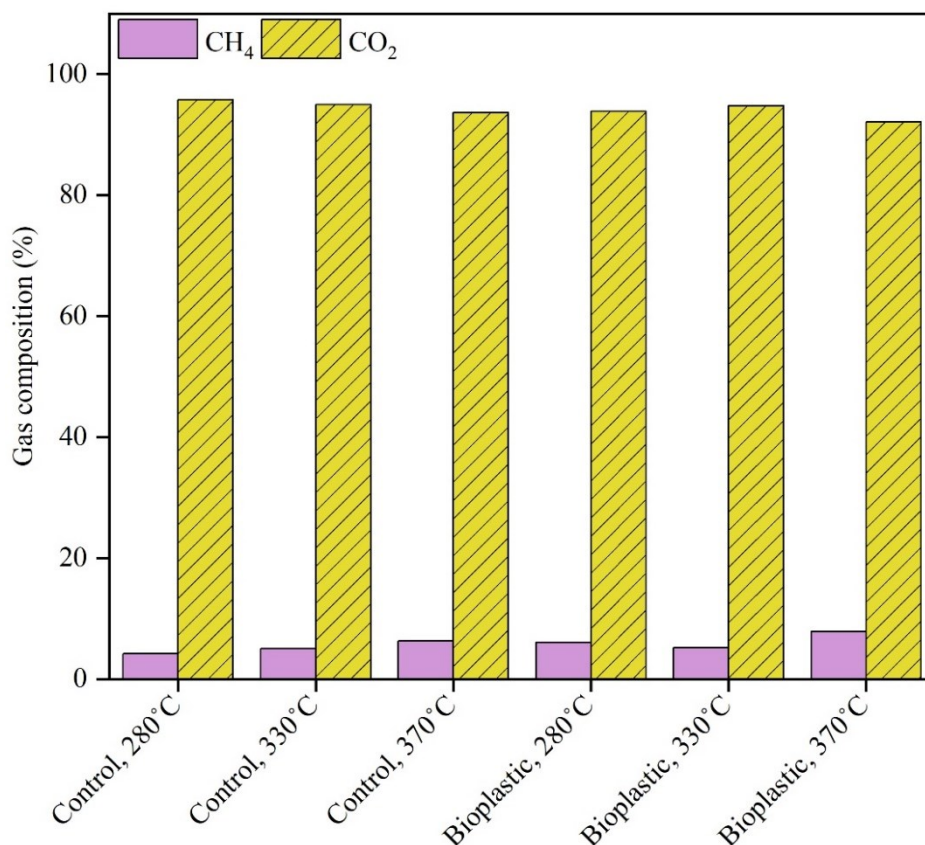


Figure 4.5. Gas chromatography-thermal conductivity detector analysis results for gaseous products from different hydrothermal liquefaction tests.

4.3.2.4. Elemental analysis, atomic ratio, and higher heating value

4.3.2.4.1. Hydrochar

Table 4.5 presents the elemental composition, HHV, H/C ratio, and O/C ratio for the HC obtained through HTL. The carbon content in the HC was significantly lower than the control and bioplastics digestate prior to HTL. This reduction can be ascribed to the progressive elimination of carbon-containing solid organic materials during the HTL process, leading to the formation of biocrude and gases, particularly at higher temperatures (Xu et al. 2018). In contrast, there was a discernible increase in the oxygen content within the same temperature

range. This can be attributed to the buildup of oxygen-containing water-insoluble salts within the solids (Xu et al. 2018; Mathanker et al. 2020b). The reduced H/C ratios observed in the solid phase indicate that hydrogen content was used, potentially generating a higher proportion of unsaturated and aromatic compounds within the solid phase (Shah et al. 2020a). In contrast, the elevated O/C ratios can be ascribed to a more extensive process of deoxygenation achieved through dehydration and decarboxylation reactions (Shah et al. 2020a).

Table 4.5. Elemental analysis and higher heating value for hydrochar at different conditions.

Hydrochar	N (wt.%)	C (wt.%)	H (wt.%)	S (wt.%)	O (wt.%)	H/C	O/C	HHV
Control digestate	2.36±0.07	36.15±0.64	4.66±0.07	0.41±0.08	56.42	0.13	1.56	8.84
Control, 280 °C	2.09±0.03	34.50±0.19	3.55±0.03	0.55±0.02	59.32	0.10	1.72	6.19
Control, 330 °C	1.82±0.02	33.11±0.84	3.49±0.11	0.51±0.04	61.07	0.11	1.84	5.33
Control, 370 °C	1.08±0.01	28.60±0.54	1.98±0.04	0.31±0.01	68.03	0.07	2.38	0.38
Bioplastic digestate	2.12±0.02	36.51±0.33	4.77±0.04	0.45±0.07	56.16	0.13	1.54	9.16
Bioplastic, 280 °C	1.69±0.03	31.43±0.32	3.52±0.05	0.44±0.06	62.91	0.11	2.00	4.47
Bioplastic, 330 °C	1.33±0.05	25.80±2.13	2.98±0.17	0.42±0.05	69.48	0.12	2.69	0.61
Bioplastic, 370 °C	1.24±0.03	26.02±0.35	3.03±0.07	0.35±0.01	69.36	0.12	2.67	0.78

The HHV of the HC samples decreased with increasing temperature. This might be related to the conversion of a major portion of the elements present in the digestates to biocrude rather than HC. As the temperature rises, the HTL process promotes the transformation of carbon-containing solid organic materials into biocrude and gases, resulting in a decrease in the HHV of the remaining solid fraction (Xu et al. 2018). The progressive removal of carbon during the HTL process decreases the energy content of the solid phase as a larger proportion of carbon is diverted towards the formation of biocrude, which possesses a higher energy content than HC (discussed later) (Niknejad et al. 2023). Therefore, the decrease in HHV observed in the HC samples can be attributed to the efficient conversion of elements into biocrude, highlighting the potential energy-rich nature of the produced biocrude.

4.3.2.4.2. Biocrude

Table 4.6 shows the elemental composition, HHV, H/C, and O/C ratio, for the biocrude obtained through HTL. The total wt.% of N and S in the biocrude were higher than those in the digestate regardless of temperature. The trend of initially increasing and then decreasing N and S contents, observed in both the control and bioplastic samples, could be because higher temperatures promote the formation of N- and S-containing organic compounds, leading to biocrude production (Xu et al. 2018). Also, when operating under subcritical conditions, ionic reactions such as dehydration occur to retain nitrogen within the biocrude (Seshasayee and Savage 2021). However, denitrogenation and desulfurization are more favorable at temperatures above 330 °C (Xu et al. 2018). Notably, the nitrogen content in the biocrude remained stable at approximately 3–4 wt% regardless of temperature. The initial low nitrogen composition makes it feasible to attain the desired levels of denitrogenation, thereby enhancing the potential utilization of the biocrude (Santillan-Jimenez et al. 2019; Seshasayee and Savage 2021). The H/C ratio represents the abundance of aromatic products in the biocrude (Seshasayee and Savage 2021). In the control biocrude, the H/C ratio was relatively stable at approximately 0.12–0.13, which was similar to the H/C ratio of the digestate (0.13). However, as the temperature of HTL increased, the O/C ratios decreased, implying that dehydration and decarboxylation reactions became more significant at higher temperatures (Shah et al. 2020a). The decrease in the O/C ratio is caused by a reduction in the concentration of oxygen-containing compounds, indicating a greater conversion of these compounds into other products. Evidently, higher temperatures enhanced the quality of the biocrude, as demonstrated by the higher C+H content, HHV, and the lowest heteroatom content (i.e., O, N, and S) (Xu et al. 2018). These heteroatoms in the biocrude originate primarily from the proteins, lipids, carbohydrates, and lignin present in the digestate (Xu et al. 2018).

Table 4.6. Elemental analysis and higher heating value for biocrude at different conditions.

Biocrude	N (wt.%)	C (wt.%)	H (wt.%)	S (wt.%)	O (wt.%)	H/C	O/C	HHV
Control, 280°C	3.92±0.02	64.53±1.59	8.58±0.09	0.88±0.08	22.09	0.13	0.34	30.20
Control, 330°C	4.10±0.01	70.60±0.16	8.53±0.01	1.20±0.00	15.57	0.12	0.22	33.38
Control, 370°C	3.23±0.03	72.52±1.21	9.04±0.03	0.76±0.09	14.45	0.12	0.20	34.91
Bioplastic, 280°C	3.39±0.02	65.44±1.38	8.38±0.05	0.54±0.05	22.24	0.13	0.34	31.26
Bioplastic, 330°C	3.87±0.04	73.95±0.08	9.84±0.05	1.05±0.02	11.29	0.13	0.15	37.14
Bioplastic, 370°C	3.57±0.02	60.58±0.97	9.03±0.10	0.33±0.03	26.49	0.15	0.44	28.67

The HHV obtained from the bioplastics digestate was greater than the control. The highest HHV for the bioplastics digestate was obtained at 330 °C, which also resulted in higher production of biocrude (see Fig.4.3). This indicates that the HTL of the bioplastics and SSO mixture leads to a larger quantity of biocrude with an improved HHV. These findings are significant for potential large-scale applications of HTL in the valorization of SSO, and are aligned with previous studies (Yuan et al. 2009; Seshasayee and Savage 2021). Yuan et al. found that the addition of sawdust facilitates the liquefaction of high-density polyethylene (HDPE) through HTL (Yuan et al. 2009). They hypothesized that sawdust had a lower decomposition temperature than HDPE, and the sawdust fragments act as active donors during the initial scission of the polymer chain, thereby accelerating depolymerization (Yuan et al. 2009). They also speculated that the hydrogen transfer process, occurring between polyolefinic chains and radicals derived from sawdust, serves to stabilize the free radicals produced during the thermal breakdown of biomass. This phenomenon leads to increased production of liquid products while reducing the formation of char and gaseous products (Yuan et al. 2009). However, these effects become weaker as the temperature increases. During the initial stages of HTL, the dominant reaction is thermal cracking. As the temperature rises, macromolecular products undergo further thermal cracking, promoting the generation of smaller radical fragments that are stabilized by active hydrogen. When there is a sufficient supply of hydrogen, the rate of oil formation accelerates with increasing temperature, resulting in a higher yield of biocrude. However, when the reaction temperature exceeds a certain threshold, the radical fragments undergo condensation reactions (Yuan et al. 2009). Consequently, the biocrude yield

decreases as the decomposition reactions occur, leading to the formation of water, carbon dioxide, and other compounds with lower energy content (Yuan et al. 2009).

At an operating temperature of 330 °C, the biocrude obtained from bioplastic digestate exhibited a lower O/C ratio. This finding aligns with the notion that the decomposition of bioplastics contributes carbon-rich components to the biocrude during the HTL process. A lower O/C ratio in the biocrude has the potential to improve its stability and viscosity, while also reducing the amount of hydrogen needed for biocrude upgrading (Shah et al. 2020a). At an operating temperature of 290 °C, the ion product of water (K_w) reaches its maximum value (Peterson et al. 2008; Seshasayee and Savage 2021). The higher concentration of H^+ ions at this temperature could facilitate the generation of furfurals from polysaccharides, leading to the production of more char from the biomass. The oxygen-rich char has the ability to interact with the hydrogen-rich plastic material, facilitating depolymerization, and consequently lowering the degradation temperatures of the bioplastics within the reactor (Yuan et al. 2009; Seshasayee and Savage 2021). However, the H/C ratios of the biocrude were still lower compared with petroleum crude (1.3–2.2) (Shah et al. 2020a). Therefore, additional upgrading techniques are necessary to remove heteroatoms, which would further enhance the feasibility of using biocrude as a petroleum fuel substitute.

4.3.2.5. FTIR spectra

Fig.4.6 illustrates the FTIR results for HC and biocrude under various conditions. The FTIR spectrum of the control sample after HTL reveals the notable influence of temperature on the characteristics of HC and biocrude (Fig.4.6a). The peaks observed in the digestate (Fig. 2) substantially decreased in intensity within the HC spectrum. Additionally, the intensity of various peaks from the HC produced at 370 °C was lower than the peaks at 330 °C or 280 °C. This indicates that elevated temperatures increased the degradation and transformation of various functional groups present in the digestate samples (Niknejad et al. 2023). The presence of peaks in the HC spectra after HTL indicates the presence of unconverted organic compounds, such as lignin, in the solid residues. These peaks suggest that despite the HTL process, some organic components require more extreme operating conditions to be fully converted (Niknejad et al. 2023). Further optimization of HTL parameters, such as temperature and residence time, may be necessary to achieve complete conversion of these residual organics.

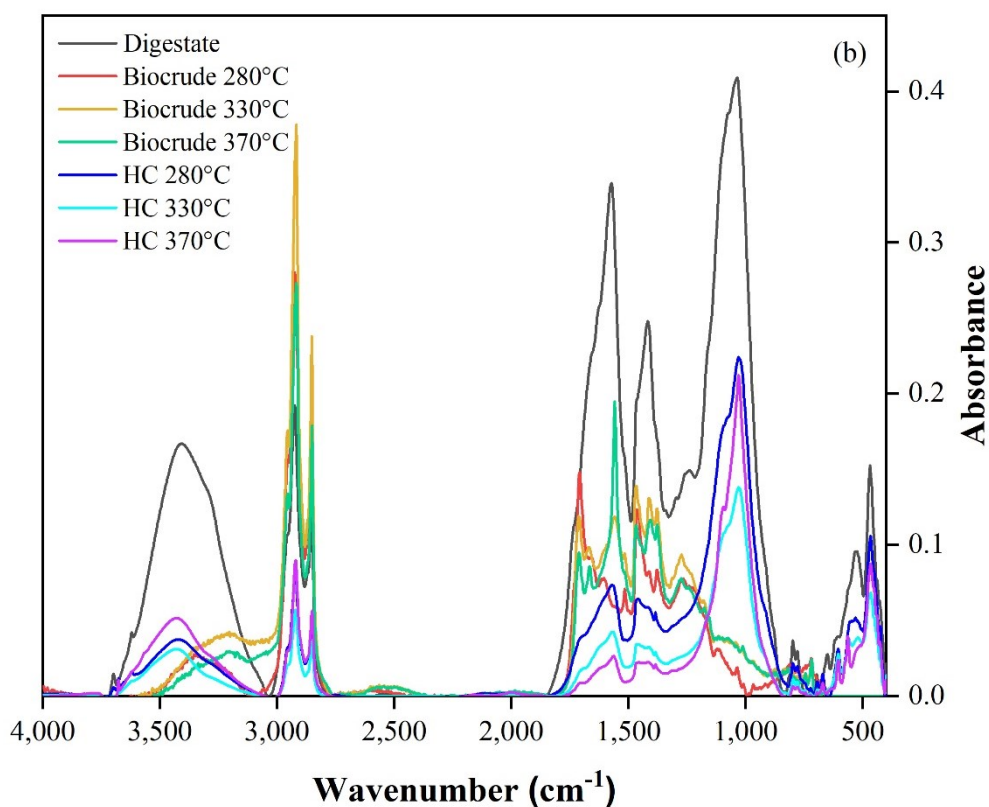
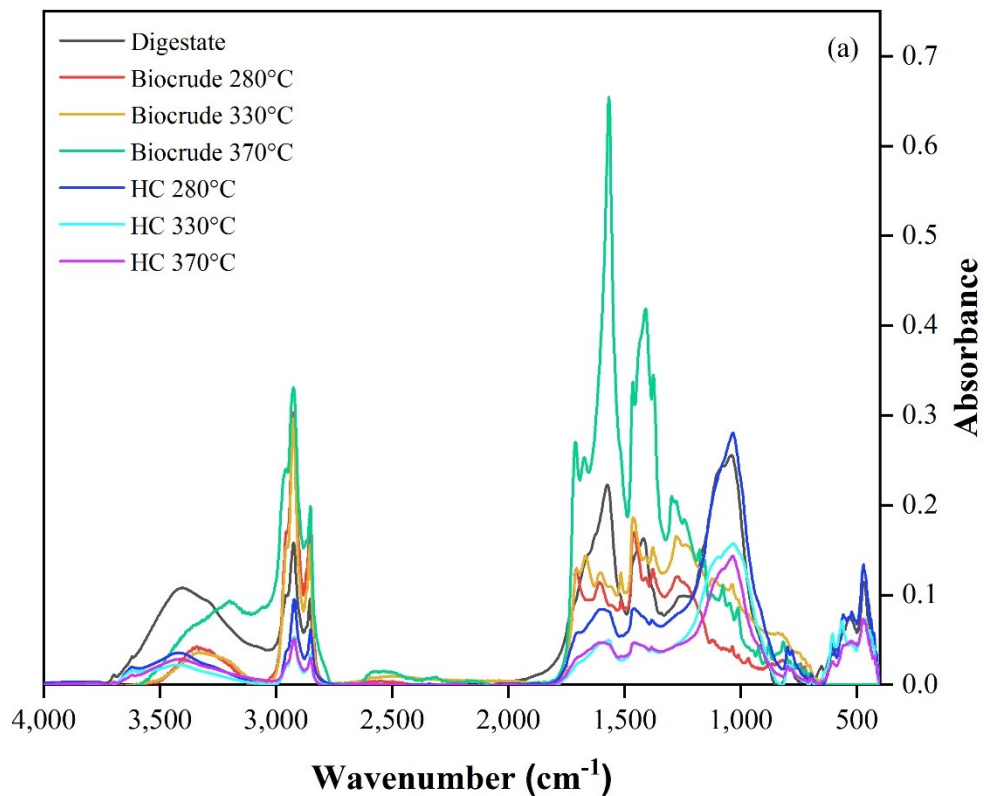


Figure 4.6. Fourier transform infrared spectroscopy of biocrude and hydrochar samples after hydrothermal liquefaction of digestate samples: (a) control, (b) bioplastic

The more intense peaks observed in the biocrude produced at 370 °C than at 280 °C highlight the influence of operating temperature on the conversion process. Temperatures around the sub- and near-critical region, close to the critical point of 373.74°C, can affect the characteristics of water, including its dielectric constant, density, and polarity (Seshasayee and Savage 2020b). These changes in water properties can enhance the hydrolysis reaction and improve the solubility of hydrophobic organic fractions, resulting in more efficient conversion of organic compounds into biocrude. Moreover, the variations in the peaks of the biocrude samples indicate that higher operating temperatures in the HTL promote the conversion of heteroatom compounds into biocrude (Xu et al. 2018). The higher peak intensity obtained at 370 °C further indicate that elevated temperatures contribute to the effective conversion of these compounds into valuable biocrude products.

The spectra of the HC and biocrude from bioplastic digestates (Fig.4.6b) revealed the disappearance of most functional groups associated with bioplastics (Fig.4.2). This suggests that HTL effectively converted or degraded bioplastics from the digestate samples. The FTIR results align with previous studies showing that an increase in reactor temperature to 250 °C causes plastics to surpass their glass transition temperature and potentially melt (Seshasayee and Savage 2020a; Niknejad et al. 2023). Furthermore, at higher temperatures such as 370 °C, coupled with a decrease in the dielectric constant of water, bioplastics are more likely to dissolve or degrade in the water phase (Seshasayee and Savage 2020a). These findings indicate that HTL holds significant potential for the substantial removal of residual bioplastic in HSAD digestate, thereby reducing the environmental risks associated with plastic pollution. The application of digestate as a biofertilizer in land application is a significant pathway for the dissemination of secondary contaminants, such as antimicrobial resistance genes (ARGs), into the environment, posing a global health threat (Mohammad et al. 2022). The presence of bioplastics can further exacerbate this concern by adsorbing antibiotics and potentially acting as carriers for ARGs (Pereira de Albuquerque et al. 2021). Therefore, the application of HTL-treated digestate can mitigate the potential negative impacts of plastic contamination (Chand et al. 2022). The efficient removal of bioplastics through HTL offers an environmentally favorable approach for the utilization of digestate to produce high-value bioproducts while decreasing environmental burden and promoting sustainable practices.

4.3.3 Principal component analysis

PCA was employed to assess the relative differences and similarities in the product distribution and the presence of distinct functional groups in biocrude, based on the specific

operating conditions. As depicted in Fig.4.7, the Control 330 °C and Bioplastics 330 °C samples were grouped together in the top-left quadrant, indicating a higher biocrude yield at 330 °C than at other operating temperatures. This suggests that at this temperature range, hydrolysis and dehydration reactions may promote ionic reactions, leading to the formation of monomers in the polar medium through initial biomass ionization (Mathanker et al. 2020a). In contrast, the Control 280 °C and Bioplastics 280 °C samples were clustered together in the bottom-left quadrant, with the HC yields and oxygenated compound loading vectors radiated towards these samples. This observation suggests that at lower temperatures, the relative abundance of HC and oxygenated compounds was higher. This can be attributed to the dominance of thermal decomposition and cracking reactions with increasing temperature, which decreases the likelihood of HC formation in the HTL process (Xu et al. 2018; Niknejad et al. 2023). Additionally, at higher temperatures, oxygenated compounds are better able to break down into smaller compounds such as hydrocarbons, decreasing the oxygen content (Xu et al. 2018; Niknejad et al. 2023). Furthermore, the loading vector of WSS shifted towards the bottom-right quadrant with Control 370 °C and Bioplastics 370 °C, indicating a higher abundance of WSS in these samples. Overall, the PCA analysis highlights the influence of operating temperature on the distribution of products and the presence of functional groups in biocrude. These findings provide valuable insights into the effect of operating conditions on the composition of biocrude in the HTL process.

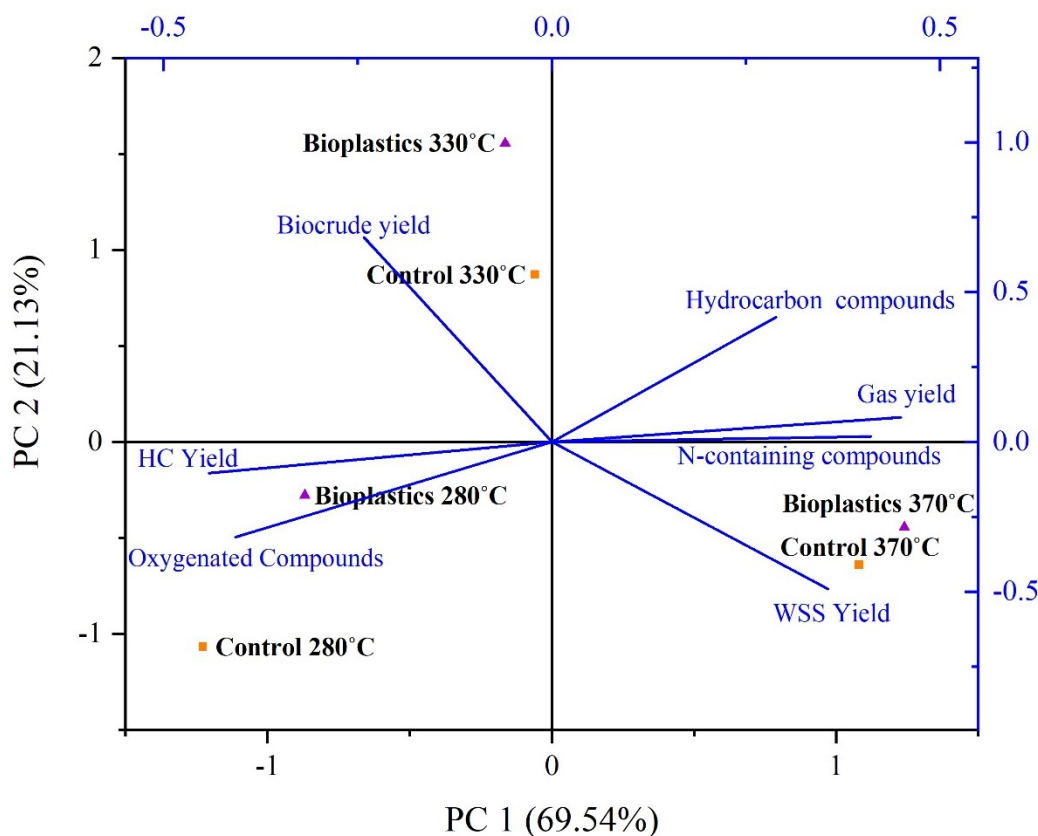


Figure 4.7. Principal component analysis of different functional groups in biocrude with products distribution.

4.4. Conclusions

This study of the co-digestion of SSO and bioplastics by HSAD followed by HTL has revealed that the presence of bioplastics in HSAD significantly reduced methane production, likely because of the breakdown of bioplastics into MPs and NPs as confirmed by FTIR analysis. However, through HTL post-processing, bioplastics were efficiently transformed into different products. Increasing the HTL temperature from 280 to 330 °C increased the weight percentage of biocrude, with the bioplastic-loaded reactor achieving the highest HHV. However, as the temperature further increased from 330 to 370°C, both the weight percentage of biocrude and HC decreased, while there was a peak rise in the weight percentage of total gas. FTIR analysis after HTL indicated the absence of bioplastics in the products, suggesting that HTL effectively removed bioplastics from the digestate by degrading and converting them into other products. These findings significantly advance our understanding of the behavior and fate of bioplastics in waste management processes and offer valuable insights for the development of sustainable waste management strategies. The knowledge gained from this study can guide

the implementation of effective measures to mitigate the environmental impact of bioplastics and optimize their utilization in a circular economy framework.

Chapter 5

Conclusions and Recommendations

5.1. Conclusion

This thesis focused on exploring the degradability of bioplastics during HSAD and their subsequent degradation during HTL under various operating conditions. Particularly, the results provided insights into the significance of HTL in converting the undegraded bioplastics in the HSAD digestate.

In an integrated process of HSAD followed by HTL, this thesis investigated the conversion of biodegradable disposables made from bioplastics into biomethane and biocrude. The results provided clear evidence that compostable plastic bags and plant-based utensils exhibited limited biodegradation in the conventional HSAD process, leading to a substantial reduction in cumulative methane yield by 29.5% and 8.99%, respectively. However, paper-based disposables showed promising results with a notable 2.6 times higher methane production compared to the control, indicating successful degradation in the HSAD process. To address the undegraded disposables, we employed HTL post-processing of the digestate, efficiently converting them into valuable biocrude. The process involved increasing the HTL temperature from 280 to 350°C, resulting in higher biocrude yields and superior biocrude quality in terms of biocrude content with higher HHV value.

To determine the impact of bioplastics on HSAD and HTL of SSO, the co-digestion of bioplastics and SSO under HSAD followed by HTL was conducted. It was found that bioplastics significantly inhibited methane production during the HSAD process, due to the breakdown of bioplastics into MPs and NPs as confirmed by FTIR analysis. However, through HTL post-processing, bioplastics were efficiently transformed into different products. Increasing the HTL temperature from 280 to 330°C led to an increase in the weight percentage of biocrude, with the bioplastic-loaded reactor achieving the highest HHV. FTIR analysis after HTL indicated the complete absence of bioplastics in the products, indicating HTL's effective removal and conversion of bioplastics into other products. Overall, these findings significantly advance our understanding of the behavior and fate of biodegradable disposables made from bioplastics in waste management processes. They offer valuable insights for the development of sustainable waste management strategies, guiding the implementation of effective measures

to mitigate the environmental impact of bioplastics and optimize their utilization within a circular economy framework.

5.2. Recommendations

- The results of this study indicated that the presence of bioplastics can inhibit methane production in the HSAD process. However, a more thorough investigation is required to comprehend the inhibitory impacts of bioplastics during this process. Delving into the specific mechanisms responsible for the decrease in methane production will facilitate the identification of potential strategies for mitigation.

- The study revealed that HTL could efficiently convert bioplastics into biocrude, biochar, and gases. However, it is imperative to assess the fate of these products, with particular attention to their potential impact on soil and water environments. Understanding the behavior of these residues is essential to ensure environmental safety on a broader scale.

- The results of this study determined that by increasing the HTL temperature up to 330°C, boost the production of biocrude in the bioplastic-loaded reactor. Nevertheless, it is essential to acknowledge that these outcomes are based on particular bioplastics employed in this investigation. Hence, further research is warranted, utilizing various bioplastics with distinct characteristics, to further validate and expand upon these findings.

- A detailed characterization of the biocrude produced through HTL is needed to explore potential upgrading techniques to improve its quality and suitability for various applications, such as biofuel production.

- A techno-economic analysis is essential to determine the economic viability of upscaling the integrated process of HSAD followed by HTL. It will evaluate costs, potential revenues, and market prospects, providing valuable insights into its commercial feasibility and competitiveness.

- It is recommended that future studies explore the potential and refinement of integrating HTL followed by AD processes. This should encompass a thorough examination of the compatibility of HTL-produced materials, specifically WSS, with AD requirements. Additionally, a comprehensive assessment of the overall feasibility of implementing this integrated approach is essential. Such endeavors hold significant promise for advancing our understanding and application of these combined technologies in the field.

- Significant research gaps persist in the utilization and safe disposal of products generated from HTL. Further investigations are needed to explore valorization methods,

treatment processes, and the environmental impact of disposal for these products. Additionally, a thorough analysis of the metal content is essential. This will contribute to a more comprehensive understanding and responsible management of the by-products generated through HTL processes.

References

- Abraham, A., Park, H., Choi, O., Sang, B.-I., 2021. Anaerobic co-digestion of bioplastics as a sustainable mode of waste management with improved energy production – A review. *Bioresour. Technol.* 322, 124537. <https://doi.org/https://doi.org/10.1016/j.biortech.2020.124537>
- Ahmed, T., Shahid, M., Azeem, F., Rasul, I., Shah, A.A., Noman, M., Hameed, A., Manzoor, N., Manzoor, I., Muhammad, S., 2018. Biodegradation of plastics: current scenario and future prospects for environmental safety. *Environ. Sci. Pollut. Res.* 25, 7287–7298. <https://doi.org/10.1007/s11356-018-1234-9>
- Ahn, J.Y., Chang, S.W., 2021. Effects of Sludge Concentration and Disintegration/Solubilization Pretreatment Methods on Increasing Anaerobic Biodegradation Efficiency and Biogas Production. *Sustain.* 2021, Vol. 13, Page 12887–13, 12887. <https://doi.org/10.3390/SU132212887>
- Akerlof, G.C., Oshry, H.I., 1950. The dielectric constant of water at high temperatures and in equilibrium with its vapor. *J. Am. Chem. Soc.* 72, 2844–2847.
- Akhtar, J., Amin, N.A.S., 2011. A review on process conditions for optimum bio-oil yield in hydrothermal liquefaction of biomass. *Renew. Sustain. Energy Rev.* 15, 1615–1624. <https://doi.org/https://doi.org/10.1016/j.rser.2010.11.054>
- Alvarez, R., Lidén, G., 2008. Semi-continuous co-digestion of solid slaughterhouse waste, manure, and fruit and vegetable waste. *Renew. Energy* 33, 726–734. <https://doi.org/https://doi.org/10.1016/j.renene.2007.05.001>
- Antero, R.V.P., Alves, A.C.F., de Oliveira, S.B., Ojala, S.A., Brum, S.S., 2020. Challenges and alternatives for the adequacy of hydrothermal carbonization of lignocellulosic biomass in cleaner production systems: A review. *J. Clean. Prod.* 252. <https://doi.org/10.1016/j.jclepro.2019.119899>
- Badoga, S., Alvarez-Majmutov, A., Xing, T., Gieleciak, R., Chen, J., 2020. Co-processing of hydrothermal liquefaction biocrude with vacuum gas oil through hydrotreating and hydrocracking to produce low-carbon fuels. *Energy & Fuels* 34, 7160–7169.
- Badrolnizam, R.S., Elham, O.S.J., Hadzifah, S.N., Husain, M.H.N., Hidayu, A.R., Mohammad,

- N.F., Daud, A.R.M., 2019. Sewage sludge conversion via hydrothermal liquefaction (HTL)—A preliminary study, in: *Journal of Physics: Conference Series*. IOP Publishing, p. 12108.
- Balagurumurthy, B., Singh, R., Bhaskar, T., 2015. Catalysts for Thermochemical Conversion of Biomass. *Recent Adv. Thermochem. Convers. Biomass* 109–132. <https://doi.org/10.1016/B978-0-444-63289-0.00004-1>
- Balat, M., 2008. Mechanisms of Thermochemical Biomass Conversion Processes. Part 3: Reactions of Liquefaction. *Energy Sources, Part A Recover. Util. Environ. Eff.* 30, 649–659. <https://doi.org/10.1080/10407780600817592>
- Balat, Mustafa, Balat, Mehmet, Kirtay, E., Balat, H., 2009. Main routes for the thermo-conversion of biomass into fuels and chemicals. Part 2: Gasification systems. *Energy Convers. Manag.* 50, 3158–3168. <https://doi.org/10.1016/J.ENCONMAN.2009.08.013>
- Barakat, A., Monlau, F., Steyer, J.-P., Carrere, H., 2012. Effect of lignin-derived and furan compounds found in lignocellulosic hydrolysates on biomethane production. *Bioresour. Technol.* 104, 90–99.
- Basar, I.A., Liu, H., Carrere, H., Trably, E., Eskicioglu, C., 2021a. A review on key design and operational parameters to optimize and develop hydrothermal liquefaction of biomass for biorefinery applications. *Green Chem.* 23, 1404–1446. <https://doi.org/10.1039/D0GC04092D>
- Basar, I.A., Liu, H., Carrere, H., Trably, E., Eskicioglu, C., 2021b. A review on key design and operational parameters to optimize and develop hydrothermal liquefaction of biomass for biorefinery applications. *Green Chem.* 23, 1404–1446. <https://doi.org/10.1039/D0GC04092D>
- Bátori, V., Åkesson, D., Zamani, A., Taherzadeh, M.J., Sárvári Horváth, I., 2018. Anaerobic degradation of bioplastics: A review. *Waste Manag.* 80, 406–413. <https://doi.org/https://doi.org/10.1016/j.wasman.2018.09.040>
- Battista, F., Frison, N., Bolzonella, D., 2021. Can bioplastics be treated in conventional anaerobic digesters for food waste treatment? *Environ. Technol. Innov.* 22, 101393. <https://doi.org/https://doi.org/10.1016/j.eti.2021.101393>

- Bayat, H., Cheng, F., Dehghanizadeh, M., Soliz, N., Brewer, C.E., Jena, U., 2019. Hydrothermal liquefaction of food waste: Bio-crude oil Characterization, Mass and Energy Balance, in: 2019 ASABE Annual International Meeting. American Society of Agricultural and Biological Engineers, p. 1.
- Biller, P., Lawson, D., Madsen, R.B., Becker, J., Iversen, B.B., Glasius, M., 2017. Assessment of agricultural crops and natural vegetation in Scotland for energy production by anaerobic digestion and hydrothermal liquefaction. *Biomass Convers. Biorefinery* 7, 467–477.
- Biller, P., Madsen, R.B., Klemmer, M., Becker, J., Iversen, B.B., Glasius, M., 2016. Effect of hydrothermal liquefaction aqueous phase recycling on bio-crude yields and composition. *Bioresour. Technol.* 220, 190–199.
- Brown, T.M., Duan, P., Savage, P.E., 2010. Hydrothermal liquefaction and gasification of *Nannochloropsis* sp. *Energy & Fuels* 24, 3639–3646.
- Cazaudehore, G., Monlau, F., Gassie, C., Lallement, A., Guyoneaud, R., 2021. Methane production and active microbial communities during anaerobic digestion of three commercial biodegradable coffee capsules under mesophilic and thermophilic conditions. *Sci. Total Environ.* 784, 146972. <https://doi.org/https://doi.org/10.1016/j.scitotenv.2021.146972>
- Chae, K.J., Jang, A., Yim, S.K., Kim, I.S., 2008. The effects of digestion temperature and temperature shock on the biogas yields from the mesophilic anaerobic digestion of swine manure. *Bioresour. Technol.* 99, 1–6. <https://doi.org/https://doi.org/10.1016/j.biortech.2006.11.063>
- Chand, R., Kohansal, K., Toor, S., Pedersen, T.H., Vollertsen, J., 2022. Microplastics degradation through hydrothermal liquefaction of wastewater treatment sludge. *J. Clean Prod.* 335, 130383. <https://doi.org/10.1016/J.JCLEPRO.2022.130383>
- Chen, G., Hu, M., Du, G., Tian, S., He, Z., Liu, B., Ma, W., 2019. Hydrothermal liquefaction of sewage sludge by microwave pretreatment. *Energy & Fuels* 34, 1145–1152.
- Chen, H., Hao, S., Chen, Z., O-Thong, S., Fan, J., Clark, J., Luo, G., Zhang, S., 2020. Mesophilic and thermophilic anaerobic digestion of aqueous phase generated from hydrothermal liquefaction of cornstalk: Molecular and metabolic insights. *Water Res.* 168, 115199. <https://doi.org/https://doi.org/10.1016/j.watres.2019.115199>

- Chen, H., Tang, M., Yang, X., Tsang, Y.F., Wu, Y., Wang, D., Zhou, Y., 2021. Polyamide 6 microplastics facilitate methane production during anaerobic digestion of waste activated sludge. *Chem. Eng. J.* 408, 127251. <https://doi.org/https://doi.org/10.1016/j.cej.2020.127251>
- Chen, W.-H., Chu, Y.-S., Liu, J.-L., Chang, J.-S., 2018. Thermal degradation of carbohydrates, proteins and lipids in microalgae analyzed by evolutionary computation. *Energy Convers. Manag.* 160, 209–219.
- Chen, W.-T., Zhang, Y., Zhang, J., Yu, G., Schideman, L.C., Zhang, P., Minarick, M., 2014. Hydrothermal liquefaction of mixed-culture algal biomass from wastewater treatment system into bio-crude oil. *Bioresour. Technol.* 152, 130–139.
- Cherad, R., Onwudili, J.A., Biller, P., Williams, P.T., Ross, A.B., 2016. Hydrogen production from the catalytic supercritical water gasification of process water generated from hydrothermal liquefaction of microalgae. *Fuel* 166, 24–28. <https://doi.org/https://doi.org/10.1016/j.fuel.2015.10.088>
- Cho, H.S., Moon, H.S., Kim, M., Nam, K., Kim, J.Y., 2011. Biodegradability and biodegradation rate of poly(caprolactone)-starch blend and poly(butylene succinate) biodegradable polymer under aerobic and anaerobic environment. *Waste Manag.* 31, 475–480. <https://doi.org/https://doi.org/10.1016/j.wasman.2010.10.029>
- Choe, S., Kim, Y., Won, Y., Myung, J., 2021. Bridging three gaps in biodegradable plastics: misconceptions and truths about biodegradation. *Front. Chem.* 9, 671750.
- Chowdhury, B., Lin, L., Dhar, B.R., Islam, M.N., McCartney, D., Kumar, A., 2019. Enhanced biomethane recovery from fat, oil, and grease through co-digestion with food waste and addition of conductive materials. *Chemosphere* 236, 124362. <https://doi.org/10.1016/J.CHEMOSPHERE.2019.124362>
- Chowdhury, B., Magsi, S.B., Ting, H.N.J., Dhar, B.R., 2020. High-solids anaerobic digestion followed by ultrasonication of digestate and wet-type anaerobic digestion for enhancing methane yield from OFMSW. *Processes* 8, 555.
- Chua, T.-K., Tseng, M., Yang, M.-K., 2013. Degradation of Poly (ϵ -caprolactone) by thermophilic *Streptomyces thermoviolaceus* subsp. *thermoviolaceus* 76T-2. *Amb Express* 3, 1–7.

- Cucina, M., Carlet, L., De Nisi, P., Somensi, C.A., Giordano, A., Adani, F., 2022a. Degradation of biodegradable bioplastics under thermophilic anaerobic digestion: A full-scale approach. *J. Clean. Prod.* 368, 133232. <https://doi.org/https://doi.org/10.1016/j.jclepro.2022.133232>
- Cucina, M., Carlet, L., De Nisi, P., Somensi, C.A., Giordano, A., Adani, F., 2022b. Degradation of biodegradable bioplastics under thermophilic anaerobic digestion: A full-scale approach. *J. Clean. Prod.* 368, 133232. <https://doi.org/10.1016/J.JCLEPRO.2022.133232>
- Cucina, M., De Nisi, P., Trombino, L., Tambone, F., Adani, F., 2021a. Degradation of bioplastics in organic waste by mesophilic anaerobic digestion, composting and soil incubation. *Waste Manag.* 134, 67–77. <https://doi.org/10.1016/J.WASMAN.2021.08.016>
- Cucina, M., De Nisi, P., Trombino, L., Tambone, F., Adani, F., 2021b. Degradation of bioplastics in organic waste by mesophilic anaerobic digestion, composting and soil incubation. *Waste Manag.* 134, 67–77. <https://doi.org/https://doi.org/10.1016/j.wasman.2021.08.016>
- Dastyar, W., Mirsoleimani Azizi, S.M., Meshref, M.N.A., Dhar, B.R., 2021a. Powdered activated carbon amendment in percolate tank enhances high-solids anaerobic digestion of organic fraction of municipal solid waste. *Process Saf. Environ. Prot.* 151, 63–70. <https://doi.org/10.1016/J.PSEP.2021.04.033>
- Dastyar, W., Mirsoleimani Azizi, S.M., Meshref, M.N.A., Dhar, B.R., 2021b. Powdered activated carbon amendment in percolate tank enhances high-solids anaerobic digestion of organic fraction of municipal solid waste. *Process Saf. Environ. Prot.* 151, 63–70. <https://doi.org/10.1016/j.psep.2021.04.033>
- Dastyar, W., Mohammad Mirsoleimani Azizi, S., Dhadwal, M., Ranjan Dhar, B., 2021c. High-solids anaerobic digestion of organic fraction of municipal solid waste: Effects of feedstock to inoculum ratio and percolate recirculation time. *Bioresour. Technol.* 337, 125335. <https://doi.org/10.1016/J.BIORTECH.2021.125335>
- de Albuquerque, F.P., Dastyar, W., Mirsoleimani Azizi, S.M., Zakaria, B.S., Kumar, A., Dhar, B.R., 2022. Carbon cloth amendment for boosting high-solids anaerobic digestion with percolate recirculation: Spatial patterns of microbial communities. *Chemosphere* 307, 135606. <https://doi.org/10.1016/J.CHEMOSPHERE.2022.135606>

- de Vlieger, D.J.M., Chakinala, A.G., Lefferts, L., Kersten, S.R.A., Seshan, K., Brilman, D.W.F., 2012. Hydrogen from ethylene glycol by supercritical water reforming using noble and base metal catalysts. *Appl. Catal. B Environ.* 111–112, 536–544. <https://doi.org/https://doi.org/10.1016/j.apcatb.2011.11.005>
- Déniel, M., Haarlemmer, G., Roubaud, A., Weiss-Hortala, E., Fages, J., 2016. Energy valorisation of food processing residues and model compounds by hydrothermal liquefaction. *Renew. Sustain. Energy Rev.* 54, 1632–1652. <https://doi.org/https://doi.org/10.1016/j.rser.2015.10.017>
- Di Cesare, A., Pinnell, L.J., Brambilla, D., Elli, G., Sabatino, R., Sathicq, M.B., Corno, G., O'Donnell, C., Turner, J.W., 2021. Bioplastic accumulates antibiotic and metal resistance genes in coastal marine sediments. *Environ. Pollut.* 291, 118161.
- Dilkes-Hoffman, L.S., Pratt, S., Lant, P.A., Laycock, B., 2019. 19 - The Role of Biodegradable Plastic in Solving Plastic Solid Waste Accumulation, in: Al-Salem, S.M.B.T.-P. to E. (Ed.), *Plastics Design Library*. William Andrew Publishing, pp. 469–505. <https://doi.org/https://doi.org/10.1016/B978-0-12-813140-4.00019-4>
- Dimitriadis, A., Bezergianni, S., 2017. Hydrothermal liquefaction of various biomass and waste feedstocks for biocrude production: A state of the art review. *Renew. Sustain. Energy Rev.* 68, 113–125. <https://doi.org/https://doi.org/10.1016/j.rser.2016.09.120>
- Dolci, G., Catenacci, A., Malpei, F., Grosso, M., 2021. Effect of Paper vs. Bioplastic Bags on Food Waste Collection and Processing. *Waste and Biomass Valorization* 12, 6293–6307. <https://doi.org/10.1007/s12649-021-01448-4>
- Endres, H.-J., Siebert-Raths, A., 2011. End-of-Life Options for Biopolymers, in: Endres, H.-J., Siebert-Raths, A.B.T.-E.B. (Eds.), . Hanser, pp. 225–243. <https://doi.org/https://doi.org/10.3139/9783446430020.006>
- Enfrin, M., Dumée, L.F., Lee, J., 2019a. Nano/microplastics in water and wastewater treatment processes—origin, impact and potential solutions. *Water Res.* 161, 621–638.
- Enfrin, M., Dumée, L.F., Lee, J., 2019b. Nano/microplastics in water and wastewater treatment processes – Origin, impact and potential solutions. *Water Res.* 161, 621–638. <https://doi.org/10.1016/J.WATRES.2019.06.049>

- Esposito, G., Frunzo, L., Giordano, A., Liotta, F., Panico, A., Pirozzi, F., 2012. Anaerobic co-digestion of organic wastes. *Rev. Environ. Sci. Bio/Technology* 11, 325–341. <https://doi.org/10.1007/s11157-012-9277-8>
- Fagbohunge, M.O., Dodd, I.C., Herbert, B.M.J., Li, H., Ricketts, L., Semple, K.T., 2015. High solid anaerobic digestion: Operational challenges and possibilities. *Environ. Technol. Innov.* 4, 268–284. <https://doi.org/10.1016/J.ETI.2015.09.003>
- Feng, S., Wei, R., Leitch, M., Xu, C.C., 2018. Comparative study on lignocellulose liquefaction in water, ethanol, and water/ethanol mixture: Roles of ethanol and water. *Energy* 155, 234–241. <https://doi.org/https://doi.org/10.1016/j.energy.2018.05.023>
- Folino, A., Karageorgiou, A., Calabrò, P.S., Komilis, D., 2020. Biodegradation of Wasted Bioplastics in Natural and Industrial Environments: A Review. *Sustain.* 2020, Vol. 12, Page 6030 12, 6030. <https://doi.org/10.3390/SU12156030>
- Garcia Alba, L., Torri, C., Samorì, C., Van Der Spek, J., Fabbri, D., Kersten, S.R.A., Brilman, D.W.F., 2012. Hydrothermal treatment (HTT) of microalgae: evaluation of the process as conversion method in an algae biorefinery concept. *Energy & fuels* 26, 642–657.
- Gollakota, A.R.K., Kishore, N., Gu, S., 2018. A review on hydrothermal liquefaction of biomass. *Renew. Sustain. Energy Rev.* 81, 1378–1392. <https://doi.org/https://doi.org/10.1016/j.rser.2017.05.178>
- Greenhalf, C., 2014. Thermochemical characterisation of various biomass feedstock and bio-oil generated by fast pyrolysis.
- Guilford, N., 2009. A new technology for the anaerobic digestion of organic waste.
- Guilford, N.G.H., Lee, H.P., Kanger, K., Meyer, T., Edwards, E.A., 2019. Solid-State Anaerobic Digestion of Mixed Organic Waste: The Synergistic Effect of Food Waste Addition on the Destruction of Paper and Cardboard. *Environ. Sci. Technol.* 53, 12677–12687. <https://doi.org/10.1021/acs.est.9b04644>
- Haffiez, N., Zakaria, B.S., Azizi, S.M.M., Dhar, B.R., 2023. Antibiotic resistance genes proliferation under anaerobic degradation of polylactic acid and polyhydroxy butyrate bioplastics. *Environ. Int.* 175, 107938.
- Haider, M.S., Castello, D., Michalski, K.M., Pedersen, T.H., Rosendahl, L.A., 2018. Catalytic

- hydrotreatment of microalgae biocrude from continuous hydrothermal liquefaction: Heteroatom removal and their distribution in distillation cuts. *Energies* 11, 3360.
- Heidari, M., Dutta, A., Acharya, B., Mahmud, S., 2019. A review of the current knowledge and challenges of hydrothermal carbonization for biomass conversion. *J. Energy Inst.* 92, 1779–1799. <https://doi.org/https://doi.org/10.1016/j.joei.2018.12.003>
- Hobbs, S.R., Harris, T.M., Barr, W.J., Landis, A.E., 2021. Life Cycle Assessment of Bioplastics and Food Waste Disposal Methods. *Sustainability*. <https://doi.org/10.3390/su13126894>
- Hoelzle, R.D., Viridis, B., Batstone, D.J., 2014. Regulation mechanisms in mixed and pure culture microbial fermentation. *Biotechnol. Bioeng.* 111, 2139–2154. <https://doi.org/https://doi.org/10.1002/bit.25321>
- Huang, H. jun, Yuan, X. zhong, Zhu, H. na, Li, H., Liu, Y., Wang, X. li, Zeng, G. ming, 2013. Comparative studies of thermochemical liquefaction characteristics of microalgae, lignocellulosic biomass and sewage sludge. *Energy* 56, 52–60. <https://doi.org/10.1016/J.ENERGY.2013.04.065>
- Jena, U., Das, K.C., Kastner, J.R., 2012. Comparison of the effects of Na₂CO₃, Ca₃(PO₄)₂, and NiO catalysts on the thermochemical liquefaction of microalga *Spirulina platensis*. *Appl. Energy* 98, 368–375.
- Kambo, H.S., Dutta, A., 2015. A comparative review of biochar and hydrochar in terms of production, physico-chemical properties and applications. *Renew. Sustain. Energy Rev.* 45, 359–378. <https://doi.org/https://doi.org/10.1016/j.rser.2015.01.050>
- Kang, J.-H., Kang, S.-W., Kim, W.-J., Kim, D.-H., Im, S.-W., 2022. Anaerobic Co-digestion of bioplastics and food waste under mesophilic and thermophilic conditions: synergistic effect and biodegradation. *Fermentation* 8, 638.
- Karamanlioglu, M., Preziosi, R., Robson, G.D., 2017. Abiotic and biotic environmental degradation of the bioplastic polymer poly(lactic acid): A review. *Polym. Degrad. Stab.* 137, 122–130. <https://doi.org/10.1016/J.POLYMDEGRADSTAB.2017.01.009>
- Karki, R., Chuenchart, W., Surendra, K.C., Shrestha, S., Raskin, L., Sung, S., Hashimoto, A., Kumar Khanal, S., 2021. Anaerobic co-digestion: Current status and perspectives. *Bioresour. Technol.* 330, 125001.

<https://doi.org/https://doi.org/10.1016/j.biortech.2021.125001>

Kaza, S., Yao, L., Bhada-Tata, P., Van Woerden, F., 2018. What a waste 2.0: a global snapshot of solid waste management to 2050. World Bank Publications.

Kumar, A., Samadder, S.R., 2020. Performance evaluation of anaerobic digestion technology for energy recovery from organic fraction of municipal solid waste: A review. *Energy* 197, 117253. <https://doi.org/https://doi.org/10.1016/j.energy.2020.117253>

Kumar, G.S., Girija, E.K., Thamizhavel, A., Yokogawa, Y., Kalkura, S.N., 2010. Synthesis and characterization of bioactive hydroxyapatite–calcite nanocomposite for biomedical applications. *J. Colloid Interface Sci.* 349, 56–62. <https://doi.org/10.1016/J.JCIS.2010.05.038>

Kumar, M., Olajire Oyedun, A., Kumar, A., 2018. A review on the current status of various hydrothermal technologies on biomass feedstock. *Renew. Sustain. Energy Rev.* 81, 1742–1770. <https://doi.org/https://doi.org/10.1016/j.rser.2017.05.270>

Lachos-Perez, D., César Torres-Mayanga, P., Abaide, E.R., Zobot, G.L., De Castilhos, F., 2022a. Hydrothermal carbonization and Liquefaction: differences, progress, challenges, and opportunities. *Bioresour. Technol.* 343, 126084. <https://doi.org/10.1016/J.BIORTECH.2021.126084>

Lachos-Perez, D., Torres-Mayanga, P.C., Abaide, E.R., Zobot, G.L., De Castilhos, F., 2022b. Hydrothermal carbonization and Liquefaction: differences, progress, challenges, and opportunities. *Bioresour. Technol.* 343, 126084.

Lallement, A., Vasmara, C., Marchetti, R., Monlau, F., Mbachu, O., Kaparaju, P., 2021. Chapter 10 - Anaerobic digestion of bioplastics, in: Tyagi, V., Aboudi, K.B.T.-C.E. and R.R. (Eds.), . Elsevier, pp. 253–270. <https://doi.org/https://doi.org/10.1016/B978-0-323-85223-4.00023-3>

Lavanya, M., Meenakshisundaram, A., Renganathan, S., Chinnasamy, S., Lewis, D.M., Nallasivam, J., Bhaskar, S., 2016. Hydrothermal liquefaction of freshwater and marine algal biomass: A novel approach to produce distillate fuel fractions through blending and co-processing of biocrude with petrocrude. *Bioresour. Technol.* 203, 228–235.

Leng, L., Li, J., Wen, Z., Zhou, W., 2018. Use of microalgae to recycle nutrients in aqueous

- phase derived from hydrothermal liquefaction process. *Bioresour. Technol.* 256, 529–542.
- León, M., Marcilla, A.F., García, Á.N., 2019. Hydrothermal liquefaction (HTL) of animal by-products: Influence of operating conditions. *Waste Manag.* 99, 49–59.
- Li, W., Khalid, H., Amin, F.R., Zhang, H., Dai, Z., Chen, C., Liu, G., 2020. Biomethane production characteristics, kinetic analysis, and energy potential of different paper wastes in anaerobic digestion. *Renew. Energy* 157, 1081–1088. <https://doi.org/10.1016/J.RENENE.2020.04.035>
- Lim, S.L., Lee, L.H., Wu, T.Y., 2016. Sustainability of using composting and vermicomposting technologies for organic solid waste biotransformation: recent overview, greenhouse gases emissions and economic analysis. *J. Clean. Prod.* 111, 262–278. <https://doi.org/https://doi.org/10.1016/j.jclepro.2015.08.083>
- Lu, J., Liu, Z., Zhang, Y., Savage, P.E., 2018. Synergistic and Antagonistic Interactions during Hydrothermal Liquefaction of Soybean Oil, Soy Protein, Cellulose, Xylose, and Lignin. *ACS Sustain. Chem. Eng.* 6, 14501–14509. <https://doi.org/10.1021/acssuschemeng.8b03156>
- Luong, D., Sephton, M.A., Watson, J.S., 2015. Subcritical water extraction of organic matter from sedimentary rocks. *Anal. Chim. Acta* 879, 48–57. <https://doi.org/https://doi.org/10.1016/j.aca.2015.04.027>
- Maragkaki, A., Tsompanidis, C., Velonia, K., Manios, T., 2023. Pilot-Scale Anaerobic Co-Digestion of Food Waste and Polylactic Acid. *Sustainability* 15, 10944.
- Marrone, P.A., Elliott, D.C., Billing, J.M., Hallen, R.T., Hart, T.R., Kadota, P., Moeller, J.C., Randel, M.A., Schmidt, A.J., 2018. Bench-Scale Evaluation of Hydrothermal Processing Technology for Conversion of Wastewater Solids to Fuels: Marrone et al. *Water Environ. Res.* 90, 329–342.
- Massardier-Nageotte, V., Pestre, C., Cruard-Pradet, T., Bayard, R., 2006. Aerobic and anaerobic biodegradability of polymer films and physico-chemical characterization. *Polym. Degrad. Stab.* 91, 620–627.
- Mathanker, A., Pudasainee, D., Kumar, A., Gupta, R., 2020a. Hydrothermal liquefaction of lignocellulosic biomass feedstock to produce biofuels: Parametric study and products

- characterization. *Fuel* 271, 117534. <https://doi.org/10.1016/J.FUEL.2020.117534>
- Mathanker, A., Pudasainee, D., Kumar, A., Gupta, R., 2020b. Hydrothermal liquefaction of lignocellulosic biomass feedstock to produce biofuels: Parametric study and products characterization. *Fuel* 271, 117534.
- Matthews, C., Moran, F., Jaiswal, A.K., 2021. A review on European Union's strategy for plastics in a circular economy and its impact on food safety. *J. Clean. Prod.* 283, 125263. <https://doi.org/10.1016/J.JCLEPRO.2020.125263>
- McKendry, P., 2002. Energy production from biomass (part 2): conversion technologies. *Bioresour. Technol.* 83, 47–54. [https://doi.org/10.1016/S0960-8524\(01\)00119-5](https://doi.org/10.1016/S0960-8524(01)00119-5)
- Meshref, M.N.A., Azizi, S.M.M., Dastyar, W., Maal-Bared, R., Dhar, B.R., 2021. Low-temperature thermal hydrolysis of sludge prior to anaerobic digestion: Principal component analysis (PCA) of experimental data. *Data Br.* 38, 107323. <https://doi.org/https://doi.org/10.1016/j.dib.2021.107323>
- Minowa, T., Zhen, F., Ogi, T., 1998. Cellulose decomposition in hot-compressed water with alkali or nickel catalyst. *J. Supercrit. Fluids* 13, 253–259. [https://doi.org/https://doi.org/10.1016/S0896-8446\(98\)00059-X](https://doi.org/https://doi.org/10.1016/S0896-8446(98)00059-X)
- Mirsoleimani Azizi, S.M., Zakaria, B.S., Haffiez, N., Dhar, B.R., 2023. Sludge Thermal Hydrolysis for Mitigating Oxidative Stress of Polystyrene Nanoplastics in Anaerobic Digestion: Significance of the Solids Content. *ACS Sustain. Chem. Eng.*
- Mishra, A., Gautam, S., Sharma, T., 2018. Effect of operating parameters on coal gasification. *Int. J. Coal Sci. Technol.* 5, 113–125. <https://doi.org/10.1007/s40789-018-0196-3>
- Mishra, S., Mohanty, K., 2020. Co-HTL of domestic sewage sludge and wastewater treatment derived microalgal biomass – An integrated biorefinery approach for sustainable biocrude production. *Energy Convers. Manag.* 204, 112312. <https://doi.org/https://doi.org/10.1016/j.enconman.2019.112312>
- Mohammad Mirsoleimani Azizi, S., Dastyar, W., Meshref, M.N.A., Maal-Bared, R., Ranjan Dhar, B., 2021a. Low-temperature thermal hydrolysis for anaerobic digestion facility in wastewater treatment plant with primary sludge fermentation. *Chem. Eng. J.* 426, 130485. <https://doi.org/10.1016/J.CEJ.2021.130485>

- Mohammad Mirsoleimani Azizi, S., Hai, F.I., Lu, W., Al-Mamun, A., Ranjan Dhar, B., 2021b. A review of mechanisms underlying the impacts of (nano)microplastics on anaerobic digestion. *Bioresour. Technol.* 329, 124894. <https://doi.org/10.1016/J.BIORTECH.2021.124894>
- Mohammad Mirsoleimani Azizi, S., Hai, F.I., Lu, W., Al-Mamun, A., Ranjan Dhar, B., 2021c. A review of mechanisms underlying the impacts of (nano)microplastics on anaerobic digestion. *Bioresour. Technol.* 329, 124894. <https://doi.org/https://doi.org/10.1016/j.biortech.2021.124894>
- Mohammad, S., Azizi, M., Haffiez, N., Zakaria, B.S., Ranjan Dhar, B., 2022. Thermal Hydrolysis of Sludge Counteracts Polystyrene Nanoplastics-Induced Stress during Anaerobic Digestion. *ACS ES&T Eng.* <https://doi.org/10.1021/ACSESTENGG.1C00460>
- Monlau, F., Sambusiti, C., Barakat, A., Quéméneur, M., Trably, E., Steyer, J.-P., Carrère, H., 2014. Do furanic and phenolic compounds of lignocellulosic and algae biomass hydrolyzate inhibit anaerobic mixed cultures? A comprehensive review. *Biotechnol. Adv.* 32, 934–951.
- Mu, L., Zhang, L., Zhu, K., Ma, J., Li, A., 2018. Semi-continuous anaerobic digestion of extruded OFMSW: Process performance and energetics evaluation. *Bioresour. Technol.* 247, 103–115. <https://doi.org/https://doi.org/10.1016/j.biortech.2017.09.085>
- Na, S.H., Kim, M.J., Kim, J.T., Jeong, S., Lee, S., Chung, J., Kim, E.J., 2021. Microplastic removal in conventional drinking water treatment processes: Performance, mechanism, and potential risk. *Water Res.* 202, 117417. <https://doi.org/10.1016/J.WATRES.2021.117417>
- Narancic, T., Cerrone, F., Beagan, N., O'Connor, K.E., 2020. Recent Advances in Bioplastics: Application and Biodegradation. *Polymers (Basel)*. <https://doi.org/10.3390/polym12040920>
- Narancic, T., Verstichel, S., Reddy Chaganti, S., Morales-Gamez, L., Kenny, S.T., De Wilde, B., Babu Padamati, R., O'Connor, K.E., 2018. Biodegradable Plastic Blends Create New Possibilities for End-of-Life Management of Plastics but They Are Not a Panacea for Plastic Pollution. *Environ. Sci. Technol.* 52, 10441–10452. <https://doi.org/10.1021/acs.est.8b02963>

- Ni, J., Qian, L., Wang, Y., Zhang, B., Gu, H., Hu, Y., Wang, Q., 2022. A review on fast hydrothermal liquefaction of biomass. *Fuel* 327, 125135. <https://doi.org/10.1016/J.FUEL.2022.125135>
- Niknejad, P., Azizi, S.M.M., Hillier, K., Gupta, R., Dhar, B.R., 2023. Biodegradability and transformation of biodegradable disposables in high-solids anaerobic digestion followed by hydrothermal liquefaction. *Resour. Conserv. Recycl.* 193, 106979. <https://doi.org/https://doi.org/10.1016/j.resconrec.2023.106979>
- Nsair, A., Onen Cinar, S., Alassali, A., Abu Qdais, H., Kuchta, K., 2020. Operational Parameters of Biogas Plants: A Review and Evaluation Study. *Energies*. <https://doi.org/10.3390/en13153761>
- Nussbaumer, T., 2003. Combustion and co-combustion of biomass: fundamentals, technologies, and primary measures for emission reduction. *Energy & fuels* 17, 1510–1521.
- Panigrahi, S., Dubey, B.K., 2019. A critical review on operating parameters and strategies to improve the biogas yield from anaerobic digestion of organic fraction of municipal solid waste. *Renew. Energy* 143, 779–797. <https://doi.org/https://doi.org/10.1016/j.renene.2019.05.040>
- Papadokonstantakis, S., Gambardella, A., Askmar, J., Ding, Y., 2018. Superstructure investigation for P-recovery technologies integration with macroalgae based hydrothermal liquefaction, in: *Computer Aided Chemical Engineering*. Elsevier, pp. 1753–1758.
- Patnaik, S., Kumar, S., Panda, A.K., 2020a. Thermal degradation of eco-friendly alternative plastics: kinetics and thermodynamics analysis. *Environ. Sci. Pollut. Res.* 27, 14991–15000. <https://doi.org/10.1007/S11356-020-07919-W/TABLES/6>
- Patnaik, S., Panda, A.K., Kumar, S., 2020b. Thermal degradation of corn starch based biodegradable plastic plates and determination of kinetic parameters by isoconversional methods using thermogravimetric analyzer. *J. Energy Inst.* 93, 1449–1459. <https://doi.org/10.1016/J.JOEI.2020.01.007>
- Patrício Silva, A.L., 2021. Future-proofing plastic waste management for a circular bioeconomy. *Curr. Opin. Environ. Sci. Heal.* 22, 100263. <https://doi.org/https://doi.org/10.1016/j.coesh.2021.100263>

- Peng, W., Wang, Z., Shu, Y., Lü, F., Zhang, H., Shao, L., He, P., 2022. Fate of a biobased polymer via high-solid anaerobic co-digestion with food waste and following aerobic treatment: Insights on changes of polymer physicochemical properties and the role of microbial and fungal communities. *Bioresour. Technol.* 343, 126079. <https://doi.org/10.1016/J.BIORTECH.2021.126079>
- Pennington, M., 2018. Anaerobic digestion facilities processing food waste in the United States in 2015. *Surv. Results. EPA.*
- Pereira de Albuquerque, F., Dhadwal, M., Dastyar, W., Mirsoleimani Azizi, S.M., Karidio, I., Zaman, H., Dhar, B.R., 2021. Fate of disposable face masks in high-solids anaerobic digestion: Experimental observations and review of potential environmental implications. *Case Stud. Chem. Environ. Eng.* 3, 100082. <https://doi.org/10.1016/J.CSCEE.2021.100082>
- Peterson, A.A., Lachance, R.P., Tester, J.W., 2010. Kinetic Evidence of the Maillard Reaction in Hydrothermal Biomass Processing: Glucose–Glycine Interactions in High-Temperature, High-Pressure Water. *Ind. Eng. Chem. Res.* 49, 2107–2117. <https://doi.org/10.1021/ie9014809>
- Peterson, A.A., Vogel, F., Lachance, R.P., Fröling, M., Antal Jr, M.J., Tester, J.W., 2008. Thermochemical biofuel production in hydrothermal media: a review of sub-and supercritical water technologies. *Energy Environ. Sci.* 1, 32–65.
- Posmanik, R., Labatut, R.A., Kim, A.H., Usack, J.G., Tester, J.W., Angenent, L.T., 2017. Coupling hydrothermal liquefaction and anaerobic digestion for energy valorization from model biomass feedstocks. *Bioresour. Technol.* 233, 134–143. <https://doi.org/10.1016/J.BIORTECH.2017.02.095>
- Posmanik, R., Martinez, C.M., Cantero-Tubilla, B., Cantero, D.A., Sills, D.L., Cocero, M.J., Tester, J.W., 2018. Acid and Alkali Catalyzed Hydrothermal Liquefaction of Dairy Manure Digestate and Food Waste. *ACS Sustain. Chem. Eng.* 6, 2724–2732. https://doi.org/10.1021/ACSSUSCHEMENG.7B04359/ASSET/IMAGES/LARGE/SC-2017-043599_0002..JPEG
- Qian, L., Wang, S., Savage, P.E., 2017. Hydrothermal liquefaction of sewage sludge under isothermal and fast conditions. *Bioresour. Technol.* 232, 27–34.

<https://doi.org/https://doi.org/10.1016/j.biortech.2017.02.017>

- Rebollo-Hernanz, M., Fernández-Gómez, B., Herrero, M., Aguilera, Y., Martín-Cabrejas, M.A., Uribarri, J., Del Castillo, M.D., 2019. Inhibition of the Maillard reaction by phytochemicals composing an aqueous coffee silverskin extract via a mixed mechanism of action. *Foods* 8, 438.
- Rocamora, I., Wagland, S.T., Villa, R., Simpson, E.W., Fernández, O., Bajón-Fernández, Y., 2020. Dry anaerobic digestion of organic waste: A review of operational parameters and their impact on process performance. *Bioresour. Technol.* 299, 122681. <https://doi.org/https://doi.org/10.1016/j.biortech.2019.122681>
- Ruggero, F., Carretti, E., Gori, R., Lotti, T., Lubello, C., 2020. Monitoring of degradation of starch-based biopolymer film under different composting conditions, using TGA, FTIR and SEM analysis. *Chemosphere* 246, 125770. <https://doi.org/10.1016/J.CHEMOSPHERE.2019.125770>
- Ruiz, H.A., Galbe, M., Garrote, G., Ramirez-Gutierrez, D.M., Ximenes, E., Sun, S.N., Lachos-Perez, D., Rodríguez-Jasso, R.M., Sun, R.C., Yang, B., Ladisch, M.R., 2021. Severity factor kinetic model as a strategic parameter of hydrothermal processing (steam explosion and liquid hot water) for biomass fractionation under biorefinery concept. *Bioresour. Technol.* 342, 125961. <https://doi.org/10.1016/J.BIORTECH.2021.125961>
- Ruiz, H.A., Rodríguez-Jasso, R.M., Fernandes, B.D., Vicente, A.A., Teixeira, J.A., 2013. Hydrothermal processing, as an alternative for upgrading agriculture residues and marine biomass according to the biorefinery concept: a review. *Renew. Sustain. Energy Rev.* 21, 35–51.
- Sánchez-Bayo, A., Rodríguez, R., Morales, V., Nasirian, N., Bautista, L.F., Vicente, G., 2019. Hydrothermal liquefaction of microalga using metal oxide catalyst. *Processes* 8, 15.
- Sangon, S., Ratanavaraha, S., Ngamprasertsith, S., Prasassarakich, P., 2006. Coal liquefaction using supercritical toluene–tetralin mixture in a semi-continuous reactor. *Fuel Process. Technol.* 87, 201–207. <https://doi.org/https://doi.org/10.1016/j.fuproc.2005.07.007>
- Santillan-Jimenez, E., Pace, R., Morgan, T., Behnke, C., Sajkowski, D.J., Lappas, A., Crocker, M., 2019. Co-processing of hydrothermal liquefaction algal bio-oil and petroleum feedstock to fuel-like hydrocarbons via fluid catalytic cracking. *Fuel Process. Technol.*

- 188, 164–171. <https://doi.org/https://doi.org/10.1016/j.fuproc.2019.02.018>
- Saqib, N.U., Sharma, H.B., Baroutian, S., Dubey, B., Sarmah, A.K., 2019. Valorisation of food waste via hydrothermal carbonisation and techno-economic feasibility assessment. *Sci. Total Environ.* 690, 261–276.
- Seshasayee, M.S., Savage, P.E., 2021. Synergistic interactions during hydrothermal liquefaction of plastics and biomolecules. *Chem. Eng. J.* 417, 129268. <https://doi.org/https://doi.org/10.1016/j.cej.2021.129268>
- Seshasayee, M.S., Savage, P.E., 2020a. Oil from plastic via hydrothermal liquefaction: Production and characterization. *Appl. Energy* 278, 115673. <https://doi.org/10.1016/J.APENERGY.2020.115673>
- Seshasayee, M.S., Savage, P.E., 2020b. Oil from plastic via hydrothermal liquefaction: Production and characterization. *Appl. Energy* 278, 115673. <https://doi.org/https://doi.org/10.1016/j.apenergy.2020.115673>
- Shah, Ayaz A., Toor, S.S., Conti, F., Nielsen, A.H., Rosendahl, L.A., 2020. Hydrothermal liquefaction of high ash containing sewage sludge at sub and supercritical conditions. *Biomass and Bioenergy* 135, 105504. <https://doi.org/10.1016/J.BIOMBIOE.2020.105504>
- Shah, Ayaz A., Toor, S.S., Conti, F., Nielsen, A.H., Rosendahl, L.A., 2020. Hydrothermal liquefaction of high ash containing sewage sludge at sub and supercritical conditions. *Biomass and Bioenergy* 135, 105504. <https://doi.org/https://doi.org/10.1016/j.biombioe.2020.105504>
- Shahriari, H., Warith, M., Hamoda, M., Kennedy, K.J., 2012. Anaerobic digestion of organic fraction of municipal solid waste combining two pretreatment modalities, high temperature microwave and hydrogen peroxide. *Waste Manag.* 32, 41–52.
- Shakya, R., Whelen, J., Adhikari, S., Mahadevan, R., Neupane, S., 2015. Effect of temperature and Na₂CO₃ catalyst on hydrothermal liquefaction of algae. *Algal Res.* 12, 80–90. <https://doi.org/https://doi.org/10.1016/j.algal.2015.08.006>
- Sharma, I., Rackemann, D., Ramirez, J., J. Cronin, D., Moghaddam, L., N. Beltramini, J., Te'o, J., Li, K., Shi, C., O.S.Doherty, W., 2022. Exploring the potential for biomethane production by the hybrid anaerobic digestion and hydrothermal gasification process: A

- review. *J. Clean. Prod.* 362, 132507. <https://doi.org/10.1016/J.JCLEPRO.2022.132507>
- Sharma, M., Singh, J., Baskar, C., Kumar, A., 2019. A comprehensive review of renewable energy production from biomass-derived bio-oil. *Biotechnol. J. Biotechnol. Comput. Biol. Bionanotechnol.* 100.
- Shin, P.K., Kim, M.H., Kim, J.M., 1997. Biodegradability of degradable plastics exposed to anaerobic digested sludge and simulated landfill conditions. *J. Environ. Polym. Degrad.* 5, 33–39.
- Siegenthaler, K.O., Künkel, A., Skupin, G., Yamamoto, M., 2012. Ecoflex® and Ecovio®: Biodegradable, Performance-Enabling Plastics BT - Synthetic Biodegradable Polymers, in: Rieger, B., Künkel, Andreas, Coates, G.W., Reichardt, R., Dinjus, E., Zevaco, T.A. (Eds.), . Springer Berlin Heidelberg, Berlin, Heidelberg, pp. 91–136. https://doi.org/10.1007/12_2010_106
- Singh, J., Gu, S., 2010. Biomass conversion to energy in India—A critique. *Renew. Sustain. Energy Rev.* 14, 1367–1378. <https://doi.org/https://doi.org/10.1016/j.rser.2010.01.013>
- Stroot, P.G., McMahon, K.D., Mackie, R.I., Raskin, L., 2001. Anaerobic codigestion of municipal solid waste and biosolids under various mixing conditions—I. digester performance. *Water Res.* 35, 1804–1816. [https://doi.org/https://doi.org/10.1016/S0043-1354\(00\)00439-5](https://doi.org/https://doi.org/10.1016/S0043-1354(00)00439-5)
- Sudibyo, H., Pecchi, M., Tester, J.W., 2022. Experimental-based mechanistic study and optimization of hydrothermal liquefaction of anaerobic digestates. *Sustain. Energy Fuels* 6, 2314–2329. <https://doi.org/10.1039/D2SE00206J>
- Sun, X., Atiyeh, H.K., Li, M., Chen, Y., 2020. Biochar facilitated bioprocessing and biorefinery for productions of biofuel and chemicals: A review. *Bioresour. Technol.* 295, 122252. <https://doi.org/https://doi.org/10.1016/j.biortech.2019.122252>
- Svoboda, P., Dvorackova, M., Svobodova, D., 2019. Influence of biodegradation on crystallization of poly (butylene adipate-co-terephthalate). *Polym. Adv. Technol.* 30, 552–562. <https://doi.org/https://doi.org/10.1002/pat.4491>
- Tang, X., Zhang, C., Yang, X., 2019. Hydrothermal Liquefaction of Model Compounds Protein and Glucose: Effect of Maillard Reaction on Low Lipid Microalgae. *IOP Conf. Ser. Mater.*

Sci. Eng. 611, 12026. <https://doi.org/10.1088/1757-899X/611/1/012026>

- Tian, C., Liu, Z., Zhang, Y., Li, B., Cao, W., Lu, H., Duan, N., Zhang, L., Zhang, T., 2015. Hydrothermal liquefaction of harvested high-ash low-lipid algal biomass from Dianchi Lake: effects of operational parameters and relations of products. *Bioresour. Technol.* 184, 336–343.
- Ting, H.N.J., Lin, L., Cruz, R.B., Chowdhury, B., Karidio, I., Zaman, H., Dhar, B.R., 2020. Transitions of microbial communities in the solid and liquid phases during high-solids anaerobic digestion of organic fraction of municipal solid waste. *Bioresour. Technol.* 317, 123951.
- Toor, S.S., Rosendahl, L., Rudolf, A., 2011. Hydrothermal liquefaction of biomass: A review of subcritical water technologies. *Energy* 36, 2328–2342. <https://doi.org/10.1016/J.ENERGY.2011.03.013>
- Tubić, A., Lončarski, M., Maletić, S., Molnar Jazić, J., Watson, M., Tričković, J., Agbaba, J., 2019. Significance of chlorinated phenols adsorption on plastics and bioplastics during water treatment. *Water* 11, 2358.
- Unmar, G., Mohee, R., 2008. Assessing the effect of biodegradable and degradable plastics on the composting of green wastes and compost quality. *Bioresour. Technol.* 99, 6738–6744. <https://doi.org/https://doi.org/10.1016/j.biortech.2008.01.016>
- Vardar, S., Demirel, B., Onay, T.T., 2022. Degradability of bioplastics in anaerobic digestion systems and their effects on biogas production: a review. *Rev. Environ. Sci. Biotechnol.* 21, 205–223. <https://doi.org/10.1007/S11157-021-09610-Z/FIGURES/2>
- Vardon, D.R., Sharma, B.K., Blazina, G. V, Rajagopalan, K., Strathmann, T.J., 2012. Thermochemical conversion of raw and defatted algal biomass via hydrothermal liquefaction and slow pyrolysis. *Bioresour. Technol.* 109, 178–187. <https://doi.org/https://doi.org/10.1016/j.biortech.2012.01.008>
- Vasmara, C., Marchetti, R., 2016. Biogas production from biodegradable bioplastics. *Environ. Eng. Manag. J.* 15.
- Venkiteswaran, K., Benn, N., Seyed, S., Zitomer, D., 2019. Methane yield and lag correlate with bacterial community shift following bioplastic anaerobic co-digestion. *Bioresour.*

Technol. Reports 7, 100198.

- Wagner, J., Bransgrove, R., Beacham, T.A., Allen, M.J., Meixner, K., Drosig, B., Ting, V.P., Chuck, C.J., 2016. Co-production of bio-oil and propylene through the hydrothermal liquefaction of polyhydroxybutyrate producing cyanobacteria. *Bioresour. Technol.* 207, 166–174.
- Weng, Y.X., Jin, Y.J., Meng, Q.Y., Wang, L., Zhang, M., Wang, Y.Z., 2013. Biodegradation behavior of poly(butylene adipate-co-terephthalate) (PBAT), poly(lactic acid) (PLA), and their blend under soil conditions. *Polym. Test.* 32, 918–926. <https://doi.org/10.1016/J.POLYMERTESTING.2013.05.001>
- Wu, S. yong, Liu, F. qi, Huang, S., Wu, Y. qing, Gao, J. sheng, 2017. Direct n-hexane extraction of wet sewage sludge at thermal and pressurized conditions: A preliminary investigation on its process and product characteristics. *Fuel Process. Technol.* 156, 90–97. <https://doi.org/10.1016/J.FUPROC.2016.07.020>
- Xu, D., Lin, G., Liu, L., Wang, Y., Jing, Z., Wang, S., 2018. Comprehensive evaluation on product characteristics of fast hydrothermal liquefaction of sewage sludge at different temperatures. *Energy* 159, 686–695. <https://doi.org/10.1016/J.ENERGY.2018.06.191>
- Xu, D., Savage, P.E., 2014. Characterization of biocrudes recovered with and without solvent after hydrothermal liquefaction of algae. *Algal Res.* 6, 1–7. <https://doi.org/10.1016/J.ALGAL.2014.08.007>
- Yagi, H., Ninomiya, F., Funabashi, M., Kunioka, M., 2014. Mesophilic anaerobic biodegradation test and analysis of eubacteria and archaea involved in anaerobic biodegradation of four specified biodegradable polyesters. *Polym. Degrad. Stab.* 110, 278–283.
- Yang, C., Wang, S., Ren, M., Li, Y., Song, W., 2019. Hydrothermal liquefaction of an animal carcass for biocrude oil. *Energy & Fuels* 33, 11302–11309.
- Yang, L., Nazari, L., Yuan, Z., Corscadden, K., Xu, C.C., 2016. Hydrothermal liquefaction of spent coffee grounds in water medium for bio-oil production. *Biomass and Bioenergy* 86, 191–198.
- Yang, W., Li, X., Liu, S., Feng, L., 2014. Direct hydrothermal liquefaction of undried

- macroalgae *Enteromorpha prolifera* using acid catalysts. *Energy Convers. Manag.* 87, 938–945.
- Yang, Y., 2007. Subcritical water chromatography: A green approach to high-temperature liquid chromatography. *J. Sep. Sci.* 30, 1131–1140.
- Ye, J., Li, D., Sun, Y., Wang, G., Yuan, Z., Zhen, F., Wang, Y., 2013. Improved biogas production from rice straw by co-digestion with kitchen waste and pig manure. *Waste Manag.* 33, 2653–2658. <https://doi.org/https://doi.org/10.1016/j.wasman.2013.05.014>
- Yoshie, N., Oike, Y., Kasuya, K., Doi, Y., Inoue, Y., 2002. Change of surface structure of poly (3-hydroxybutyrate) film upon enzymatic hydrolysis by PHB depolymerase. *Biomacromolecules* 3, 1320–1326.
- Yu, C., Dongsu, B., Tao, Z., Xintong, J., Ming, C., Siqi, W., Zheng, S., Yalei, Z., 2023. Anaerobic co-digestion of three commercial bio-plastic bags with food waste: Effects on methane production and microbial community structure. *Sci. Total Environ.* 859, 159967.
- Yuan, X., Cao, H., Li, H., Zeng, G., Tong, J., Wang, L., 2009. Quantitative and qualitative analysis of products formed during co-liquefaction of biomass and synthetic polymer mixtures in sub- and supercritical water. *Fuel Process. Technol.* 90, 428–434. <https://doi.org/https://doi.org/10.1016/j.fuproc.2008.11.005>
- Zhang, L., Li, W., Lu, J., Li, R., Wu, Y., 2021. Production of platform chemical and bio-fuel from paper mill sludge via hydrothermal liquefaction. *J. Anal. Appl. Pyrolysis* 155, 105032. <https://doi.org/10.1016/J.JAAP.2021.105032>
- Zhang, L., Wu, W., Siqu, N., Dekyi, T., Zhang, Y., 2019. Thermochemical catalytic-reforming conversion of municipal solid waste to hydrogen-rich synthesis gas via carbon supported catalysts. *Chem. Eng. J.* 361, 1617–1629. <https://doi.org/https://doi.org/10.1016/j.cej.2018.12.115>
- Zhang, S., Zhou, S., Yang, X., Xi, W., Zheng, K., Chu, C., Ju, M., Liu, L., 2020. Effect of operating parameters on hydrothermal liquefaction of corn straw and its life cycle assessment. *Environ. Sci. Pollut. Res.* 27, 6362–6374. <https://doi.org/10.1007/s11356-019-07267-4>
- Zhao, X., Cornish, K., Vodovotz, Y., 2020. Narrowing the Gap for Bioplastic Use in Food

Packaging: An Update. *Environ. Sci. Technol.* 54, 4712–4732.
<https://doi.org/10.1021/acs.est.9b03755>

Zhou, Y., Schideman, L., Zheng, M., Martin-Ryals, A., Li, P., Tommaso, G., Zhang, Y., 2015. Anaerobic digestion of post-hydrothermal liquefaction wastewater for improved energy efficiency of hydrothermal bioenergy processes. *Water Sci. Technol.* 72, 2139–2147.

Zhu, Z., Rosendahl, L., Toor, S.S., Yu, D., Chen, G., 2015. Hydrothermal liquefaction of barley straw to bio-crude oil: Effects of reaction temperature and aqueous phase recirculation. *Appl. Energy* 137, 183–192.
<https://doi.org/https://doi.org/10.1016/j.apenergy.2014.10.005>

Zhu, Z., Toor, S.S., Rosendahl, L., Chen, G., 2014. Analysis of product distribution and characteristics in hydrothermal liquefaction of barley straw in subcritical and supercritical water. *Environ. Prog. Sustain. Energy* 33, 737–743.

Appendix A

Supplementary Information for Chapter 3

Table A-1. Summary of literature used for identifying different functional groups present in samples based on their wavenumber.

Sample	Wavelength (cm^{-1})	Compounds/functional groups	Reference considered for identifying functional group
Control	1,038	Carbohydrates, polysaccharides, and aromatic ethers	(Chowdhury et al., 2019; Mohammad Mirsoleimani Azizi et al., 2021a)
	1,657	Proteins, esters carbonyl, etc.	(Mohammad Mirsoleimani Azizi et al., 2021a)
	2,926 and 1,454	Aliphatic <i>C – H</i> stretching and bending	(Chowdhury et al., 2019; Mohammad Mirsoleimani Azizi et al., 2021a)
	3,296	<i>O – H</i> vibration of carboxylic and alcoholic groups	(Chowdhury et al., 2019)
Paper-based products	1,027	Hydrogen atoms on the phenyl ring	(Peng et al., 2022; Weng et al., 2013)
	1,317	Symmetric bending vibration of CH	(Peng et al., 2022; Weng et al., 2013)
	2,927	Symmetric stretching vibrations of CH_3	(Peng et al., 2022; Weng et al., 2013)
	3,320	<i>O – H</i> stretching vibration	(Peng et al., 2022; Weng et al., 2013)
Plastic bags and utensils	729	Bending vibration absorption of the CH-plane of the benzene ring	(Peng et al., 2022; Weng et al., 2013)
	874	Esters	(Peng et al., 2022; Weng et al., 2013)
	1,018	bending vibration adsorption at the surface of the adjacent hydrogen atoms on the phenyl ring	(Peng et al., 2022; Weng et al., 2013)
	1,103	<i>C – O</i> left-right symmetric stretching vibration adsorption	(Peng et al., 2022; Weng et al., 2013)
	1,182 and 1,167	<i>C – O – C</i> stretching vibration	(Peng et al., 2022; Weng et al., 2013)
	1,269	Symmetric stretching vibration of C-O	(Peng et al., 2022; Weng et al., 2013)
	1,360	Symmetric bending vibration of CH	(Peng et al., 2022; Weng et al., 2013)
	1,409	Trans- CH_4 -plane bending vibration	(Peng et al., 2022; Weng et al., 2013)

	1,713	Stretching vibration of C-O	(Peng et al., 2022; Weng et al., 2013)
	1,755	Stretching vibration of carbonyl C = O	(Peng et al., 2022; Weng et al., 2013)
	2,922	Asymmetric stretching vibration of CH ₂	(Peng et al., 2022; Weng et al., 2013)

Table A-2. GC-MS results for heavy oil (HO) from different digestate samples under different HTL experimental condition: **(a)** Control (280 °C) **(b)** Control (350 °C) **(c)** Paper-based disposables (280 °C) **(d)** Paper-based disposables (350 °C) **(e)** Compostable plastic bag (280 °C) **(f)** Compostable plastic bag (350 °C) **(g)** Plant-based utensils (280 °C) **(h)** Plant-based utensils (350 °C)

(a) Control (280 °C)

RT	Name	Area%
3.01	5-Hexen-2-one	1.55
3.48	Propanoic acid	0.95
3.48	Propanal	0.95
4.02	3-Penten-2-one, 4-methyl-	6.51
4.02	3-Hexen-2-one	6.51
4.89	Acetamide	1.33
5.47	2-Acetoxyisobutyryl chloride	1.30%
7.4	2-Pentanone, 4-amino-4-methyl-	1.39
8.1	Butane, 2-methoxy-2,3,3-trimethyl-	14.47
10.27	Fumaric acid, dipropargyl ester	5
14.5	p-Cresol	1.1
15.32	2-Pyrrolidinone	7.76
15.63	4-Piperidinone, 2,2,6,6-tetramethyl-	9.44
15.93	Isopropyldimethylsilane	2.7
17.22	Pyrrolidine, 1-acetyl-	4.06
17.5	Phenol, 4-ethyl-	1.2
18.83	Benzoic acid	7.43
19.6	1,3-Cyclohexanedione, 2,5,5-trimethyl-	1.02
20.68	Caprolactam	1.56
21.01	1,3-Dioxolane, 2-propyl-	1.71
22.63	2,3-Dimethoxyphenol	1.64
23.18	Hydrocinnamic acid	2.36
25.23	Undecanoic acid	0.83
25.83	2-Oxo-1-methyl-3-isopropylpyrazine	1.84
29.81	Benzophenone	0.79
26.04	Undecylenic acid	1.4
32.79	3,6-Diisopropylpiperazin-2,5-dione	1.01
33.06	3-Methyl-2,3,6,7,8,8a-hexahydropyrrolo[1,2-a]pyrazine-1,4-dione	1.9
33.7	Phenanthrene	1.1
35.65	Pentadecanoic acid	0.91
36.42	Cyclo(L-prolyl-L-valine)	1.24
39.26	Octahydrodipyrrolo[1,2-a:1',2'-d]pyrazine-5,10-dione-, (5aR,10aR) (isomer 1)	2.19

39.69	Hexahydro-3-(1-methylpropyl)pyrrolo[1,2-a]pyrazine-1,4-dione	1.36
43.82	Pyrene	1.29

(b) Control (350 °C)

RT	Name	Area%
4.02	Ethanimidic acid, ethyl ester	1.35
6.55	Oxygen	2.65
8.1	Butane, 2-methoxy-2,3,3-trimethyl-	6.24
10.27	Fumaric acid, dipropargyl ester	7.12
10.82	2,4-Dihydroxy-3-methylbenzaldehyde, 2TMS	0.75
14.5	p-Cresol	0.76
14.91	2-Pyrrolidinone	1.93
14.95	p-Cresol	0.8
15.51	4-Piperidinone, 2,2,6,6-tetramethyl-	2.38
16.81	Benzene, 1-methoxy-4-methyl-	0.76
17.5	Phenol, 4-ethyl-	1.2
18.33	2-Acetyl-5-methylthiophene	1.75
19.1	3-(1-Pyrrolidinylcarbonyl)piperidine	1.45
20.36	Phenol, 4-ethyl-2-methoxy-	2.1
21.07	Indole	1.24
21.38	Naphthalene, 1-methyl-	1.5
22.39	7-Methylthieno[3,2-b]pyridine	1.56
22.63	2,3-Dimethoxyphenol	1.44
22.91	Phenol, 2-methoxy-4-propyl-	0.76
23.64	1H-Indole, 4-methyl-	1.28
23.71	4-Tetradecene, (E)-	3.2
25.66	1-Naphthoic acid, 2,5-dichlorophenyl ester	3.68
26.17	3-Ethyl-1H-indole	1.64
26.37	1-Tetradecene	1.77
26.84	Pentanoic acid, 5-hydroxy-, 2,4-di-t-butylphenyl esters	3.61
27.56	Pyridine, 2-methyl-5-phenyl-	0.93
27.98	1-Tetradecene	2.43
28.64	Dodecanoic acid	2.43
28.89	1-Heptadecene	2.31
29.52	1H-Indole, 2-(1,1-dimethylethyl)-	1.57
29.81	Benzophenone	0.75
30.29	Cyclotetrasiloxane, octamethyl-	1
30.48	1,7-Trimethylene-2,3-dimethylindole	1.6
30.96	n-Tridecan-1-ol	2.14
31.28	1-Heptadecene	1.93
31.66	1-Tetradecanamine, N,N-dimethyl-	1.67
32.08	Benzene, (1-hexylheptyl)-	1.3
32.61	Cyclotetradecane	3.14
33.18	2-Dodecanone	0.89
33.47	Tetradecanoic acid	1.1
33.7	Phenanthrene	1.42
34.11	1-Heptadecene	0.83

35.65	Pentadecanoic acid	0.91
36	1,1'-Biphenyl, 2-azido-	1.38
36.28	2,4,6,8-Tetramethyl-1-undecene	0.72
39.24	Octahydrodipyrrolo pyrazine-5,10-dione-, (5aR,10aR) (isomer 1)	1.66
40.35	n-Hexadecanoic acid	1.85
40.96	1-Heptadecene	1
41.13	Acetic acid, hydrazide	1.26
42.52	Fluoranthene	0.87
43.82	Pyrene	1.18
44.84	beta.-Alanine, n-pentafluoropropionyl-, hexadecyl ester	1.18
45.29	Octadecanoic acid	1
45.87	11-Tricosene	0.78

(c) Paper-based disposables (280 °C)

RT	Name	Area%
11.11	Phenol	0.75
14.41	Phenol, 2-methoxy-	2.93
17.34	Phenol, 4-ethyl-	0.89
17.82	Benzene, 1,2-dimethoxy-	0.75
20.38	Phenol, 4-ethyl-2-methoxy-	2.01
21.05	Indole	1.31
21.4	Naphthalene, 1-methyl-	2.18
22.56	Phenol, 2,6-dimethoxy-	1.83
22.92	Phenol, 2-methoxy-4-propyl-	1.2
23.33	Quinoline, 3-methyl-	0.8
23.65	1H-Indole, 6-methyl-	5.87
24.54	Probarbital	0.77
25.28	trans-Isoeugenol	3.33
26.17	3-Ethyl-1H-indole	2.72
26.39	1H-Indole, 2,3-dimethyl-	1.43
26.83	2,4-Di-tert-butylphenol	3.14
27.12	5-tert-Butylpyrogallol	2.3
27.58	Pyridine, 2-methyl-5-phenyl-	1.13
28.02	3-Ethyl-4-methyl-1H-indole	2.78
28.55	Undecanoic acid	3.73
28.91	3-Octadecene, (E)-	2.86
29.08	Hexadecane	1.37
29.2	2,6-Dimethoxy-4-propylphenol	1.84
29.82	Benzophenone	1.84
30.47	1,7-Trimethylene-2,3-dimethylindole	3.15
30.98	Dichloroacetic acid, nonyl ester	2.43
31.28	1-Heptadecene	1.16
31.46	Heptadecane	1.82
31.75	1-Undecanamine, N,N-dimethyl-	1.305
32.1	1-Isoleucine, N-allyloxycarbonyl-, nonyl ester	1.338
32.32	Octadecanoic acid	0.93
32.79	7-Methoxy-6-methylcoumarin	2.86

33.42	Tridecanoic acid	1.86
33.72	Phenanthrene	1.47
34.13	5-Octadecene, (E)-	1.32
34.36	3,5-Dimethyl-4-octanone	0.95
35.66	Pentadecanoic acid	1.7
35.99	Pentadecanoic acid	2.42
39.1	Tridecanoic acid	1.53
39.61	2-Methyl-1,8-octanediol	1.58
40.37	1-(+)-Ascorbic acid 2,6-dihexadecanoate	3.44
40.98	1-Heptadecene	1.18
42	Heptadecanoic acid	0.75
42.54	Pyrene	0.75
44.38	Undecanoic acid, 2-methyl-	1.7
45.29	Octadecanoic acid	0.82
45.6	Nonanamide	0.8
56.59	Cholestane, 3-(ethylthio)-, (3.beta.,5.alpha.)-	0.82
60.76	Epicholestanol	0.83

(d) Paper-based disposables (350 °C)

RT	Name	Area%
6.49	2-Pentanone, 4-amino-4-methyl-	2.13
10.81	Cyclotetrasiloxane, octamethyl-	0.81
14.01	1,2,3-Trimethylpiperidin-4-one	0.82
14.48	Phenol, 3-methyl-	1
14.83	p-Cresol	0.75
15.3	3-Aminopyridine	0.82
15.53	4-Piperidinone, 2,2,6,6-tetramethyl-	2.63
16.76	Phenol, 3,4-dimethyl-	0.83
17.41	Phenol, 4-ethyl-	1.1
18.13	Hexyl ethylphosphonofluoridate	1.42
19.1	5-Formyl-3-methyluracil	1.4
20.32	Protopine	1.33
20.65	2-Ethyl-3,5-dimethylpyridine	0.75
21.05	Indole	1.01
21.39	Naphthalene, 1-methyl-	1.97
22.55	Phenol, 2,6-dimethoxy-	2.53
22.91	Phenol, 2-methoxy-4-propyl-	1.1
23.3	Quinoline, 4-methyl-	1.5
23.65	1H-Indole, 4-methyl-	2.74
23.92	Undecane, 3,7-dimethyl-	1.42
24.79	3,4-Dihydroxy-5-methoxybenzaldehyde	2.76
25.69	Pyridine, 2-phenyl-	1.28
26.17	3-Ethyl-1H-indole	1.61
26.37	Cetene	1.84
26.87	2,4-Di-tert-butylphenol	3.66
27.56	Pyridine, 2-methyl-5-phenyl-	1.05
27.98	Cetene	2.63

28.64	Fluorene	2.16
28.89	1-Heptadecene	3.03
29.54	4H-Pyrrolo[3,2,1-ij]quinoline, 1,2,5,6-tetrahydro-6-methyl-	1.01
29.81	Benzophenone	1.71
30.44	1H-Indole, 2-(1,1-dimethylethyl)-	2.62
30.96	Formic acid, dodecyl ester	2.2
31.28	1-Heptadecene	1.27
31.45	Heptadecane	0.78
31.64	1-Tetradecanamine, N,N-dimethyl-	1.75
32.13	1-Nonadecene	1.37
32.61	n-Tridecan-1-ol	2.96
33.18	2-Hexadecanone	0.98
33.42	Undecanoic acid	1.03
33.71	Phenanthrene	1.51
34.13	1-Heptadecene	0.73
34.33	6-Methoxy-7-(3-methylbut-2-enoxy)chromen-2-one	1.25
35.63	Undecanoic acid	1.15
35.98	meso-2,5-Dimethyl-3,4-hexanediol	1.29
37.45	1-Hexadecanol	0.75
38.35	Dimethyl palmitamine	0.79
38.93	Pentadecanoic acid, 14-methyl-, methyl ester	1.78
40.34	n-Hexadecanoic acid	1.8
41.23	2-Decanone	0.82
41.97	Heptadecanoic acid	0.82
42.54	Pyrene	0.75
43.83	Pyrene	1.13
44.37	Methyl stearate	0.8
45.45	2-(2-Hydroxycyclooctyl)-furan	2.1
45.87	11-Tricosene	1.1
47.94	1-Docosene	0.75

(e) Compostable plastic bag (280 °C)

RT	Name	Area%
4.91	Pyridine, 2-methyl-	2.55
7.16	1-Butanol, TMS derivative	1.55
8.4	Butyrolactone	0.75
17.05	1,3-Butanediol, (S)-	51.88
17.76	L-Lactic acid	2.42
18.24	2-Pyrrolidinone, 1-ethenyl-	1.4
18.95	Ethylmethylsilane	4.81
19.55	3-Aminopyridine	1.905
20.09	3-Pyridinol	2.65
20.59	Benzoic acid	3.69
20.87	Phenol, 4-amino-	2.391
21.58	Triethylene glycol	0.75
22.01	Benzeneacetic acid	1.21
22.52	Benzoic acid, 4-methyl-	1.79

22.86	6-Heptenoic acid	1.73
23.38	2-Pyrrolidinone, 1-methyl-	0.75
23.77	1H-Indole, 4-methyl-	1.86
24.02	Benzene, 1-fluoro-4-(4-methyl-4-pentenyl)-	0.93
25.06	1-Butanol, 4-butoxy-	2.15
26.65	Apocynin	5.98
27.32	phosphorane, (3,5-dimethylphenyl)dimethyl-, oxide	0.75
29.32	2,6-Dimethoxy-4-propylphenol, acetate	2.57
30.94	1-Tetradecanol	1.21

(f) Compostable plastic bag (350 °C)

RT	Name	Area%
3.96	3-Hexen-2-one	1.37
10.62	1,4-Butanediol	16.04
10.82	2,4-Dihydroxy-3-methylbenzaldehyde, 2TMS	1.31
14.48	Phenol, 3-methyl-	1
14.77	2-Pyrrolidinone	1.2
14.85	p-Cresol	1.54
15.44	3-Cyclohexene-1-carboxaldehyde, 4-methyl-	1
17.38	Quinoline, 1,2,3,4-tetrahydro-	1.33
19.15	Benzoic acid	9.73
19.2	Phenol, 4-ethyl-2-methyl-	1.12
20.28	2-Cyclohexen-1-one, 5-methyl-2-(1-methylethyl)-	1.38
21.09	Indole	0.82
21.37	Naphthalene, 1-methyl-	0.86
21.88	4-Ethylformanilide	1.08
22.73	Benzamide	3.45
23.65	1H-Indole, 4-methyl-	4.38
24.81	Benzamide, N-ethyl-	2.25
25.97	1-Undecanol	2.6
26.17	3-Ethyl-1H-indole	1.523
26.4	1H-Indole, 2,3-dimethyl-	1.85
26.55	Tetraethylene glycol	0.78
26.83	2,4-Di-tert-butylphenol, acetate	1.84
27.59	Pyridine, 2-methyl-5-phenyl-	1.92
28.03	3-Ethyl-4-methyl-1H-indole	2.55
28.51	Dodecanoic acid	2.14
28.89	1,2,3,7-Tetramethylindole	2.33
29.74	2-Ethyl-8-quinolinol	2.66
30.46	p-Cyanophenyl p-(2-methylbutoxy)benzoate	2.22
30.95	1-Tetradecanol	1.81
31.27	1-Heptadecene	2.05
31.68	N-Dimethylaminomethyl-tert.-butyl-isopropylphosphine	1
32.07	Benzene, (1-hexylheptyl)-	1
32.59	Cyclotetradecane	1.62
32.79	5-Nitrothiophene-2-carboxamide	1.12
33.39	Tetradecanoic acid	1.85

33.7	Diphenylacetylene	1.14
34.33	Scopoletin, O-acetyl-	1
35.56	Pentadecanoic acid	1.41
35.88	4-Pentadecanol	1.24
39.23	Octahydrodipyrrolo[1,2-a:1',2'-d]pyrazine-5,10-dione-, (5aR,10aR) (isomer 1)	1.1
40.36	n-Hexadecanoic acid	4.11
42.17	Octadecanamide	1
43.36	1-Heptadecene	0.75
45.28	Octadecanoic acid	2.7

(g) Plant-based utensils (280 °C)

RT	Name	Area%
9.99	Formamide	10.24
10.02	Formamide	1.15
13.19	Pyridine, 5-ethyl-2-methyl-	1.21
14.38	p-Cresol	4.41
15.31	1H-Imidazole, 1-methyl-4-nitro-	0.82
15.69	N,N-Dimethylformamide ethylene acetal	1.33
17.38	Phenol, 4-ethyl-	0.75
20.37	Phenol, 4-ethyl-2-methoxy-	0.75
21.38	Naphthalene, 2-methyl-	2.36
23.39	4(1H)-Pyrimidinone, 2-amino-6-mercapto-	0.64
23.67	Indolizine, 1-methyl-	1.73
23.71	Cetene	0.76
25.12	2-Oxo-1-methyl-3-isopropylpyrazine	1.99
25.97	1-Dodecanol	1.23
26.18	3-Ethyl-1H-indole	1.77
26.82	2,4-Di-tert-butylphenol	1.23
27.05	N-Dimethylaminomethyl-tert.-butyl-isopropylphosphine	1.38
27.6	Pyridine, 2-methyl-5-phenyl-	0.76
27.88	Carbon monoxide	1.76
28.5	Dodecanoic acid	2.4
28.89	Cetene	1.97
29.5	1H-Indole, 2-(1,1-dimethylethyl)-	1.13
29.81	Benzophenone	1.2
30.47	1,7-Trimethylene-2,3-dimethylindole	1.64
30.96	1-Dodecanol	1.94
31.45	Heptadecane	2.28
31.74	1-Undecanamine, N,N-dimethyl-	1.278
32.33	3-Pyridinecarboxamide, N-phenyl-	1.97
32.82	p-Anisic acid, 3,4-dichlorophenyl ester	1.53
33.17	2-Hexadecanone	1.06
33.39	Tetradecanoic acid	1.3
33.71	9H-Fluorene, 9-methylene-	1.47
34.34	3,4-Heptadien-2-one, 3-cyclopentyl-6-methyl-	0.84
35.55	Pentadecanoic acid	0.88

35.89	2-methylhexanoic Acid, 2,2,2-trifluoroethyl ester	1.91
38.43	N-Dimethylaminomethyl-tert.-butyl-isopropylphosphine	0.57
39.25	l-Proline, N-butoxycarbonyl-, heptyl ester	1.44
40.37	n-Hexadecanoic acid	3.74
40.98	11-Tricosene	2.48
41.97	Heptadecanoic acid	0.82
42.53	Pyrene	2.06
43.39	1-Octadecanol	1.94
43.83	Fluoranthene	1.52
44.38	Methyl stearate	0.76
44.85	6-Tridecene	2.41
45.29	Octadecanoic acid	1.51
45.66	Butyl citrate	2.8
47.6	8-Pentadecanone	1.03
48.33	Nickel tetracarbonyl	0.97
56.16	Cholest-4-ene	0.77
56.58	Cholest-2-ene	0.93

(h) Plant-based utensils (350 °C)

RT	Name	Area%
9.99	Formamide	11.39
10.83	Hydrazinecarboxamide	0.78
13.19	Pyridine, 3-ethyl-4-methyl-	1.22
14.38	Phenol, 3-methyl-	5.42
15.31	1H-Imidazole, 1-methyl-4-nitro-	0.94
15.69	Ethylmethylsilane	1.33
17.37	Phenol, 3-ethyl-	0.82
19.65	Carbonic acid, monoamide, N-isobutyl-, ethyl ester	0.77
20.37	Benzene, 1,4-dimethoxy-2-methyl-	0.75
21.38	Naphthalene, 1-methyl-	1.96
22.92	Phenol, 2-methoxy-4-propyl-	2.01
23.67	Indolizine, 3-methyl-	1.94
25.12	Undecanoic acid	2
25.97	1-Undecanol	1.12
26.18	Benzonitrile, 2,4,6-trimethyl-	1.77
26.82	2,4-Di-tert-butylphenol	1.33
27.05	N-Dimethylaminomethyl-tert	1.18
27.6	Pyridine, 2-methyl-5-phenyl-	0.86
27.88	Nitrogen	1.75
28.5	Undecanoic acid	1.95
28.89	3-Hexadecene, (Z)-	1.97
29.52	1H-Indole, 2,3-dihydro-1,3,3-trimethyl-2-methylene-	1.63
29.81	Benzophenone	1.39
30.43	2H-Isoindole, 4,5,6,7-tetramethyl-	0.75
30.47	3-Buten-2-one,4-(2,5,6,6-tetramethyl-1-cyclohexen-1)	0.95

30.96	1-Dodecanol	2.04
31.45	Heptadecane	2.18
31.74	1-Tetradecanamine, N,N-dimethyl-	1.3
32.33	3-Pyridinecarboxamide, N-phenyl-	1.77
32.82	p-Anisic acid, 3,4-dichlorophenyl ester	0.94
32.98	Fumaric acid, pentyl 2-phenylethyl ester	1.53
33.17	2-Dodecanone	1.1
33.39	Tetradecanoic acid	1.49
33.71	Anthracene	1.67
34.12	1-Heptadecene	0.73
35.55	Undecanoic acid	1.3
35.89	Heptanoic acid, 4-octyl ester	1.7
39.25	l-Proline, N-butoxycarbonyl-, heptyl ester	1.93
40.37	n-Hexadecanoic acid	5.2
40.98	11-Tricosene	1.76
41.97	1,1-Diisobutoxy-butane	0.81
42.18	Heptadecanoic acid	0.75
42.53	Pyrene	1.2
43.39	1-Octadecanol	0.92
43.84	Fluoranthene	1.56
44.38	Methyl stearate	1.76
44.85	6-Tridecene	2.41
45.29	Octadecanoic acid	1.8
45.66	Adipic acid, butyl non-5-yn-3-yl ester	2.97
47.6	8-Pentadecanone	1.1
48.33	Nickel tetracarbonyl	1
56.16	Cholest-4-ene	0.89
56.58	Cholest-2-ene	0.98

Appendix B

Supplementary Information for Chapter 4

Table B-1. GC-MS results for heavy oil (HO) from different digestate samples under different HTL experimental condition: **(a)** Control (280 °C) **(b)** Control (330 °C) **(c)** Control (370 °C) **(d)** Bioplastic (280 °C) **(e)** Bioplastic (330 °C) **(f)** Bioplastic (370 °C)

(a) Control (280 °C)

RT	Name	Area%
11.91	1-Propanol, 2,2-dimethyl-	2.74
11.98	N-Dimethylaminomethyl-tert.-butyl isopropylphosphine	2.78
13.11	Pentanoic acid	6.96
17.02	Phenol, 2-methoxy-	6.06
17.02	Mequinol	2.05
18.89	Nonanamide	0.79
19.16	Benzenamine, 2-ethyl-6-methyl-	0.78
20.03	Phenol, 3-ethyl-	1.91
20.41	2-Methoxy-5-methylphenol	1.15
21.75	Monobenzene	0.84
23.07	Phenol, 4-ethyl-2-methoxy-	3.09
23.30	p-Propionotoluidide	0.79
23.48	Benzeneacetic acid	0.80
23.63	Indole	2.18
25.25	Phenol, 2,6-dimethoxy-	2.45
25.59	Phenol, 2-methoxy-4-propyl-	2.75
25.81	Hydrocinnamic acid	1.38
25.99	7-Hexadecene, (Z)-	2.05
26.25	1H-Indole, 4-methyl-	3.67
26.99	Benzeneacetamide	0.80
27.85	Phenol, 2-methoxy-4-(1-propenyl)-	1.53
28.94	Ethanone, 1-(2-hydroxy-4-methoxyphenyl)-	0.89
29.32	N-Dimethylaminomethyl-tert.-butylisopropylphosphine	1.58
29.83	4-Ethyl-2,6-dimethoxyphenol	1.20
31.02	cis-Inositol	2.94
31.17	5-Octadecene, (E)-	1.50
31.33	Nonadecane	1.83
31.33	Tetradecane, 1-iodo-	0.89
32.52	Benzophenone	1.03
33.55	4,4'-Isopropylidene-bis(2-chlorophenol)	0.82

37.14	Sebacic acid, di(4-heptyl) ester	3.11
37.65	5-Eicosene, (E)-	1.15
39.19	2-Propanesulfinic acid, 2-methyl-, methyl ester	0.87
39.43	2,6,10,14-Tetramethylpentadecan-6-ol	1.41
41.87	Hexadecanoic acid, methyl ester	1.23
42.47	Succinic acid, 8-chlorooctyl tetrahydrofurfuryl ester	0.95
43.33	n-Hexadecanoic acid	7.63
43.36	n-Hexadecanoic acid	0.75
43.55	Nonanamide	0.95
43.60	5-Eicosene, (E)-	2.06
47.18	Oxazole, 4,5-dimethyl-	2.12
47.49	Heptenyl angelate, 3Z-	2.61
47.85	Octadecanoic acid	2.64
48.23	Hexadecanamide	2.82
51.39	Cyclooctaneacetic acid, 2-oxo-	1.81
51.97	Permethyl 2"-O-rhamnosylisovitexin	0.81
52.15	Nonanamide	1.27

(b) Control (330 °C)

RT	Name	Area%
9.82	3-Octanamine	14.7
10.13	Nickel,[[2,2'-[1,7-heptanediy]bis(nitrilomethylidyne)]bis[phenolato]](2-)-N,N',O,O']-	3.3
11.62	Tetrabenzo[a,c,hi,qr]pentacene	1.8
16.36	2-Piperidinecarboxylic acid, 1-acetyl-, ethyl ester	1.3
16.72	Imidazo[4,5-d]imidazole, 1,6-dihydro-	1.0
17.84	4-Piperidinone, 2,2,6,6-tetramethyl-	3.2
19.69	(2S,6R,7S,8E)-(+)-2,7-Epoxy-4,8-megastigmadiene	1.3
20.03	Phenol, 3-ethyl-	1.9
20.41	2-Methoxy-5-methylphenol	1.2
21.62	Pyridine, 3-(ethylthio)-	0.9
22.63	2,3-Dimethoxyphenol	1.4
22.91	Phenol, 2-methoxy-4-propyl-	0.9
23.64	4-Tetradecene, (E)-	3.2
25.22	9H-Carbazole, 3,6-dinitro-	2.0
26.28	3,4-Dimethylphenyl undecyl ether	1.1
27.98	1-Tetradecene	3.5
28.64	Dodecanoic acid	3.8
30.64	1,3-Dioxolane, 2-heptyl-	2.1
30.96	n-Tridecan-1-ol	4.3
31.37	1-Heptadecene	4.4
35.65	Pentadecanoic acid	2.9

36.84	Tetradecanoic acid	3.6
39.18	4-Octene, 2,2,3,7-tetramethyl-, [S-(E)]-	1.0
39.72	l-Norvaline, n-propargyloxycarbonyl-, pentyl ester	0.8
41.83	Methyl 2-O-methyl-.beta.-D-xylopyranoside	0.8
42.45	2-Oxatricyclo[20.2.2.1(3,7)]heptacos-3,5,7(27),22,24,25-hexaene	1.2
43.14	Propanamide, N-(1-oxopropyl)-	15.3
43.77	Androstenediol, 2TBDMS derivative	1.0
45.87	11-Tricosene	1.8
47.23	2-Pyridone, 3,5-diiodo-N-methyl-	4.3
47.70	Octadecanoic acid	3.8
48.10	Nonanamide	1.7

(c) Control (370 °C)

RT	Name	Area%
12.69	Benzenepropanoic acid, 3,5-bis(1,1-dimethylethyl)-4-hydroxy-, octadecyl ester	1.09
13.22	Phenol	1.73
16.53	p-Cresol	1.64
19.54	Silane, 1,3-butadiynyltrimethyl-	1.14
23.45	Indole	0.87
23.79	Estra-1,3,5(10)-trien-6-one, 3,17-bis(acetyloxy)-2-methoxy-, (17.beta.)-	1.13
24.85	2,4(1H,3H)-Pyrimidinedione, 6-methyl-1-phenyl-	2.62
26.14	Acetic acid, cesium salt	2.80
28.25	Kaempferol-3,7-O-diglucoside, tms-	1.43
28.74	N-Ethylcathinone, N-trimethylsilyl-	1.08
28.86	1H-Indole, 2,6-dimethyl-	1.10
30.28	1,4-Ethanoisoquinoline, 1,2,3,4-tetrahydro-2-methyl-	1.14
30.70	n-Decanoic acid	2.63
31.13	Cyanamide, dimethyl-	1.97
31.28	1-Heptadecene	4.12
31.45	Heptadecane	4.78
31.64	1-Tetradecanamine, N,N-dimethyl-	1.75
32.13	1-Nonadecene	5.98
32.61	n-Tridecan-1-ol	2.96
33.18	2-Hexadecanone	0.98
33.42	Undecanoic acid	1.03
33.21	1,3,5-Triazin-2-amine, N,N-dihexyl-4,6-bis[(4-methylphenyl)thio]-	1.58
35.26	Cyanamide, dimethyl-	3.09
36.81	Pentanoic acid, 2-hydroxy-, ethyl ester	2.32
37.96	D:A-Friedooleanane-1,3-dione, 7-hydroxy-, (7.alpha.)-	1.40
39.14	2-Deoxy-.alpha.-ecdysone, 22-O-benzoate	1.47
39.59	Hexadecyl pentadecanoate	1.40

41.17	2-Propenoic acid, methyl ester	1.01
41.83	Methyl 2-O-methyl-.beta.-D-xylopyranoside	1.22
42.59	Ursan-16-one, 3-hydroxy-, (3.beta.,18.alpha.,19.alpha.,20.beta.)-	1.88
43.24	n-Hexadecanoic acid	8.44
43.93	4-Iodo-2,5-dimethoxyphenethylamine, N-trifluoroacetyl-	1.30
43.93	Batrachotoxinin a, 7,8-dihydro-, (8.beta.)-	1.60
44.52	L-Leucine, N-methyl-N-(octyloxycarbonyl)-, dodecyl ester	1.02
44.72	Isonipecotic acid, N-(3-phenylpropionyl)-, hexyl ester	1.09
45.54	Benzamide, N,N-dioctyl-4-ethyl-	1.54
45.54	15.beta.-Hydroxy-7,8,-dimethoxy-13.beta.-carbomethoxy-14.beta	1.19
45.87	11-Tricosene	1.10
47.94	1-Docosene	1.75
47.24	5,7-Dihydroxy-3-[2,3-dihydro-4-hydroxy-2-(2-hydroxyisopropyl)benzofuran-7-yl]chromone	1.40
47.71	beta.-l-Arabinopyranoside, methyl	1.45
48.11	Nonanamide	3.28
48.35	4H-1,16-Etheno-5,15-(propaniminoethano)furo	0.85
51.72	N-[(p-Nitrophenyl)sulfonyl]-hydroxyproline	0.75

(d) Bioplastic (280 °C)

RT	Name	Area%
16.54	p-Cresol	1.7
17.37	Pentanoic acid	1.9
19.63	Silane, 1,3-butadiynyltrimethyl-	5.4
22.94	Resorcinol, 2-acetyl-	1.3
24.81	Butanoic acid, 3-methyl-, 2-phenylethyl ester	1.8
25.67	Pentanoic acid	4.6
25.85	Quinoline, 6-methyl-	2.8
26.09	Indolizine, 3-methyl-	1.4
30.73	Pentanoic acid, 2-hydroxy-, ethyl ester	3.0
30.96	1-Dodecanol	1.9
31.45	Heptadecane	2.3
36.92	Ethane-1,1-diol dibutanoate	6.2
36.96	Nonanoic acid	1.2
37.60	Formic acid, 4,4-dimethylpent-2-yl ester	1.2
38.74	24s-Cycloartane-3,16,24,25-tetraacetate	2.1
39.20	2-Butene, 1-butoxy-, (E)-	1.1
40.09	4-Methylcyclohexaneacetic acid (stereoisomer 1)	1.0
40.98	11-Tricosene	3.6
41.84	Methyl 2-O-methyl-.beta.-D-xylopyranoside	2.8
43.39	n-Hexadecanoic acid	5.2
43.39	Dodecanoic acid	4.2
43.58	Nonanamide	1.5
43.58	Octadecanamide	0.9
44.85	6-Tridecene	2.4
47.30	Glutaric acid, 2,2,3,3,4,4,5,5-octafluoropentyl pentafluorobenzyl ester	4.4
47.60	8-Pentadecanone	1.0
47.80	Octadecanoic acid	7.1
48.16	Nonanamide	5.6
48.26	2-Oxa-6-azatricyclo[3.3.1.1(3,7)]decan-4-ol, 6-(phenylsulfonyl)	1.0
51.45	Benzeneacetic acid, 2,4,5-tris[(trimethylsilyl)oxy]-, trimethylsilyl ester	1.5
51.61	L-Leucine, N-methyl-N-(hexyloxycarbonyl)-, pentadecyl ester	1.1
52.08	2-Propanol, 2-methyl-	2.2

(e) Bioplastic (330 °C)

RT	Name	Area%
16.71	Sulfamic acid, N,N-dimethyl-, 4-nitrophenyl ester	1.47
17.38	Quinoline, 1,2,3,4-tetrahydro-	1.33
17.85	4-Piperidinone, 2,2,6,6-tetramethyl-	1.84
19.72	(2S,6R,7S,8E)-(+)-2,7-Epoxy-4,8-megastigmadiene	1.44
21.09	Indole	0.82
21.61	Ethyl 5-fluoro-3-iodo-1H-indole-2-carboxylate	0.76
24.81	Benzamide, N-ethyl-	2.25
25.05	5-Methyl-4-hexene-1-yl acetate	1.74
25.62	Benserazide	2.94
25.97	1-Undecanol	2.60
26.10	Indolizine, 3-methyl-	1.29
28.88	Diethyl 3,3'-(methyylimino)dipropionate	0.76
30.59	Indolizine, 2-methyl-6-ethyl-	2.45
30.95	1-Tetradecanol	1.81
31.27	1-Heptadecene	8.82
36.91	n-Decanoic acid	5.40
38.87	1,3-Dioxolane, 2-heptyl-	1.02
39.47	Veralkamine	6.08
42.17	Octadecanamide	1.00
43.29	Thietane, 2,4-dimethyl-	9.99
43.36	1-Heptadecene	7.05
43.70	Silane, diethyl(pentafluorobenzyloxy)tetradecyloxy-	4.38
45.28	Octadecanoic acid	2.70
47.71	4-Phenyl-3-butyn-2-one	4.69
47.75	Octadecanoic acid	6.31
48.13	Nonanamide	2.92
51.30	2',3',4',5,7-Pentamethoxyflavone	1.34
51.30	N-Methyl-N-vinylthio-naphthalene-1-amine	1.23

(f) Bioplastic (370 °C)

RT	Name	Area%
9.99	Ethylamine, 2-((p-bromo-.alpha.-methyl-.alpha.-phenylbenzyl)oxy)-N,N-dimethyl-	10.2
10.47	Ethylamine, 2-((p-bromo-.alpha.-methyl-.alpha.-phenylbenzyl)oxy)-N,N-dimethyl-	8.8
10.47	N-Dimethylaminomethyl-tert.-butyl-isopropylphosphine	3.3
13.78	Phenol	1.3
14.67	Trifluomeprazine	1.4
16.45	Furazan-3,4-diamine, N,N'-bistrifluoroacetyl-	2.2
16.84	p-Cresol	1.5
17.88	4-Piperidinone, 2,2,6,6-tetramethyl-	3.0
19.57	1-Naphthoic acid, 2,2,3,3,4,4,5,5-octafluoropentyl ester	2.8
20.02	Carbonic acid, monoamide, N-(2-butyl)-N-tetradecyl-, decyl ester	2.4
21.59	Pyridine, 2-[2-(3-nitrophenyl)ethenyl]-, trans-	1.0
23.92	Undecane, 3,7-dimethyl-	1.4
24.84	Aspidospermidine-3-carboxylic acid, 2,3-didehydro-1-methyl-, methyl ester	4.1
26.11	Indolizine, 3-methyl-	1.5
26.37	Cetene	4.8
28.63	4-(3-Hydroxy-2-oxo-propylamino)-benzonitrile	0.9
28.89	1-Heptadecene	3.0
30.64	Xylose	1.5
31.22	4-Hydroxy-3-nitroacetophenone	0.8
34.26	Bufotenine, N,O-bis(heptafluorobutyryl)-	3.0
36.81	Pentanoic acid	2.5
41.17	Heptane, 3,3,4-trimethyl-	2.1
43.16	n-Hexadecanoic acid	11.8
43.16	n-Decanoic acid	0.9
46.38	Bicyclo[4.1.0]heptan-2-one, 3,7,7-trimethyl-	1.2
47.24	9H-Carbazole-1-carboxylic acid, 4-(1H-indol-3-yl)-, methyl ester	1.6
47.70	Octadecanoic acid	2.2
48.09	Nonanamide	4.1
50.24	1,3,4-Oxadiazole, 2-(2-phenylethenyl)-5-(4-biphenyl)-	0.8
52.04	Nonanamide	1.1
58.81	2-Chloropropionic acid, 3-methylphenyl ester	1.1
59.30	Benzene, propoxy-	0.8